The Impact of Peptide Insertions
on Adeno-Associated Viral Vector Fate

Inaugural-Dissertation

zur

Erlangung des Doktorgrades

Dr.nat.med.

der Medizinischen Fakultät

und

der Mathematisch-Naturwissenschaftlichen Fakultät

der Universität zu Köln

vorgelegt von

Silke Uhrig

aus Köln

Hundt Druck GmbH, Köln

2010

Berichterstatter/-in: Prof. Dr. Herbert Pfister

                         Prof. Dr. Dagmar Knebel-Mörsdorf

Tag der letzten mündlichen Prüfung: 1. Juni 2010

Für meine Eltern

*Ihrer wahren Wesensbestimmung nach ist die Wissenschaft
das Studium der Schönheit der Welt.*

Simone Weil (1909-1943)

Table of contents

List of figures

List of tables

List of abbreviations

aa	amino acid
AAV	adeno-associated virus
AAVS1	AAV integration site 1
Ad	adenovirus
Alasl	δ-aminolevulinate synthase I
ALV	avian leucosis virus
ApoE	apolipoprotein E
APS	ammonium persulfate
ATP	adenosine triphosphate
B-CLL	B cell chronic lymphocytic leukemia
bp	base pair
CAR	coxsackie and adenovirus receptor
CD	cluster of differentiation
cDNA	complementary DNA
CPZ	chlorpromazine
Cy5	cyanine 5
DAPI	4′,6-diamidino-2-phenylindol
DMSO	dimethyl sulfoxide
DNA	deoxyribonucleic acid
DOC	deoxycholic acid
DTT	dithiothreitol

EDTA	ethylenediaminetetraacetic acid
e.g.	*lat.* exempli gratia ("for example")
EGF(R)	epidermal growth factor (receptor)
ELISA	enzyme-linked immunosorbent assay
EPO	erythropoietin
FACS	fluorescence activated cell sorting
FCS	fetal calf serum
FGF(R)	fibroblast growth factor (receptor)
FITC	fluorescein-5-isocyanate
g.p.	genomic particles
GFP	green fluorescent protein
gp	glycoprotein
HGF(R)	hepatocyte growth factor (receptor)
HIV	human immunodeficiency virus
HLA	human leucocyte antigen
HRP	horseraddish peroxidase
HSPG	heparan sulphate proteoglycan
i.e.	*lat.* id est ("that is")
IGF	insulin-like growth factor
i.g.p.	intracellular genomic particles
ITR	inverted terminal repeat
kb	kilo bases
LamR	laminin receptor
LB	Luria-Bertani
LDL(R)	low-density lipoprotein (receptor)
LH	luteinizing hormone
MG-132	carbobenzoxy-Leu-Leu-leucinal
MLV	murine leukemia virus
NPC	nuclear pore complex
nt	nucleotide
OD	optical density
ORF	open reading frame
p.i.	post infection
p.t.	post transduction
PAGE	polyacrylamid gel electrophoresis
PBS	phosphate buffered saline
PCR	polymerase chain reaction
PDGF(R)	platelet derived growth factor (receptor)
PEG	polyethylenglycol
PEI	polyethylenimine

PFA	paraformaldehyde
PI3K	phosphatidylinositol-3 kinase
PIPES	piperazine-N,N′-bis(2-ethanesulfonic acid)
PLA_2	phospholipase A_2
Plat	plasminogen activator
qPCR	quantitative PCR
rAAV	recombinant adeno-associated viral vector
Rab	Ras-related in brain
Rac1	Ras-related C3 botulinum toxin substrate 1
RIPA	radioimmunoprecipitation assay
RNA	ribonucleic acid
RT-PCR	reverse transcriptase PCR
scFv	single-chain fragment of variable region
SDS	sodium dodecyl sulphate
TBE	tris borate EDTA
TEMED	N,N,N,N-tetramethylethylenediamine
TMB	3,3', 5,5'-tetramethylbenzidine
Tris	tris(hydroxymethyl)aminomethane
VAP	viral attachment protein
VP	viral protein
VSV	vesicular stomatitis virus

Commonly used abbreviations and SI units are not separately listed.

Zusammenfassung

Rekombinante Adeno-assoziierte virale (rAAV) Vektoren besitzen eine Reihe für einen Vektor vorteilhafter Eigenschaften, darunter sind eine geringe Immunogenität, hohe Stabilität, langlebige Transgenexpression und das Potential zur ortsspezifischen Integration ohne bisher bekannte Nebenwirkungen zu nennen. Der Einsatz von rAAV-Vektoren in der Gentherapie wird jedoch dadurch limitiert, dass AAV einen breiten Gewebetropismus aufweist, der zu einer unerwünschten Transduktion von Nicht-Zielzellen führen kann. Kürzlich wurde demonstriert, dass die genetische Modifizierung des AAV-Kapsids durch Insertion rezeptorspezifischer Liganden („AAV targeting") die Transduktion von Zellen unabhängig vom Vorhandensein der natürlichen AAV-Rezeptoren ermöglicht. Die „AAV-targeting"-Technologie führt darüber hinaus zu einer Erhöhung der Transduktionseffizienz auf Wildtyp-AAV-permissiven Zellen und bietet die Möglichkeit zu einem AAV-vermittelten, zelltypspezifischen Gentransfer.

Die vorliegende Arbeit zeigt erstmals, dass der inserierte Ligand sowohl den Mechanismus der Internalisierung des AAV-Vektors bestimmt, als auch die Effizienz, mit der Vektoren in die Zelle und Vektorgenome in den Zellkern übertragen werden. Mit Hilfe von „AAV peptide display" wurden vier rAAV-Peptidinsertionsmutanten selektiert, die sich in der inserierten Sequenz und der Nettoladung der Insertion unterscheiden, und im Hinblick auf ihre Vektor-Zell Interaktion im Vergleich zu rAAV2 analysiert. Mutanten (A2 und C2) mit neutralen Peptidliganden transduzierten Zellen unabhängig vom AAV2-Primärrezeptor Heparansulfat-Proteoglykan (HSPG), während die Affinität der Mutanten B1 und D5 zu HSPG mit der positiven Nettoladung Ihrer Liganden korrelierte. Im Vergleich zu rAAV2 wies B1 eine niedrigere Affinität zu HSPG auf, D5 hingegen eine wesentlich höhere. Die neue Liganden-Rezeptor Interaktion führte zu einer Clathrin-vermittelten Aufnahme von A2 und C2, während D5 auf einem Clathrin-unabhängigen Weg in die Zelle eintrat – vermutlich über HSPG. Obwohl sich B1 nur in einer Aminosäure von C2 unterscheidet, war B1 in der Lage, sowohl Clathrin-vermittelt, als auch Clathrin-unabhängig in die Zelle aufgenommen zu werden. Vermittelt durch ihre Fähigkeit, an HSPG zu binden, traten B1 und D5 – im Gegensatz zu A2 und C2 – effizient in verschiedene Zelltypen ein. Effiziente Transgenexpression war hingegen von der Aufnahme der AAV-Vektoren über Clathrin-vermittelte Endozytose abhängig. Während die Transgenexpression bei allen AAV-Vektoren zu einem ähnlichen Zeitpunkt begann, erreichten Clathrin-vermittelt internalisierte Vektoren (rAAV2, A2 und C2) ein sigifikant höheres Genexpressionsniveau, was vermuten lässt, dass dieser Eintrittsmechanismus für eine effiziente intrazelluläre Prozessierung ausschlaggebend ist. In Übereinstimmung mit diesem Ergebnis wurden von B1 und D5, die Clathrin-unabhängig in die Zelle gelangten, signifikant weniger Vektorgenome in den Kern übertragen, als von

rAAV2. Statt dessen waren die Vektorgenome von B1 und D5 hauptsächlich mit membranumhüllten Zellorganellen – vermutlich Endosomen – assoziiert, was vermuten lässt, dass die intrazelluläre Prozessierung von Vektoren nach Proteoglykan-abhängiger Internalisierung im Vergleich zur effizienten Prozessierung von rAAV2 beeinträchtigt ist.

Abstract

Recombinant adeno-associated viral (rAAV) vectors possess a number of attractive properties including low immunogenicity, high stability, longevity of transgene expression and the potential to integrate site-specifically without known side-effects. The major limitation regarding the use of AAV vectors for gene therapy is the broad tissue tropism of AAV following *in vivo* gene tranfer application. Recently, genetic modification of the AAV capsid by insertion of receptor-specific ligands (AAV targeting) was demonstrated to enable the transduction of cells in the absence of AAV's natural receptors, to improve transduction efficiency in wild-type-AAV-permissive cells and to provide the opportunity of rAAV-mediated, cell-type-specific gene transfer.

This study shows for the first time, that the inserted ligand both alters the mechanism of AAV vector internalization and determines the efficiency of cell entry and nuclear delivery of vector genomes. Using AAV peptide display, four rAAV peptide insertion mutants differing in sequence and net charge of the inserted ligand were selected and analyzed regarding their vector-cell interplay in comparison to rAAV2. Mutants (A2 and C2) displaying neutral peptide ligands transduced cells independent of AAV2's primary receptor heparan sulphate proteoglycan (HSPG), whereas the affinity of the mutants B1 and D5 to HSPG correlated with the net positive charge of their ligands. Compared to rAAV2, the affinity to HSPG was lower for B1, but notably higher for D5. Ligand-receptor interaction led to clathrin-dependent uptake of A2 and C2, while D5 entered cells clathrin-independently, presumably via HSPG. Interestingly, B1, differing in a single amino acid from C2, was able to use both entry routes. Mediated by their ability to bind to HSPG, B1 and D5 – in contrast to A2 and C2 – entered efficiently into different cell lines. However, efficient transgene expression was dependent on vector entry by clathrin-mediated endocytosis. While the onset of gene expression happened in a similar time frame for all AAV vectors, those vectors internalized in a clathrin-mediated fashion (rAAV2, A2 and C2) reached significantly higher gene expression levels, demonstrating that this entry route is pivotal for efficient intracellular processing. In line with this observation, B1 and D5 – which entered the cell clathrin-independently – delivered significantly less vector genomes to the nucleus than rAAV2, but were mostly present inside membrane-coated cellular compartments – most likely inside endosomes – revealing that vector trafficking following proteoglycan-dependent endocytosis is impaired compared to the efficient intracellular processing of rAAV2.

1 Introduction

1.1 Gene therapy vectors

Gene therapy can be defined as the use of genetic material to modify a patient's cells for the treatment of an inherited or acquired disease. In general, a gene must be delivered to the cell using a carrier, or vector. The vector systems currently used in gene therapy can be divided into viral and non-viral vectors. Since viruses have evolved specialized molecular mechanisms to efficiently transport their genomes into cells, they possess ideal characteristics as a gene transfer vehicle. Indeed, the most common type of vectors used today is based on virions that have been genetically altered to carry a transgene instead of their viral genome and are termed viral vectors. Such a viral vector can transduce cells and deliver its transgene but does not produce progeny, which is a key property regarding vector safety. The most popular viral gene therapy vectors are based on retro/lentiviruses, adenoviruses (Ad) and adeno-associated virus (AAV), which have different mechanisms to enter a host cell [1] (Figure 1).

Ad is a non-enveloped, double-stranded DNA virus with an icosahedral capsid consisting of hexon (240 trimers), fiber (12 monomers) and penton (5 pentamers) [2]. Fiber and penton mediate binding to cell surface receptors followed by internalization. The uptake of Ad serotype 5, a common platform of Ad-based vectors, involves the attachment of Ad5 to the coxsackie and adenovirus receptor (CAR), conducted by the fiber knob, followed by interactions between penton base components and α_v integrins leading to internalization of Ad5 [3],[4] (Figure 1a).

AAV is a non-enveloped virus with a single-stranded DNA genome. The icosahedral capsid of AAV is built by 60 monomers of the three viral proteins VP1, VP2 and VP3 in a ratio of ~1:1:10 [5]. Similar to Ad, the AAV capsid mediates binding to cellular attachment and internalization receptors. AAV serotype 2, the best characterized AAV serotype and a promising vector platform, makes its first contact with the cell by attaching to the primary receptor HSPG, which might be enhanced by co-receptors such as fibroblast growth factor receptor (FGFR) and/or hepatocyte growth factor receptor (HGFR) [6],[7]. Subsequent binding to integrins leads to endocytosis of AAV2 via clathrin-coated pits [8-11] (Figure 1b). In addition to clathrin-mediated endocytosis, caveolin-dependent uptake is involved in the uptake of AAV serotype 5, which binds to the cell via sialic acid and platelet-derived growth factor receptor (PDGFR) [12-15].

Retro-/lentiviruses are enveloped viruses with a diploid single-stranded, positive sense RNA genome [1]. The viral genome is surrounded by a protein shell, the nucleocapsid, and a lipid bilayer, the viral envelope, carrying the Envelope glycoproteins (Env proteins) [3]. The first

step in lentiviral cell entry is a fusion between the viral envelope and the cellular membrane mediated by Env proteins [16] (Figure 1c). HIV entry into target cells, for example, is mediated by the viral Env proteins gp120 and gp41 upon binding to the cellular CD4 molecule and a co-receptor on the target cell plasma membrane. Subsequent conformational changes in gp41 bring the viral and cellular membranes in close proximity and allow fusion pore formation. Finally, the nucleocapsid is released to the cytosol [1],[16].
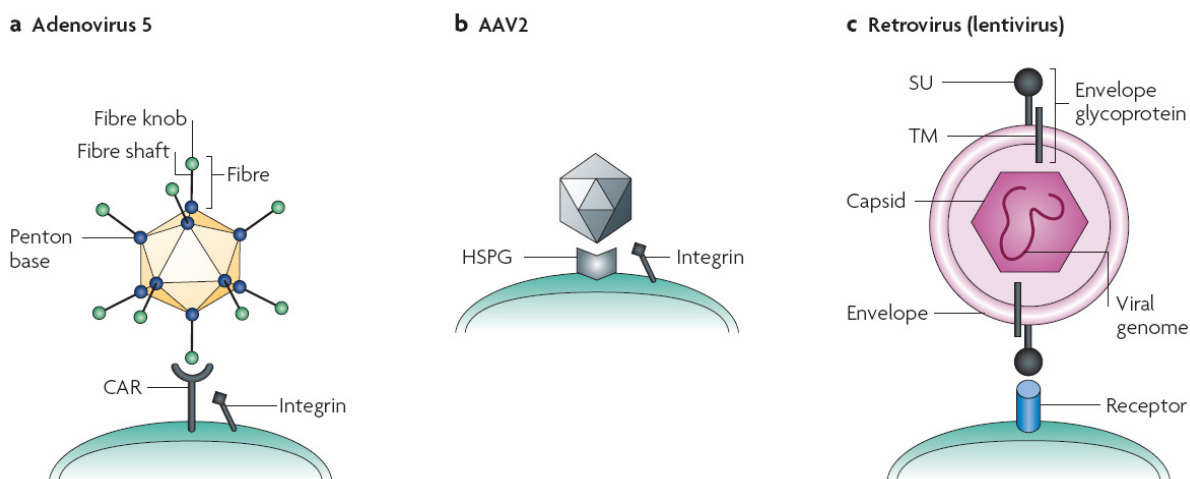
Figure 1: Entry mechanisms of unmodified viral vectors

a: Adenovirus (Ad): Ad serotype 5 binds to its receptor CAR (coxsackie and adenovirus receptor) through its fiber knob. Subsequently, integrins interact with the RGD peptide motif in the penton base and facilitate cell entry by endocytosis.

b: Adeno-associated virus (AAV): Several residues of the AAV2 (adeno-associated virus serotype 2) capsid are involved in binding to heparan sulphate proteoglycan (HSPG) and then to the co-receptors, which can be integrins (shown here), FGFR, HGFR or others. Subsequently, the virus is internalized by endocytosis.

c: Retrovirus (lentivirus): Membrane fusion is the main mechanism whereby enveloped viruses deliver their genomes into target cells. After initial non-specific adhesion of the virus to the cell surface, viral attachment glycoproteins bind specifically to their cognate receptors, whereupon binding becomes irreversible. Subsequent steps in the viral entry process vary between different viruses but always result in fusion between the lipid membranes of the virus and the host cell, following which the viral nucleocapsid is released into the cytoplasm. In most cases, receptor binding triggers conformational changes in the viral proteins that mediate membrane fusion. SU, surface subunit; TM, transmembrane subunit. *Reprinted by permission of Macmillan Publishers Ltd: Nature Reviews Genetics* [3]*, © 2007*

Besides viral vectors, non-viral systems – usually a polymer-DNA or lipid-DNA complex – have been used to deliver exogenous DNA into cells. Cationic polymers and lipids interact with negatively charged DNA through electrostatic interactions leading to polyplexes and

lipoplexes, respectively [17]. Cationic carriers were shown to bind to cell surface HSPGs and enter the cell by endocytosis or phagocytosis followed by endosomal trafficking of the DNA-containing complex [18-23]. Cationic lipoplexes can deliver the complexed DNA into the cytoplasm by de-stabilizing the endosomal membrane ("flip-flop" of anionic lipids) [24],[25], whereas the ionizable amine groups of cationic polymers are able to cause osmotic swelling and rupture of the endosomal membrane ("proton-sponge" hypothesis) [26]. Advantages associated with these kinds of vectors include their large-scale manufacture, their low immunogenecity and the capacity to carry large DNA molecules [17],[27]. However, compared to viral vectors, non-viral vectors are still less efficient with respect to transgene expression, i.e. successful cell transduction [1],[17].

Despite the ability of efficient gene delivery at least into certain cell types, there are still numerous problems regarding the use of viral vectors for gene therapy. To achieve therapeutic success, gene transfer vehicles not only have to mediate efficient gene delivery and expression, but they also have to be capable of transducing target cells without harming non-target cells. The first drawback associated with unmodified viral vectors is the inefficient transduction of therapeutically relevant cell types, while the second is caused by the tropism of natural viral variants that is not restricted to certain cells or tissues. Hence, to achieve efficient and specific gene transfer *in vivo*, novel viral vectors with user-defined gene delivery properties have to be developed.

Several techniques have been utilized in viral vector engineering which modify the viral capsid or envelope, among them pseudotyping, the use of adaptors and genetic targeting approaches [3].

1.1.1 Vector targeting by pseudotyping

A major limitation of gene therapy approaches is the poor transduction of therapeutically relevant cell types caused by the absence of receptors for viral attachment proteins (VAPs) [28],[29]. This constraint can be circumvented by pseudotyping, a technique involving the transfer of VAPs between different viral serotypes, thereby broadening the viral tropism. In addition, mosaic or chimeric vectors can be built by mixing VAPs from different variants or by swapping smaller VAP domains between serotypes [1].

Pseudotyping has most extensively been used to modulate the tropism of lentiviral vectors because they are highly permissive for incorporation of heterologous attachment glycoproteins into their lipid envelope [30],[31] (Figure 2A). The use of VSV-G (the glycoprotein of vesicular stomatitis virus) or Env proteins of γ-retroviruses as VAPs in a pseudotyped lentiviral vector confers a broad tropism, making it possible to achieve gene transfer into basically all human and murine cell types [16],[32],[33].

Pseudotyping has also been used for the non-enveloped vectors Ad and AAV, where the VAP must be incorporated into a protein capsid instead of a lipid bilayer (Figure 2B and C). Chimeric Ad particles, generated by exchanging fibers or hexons between Ad5 and other serotypes, have the potential to alter the viral tropism. Fibers from different serotypes in the context of the Ad5 capsid were shown to improve transduction of some cancer and primary cell lines [34],[35], and chimeric Ad vectors with fiber-like proteins from T4 bacteriophage or reovirus could be targeted to alternate receptors [36],[37].

Pseudotyped or pseudopackaged AAV vectors can be generated by packaging vector genomes flanked by the AAV2-ITR sequences into capsids of a different serotype [7]. Chimeric and mosaic AAV vectors are built by swapping capsid monomers or domains from one serotype to another, thereby generating vectors with the combined gene delivery properties of the parent serotypes [38-40]. For example, an AAV1/AAV2 chimeric vector achieved gene expression levels similar to those of AAV1 in muscle and AAV2 in liver, and could be purified by heparin affinity chromatography like wild-type AAV2 [38]. An AAV3/AAV5 mosaic vector was shown to share both receptor binding abilities of the parent serotypes, as it could bind to heparan sulphate (like AAV3) and mucin (like AAV5) [39]. Moreover, vectors composed of various monomeric capsid proteins or capsid domains from different serotypes gained novel functions not found among natural variants [39-42].

Pseudotyped viral vectors have an expanded tropism to cell types that are refractory to the natural variant. However, de-targeting from the natural tropism often needs further modifications of the pseudotyped vector that require structural knowledge of the VAP.
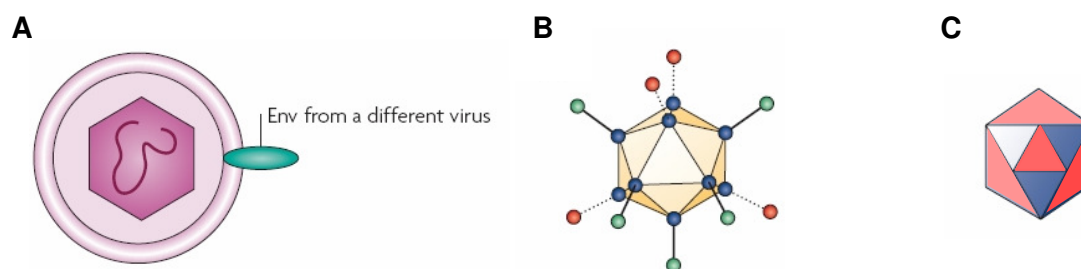
Figure 2: Pseudotyping viral vectors

A retroviral/lentiviral vector is pseudotyped with an envelope protein (Env) from a different virus (**A**). Pseudotyping of adenoviral vectors is achieved by exchanging fibers or hexons between different serotypes (**B**). AAV can be pseudotyped by swapping capsid proteins or capsid protein domains between different serotypes (**C**). *Adapted by permission of Macmillan Publishers Ltd: Nature Reviews Genetics* [3]*, © 2007*

1.1.2 Vector targeting using adaptors

The use of adaptor proteins has been explored as a technique that is applicable even with limited knowledge of the viral structure [3]. Adaptors are molecules with dual specificities: one end binds to the viral vector and the other end binds to the receptor on the target cell. The advantage of this approach is the ability to change viral properties in a highly modular manner and that most adaptors can achieve the two main goals of targeted delivery: ablating native tropism and conferring a novel tropism towards the desired target [3].

Bi-specific linker molecules have commonly been applied to retroviral vector systems. Typically, the adaptors are fusion proteins composed of a viral receptor, which interacts with the vector particle via the Env protein, and a targeting ligand, which interacts with its cognate receptor on the target cells [1] (Figure 3A). Two adaptors composed of EGF and either avian leucosis virus A (ALV-A) receptor (TVA) or ALV-B receptor (TVB) achieved efficient ALV-A- or ALV-B-mediated transduction of cells expressing EGFR [43]. In a more complex linker approach, the protein A IgG-binding ZZ domain from *Staphylococcus aureus* [44] was inserted into the receptor binding site of Sindbis virus E2 Env protein [45],[46]. This allowed for example the incorporation of targeting antibodies against CD4 or human leukocyte antigen (HLA) into virus particles leading to preferential transduction of CD4$^+$ and HLA$^+$ cells by the re-targeted, pseudotyped retroviral vectors [45].

Different bi-specific adaptors have been developed for targeting Ad vectors (Figure 3B). Fusion of the CAR ectodomain with EGF reduced vector binding to CAR$^+$ cells by 90% and enhanced transduction of EGFR-expressing cells by the targeted vector up to 12-fold compared to an untargeted Ad [47]. Likewise, fusing the ectodomain of CAR with CD40 ligand successfully targeted Ad vectors to dendritic cells expressing CD40 [48]. Chemical conjugation is a method for coupling adaptors to vectors in which the targeting ligand is covalently linked to the vector. Polyethylene glycol (PEG) has been used to couple Ad vectors to ligands such as FGF2 or an RGD-containing peptide in order to target ovarian cancer cells or endothelial cells [49], [50]. An extension of the chemical conjugation approach combines the flexibility of adaptor systems with the advantage of stable covalent bonds that are provided by genetic targeting (see below). Reactive thiol groups were introduced into the Ad capsid by genetically inserting cysteines at exposed positions. The thiol groups were then coupled to transferrin, which mediated the successful targeting of the vector to cells expressing transferrin receptor [51].

Chemical coupling methods have also been developed through biotinylation of the AAV capsid. Streptavidin-EGF and Streptavidin-FGF fusion proteins mediated increased transduction of EGFR$^+$ or FGFR$^+$ cells by the targeted AAV vectors but no difference was observed between targeted and unmodified vectors on an EGFR-negative cell line [52],

indicating that the modified vector had retained its natural tropism. Also bi-specific adaptors have been studied: a bi-specific antibody that recognizes both the intact AAV2 capsid and $\alpha_{IIb}\beta_3$ integrin has been used to re-target AAV2 (Figure 3C). This vector demonstrated enhanced binding to wtAAV2-non-permissive cells and increased transduction up to 70-fold on these cell lines [53]. In an approach of combining genetic peptide insertion (see below) and the use of an adaptor, the protein A IgG-binding domain from *S. aureus* was genetically introduced into the AAV capsid and coupled to antibodies against CD29, CD117 and CXCR4 leading to specific transduction of human hematopoietic cell lines, however with low efficiency [54] (Figure 3D).
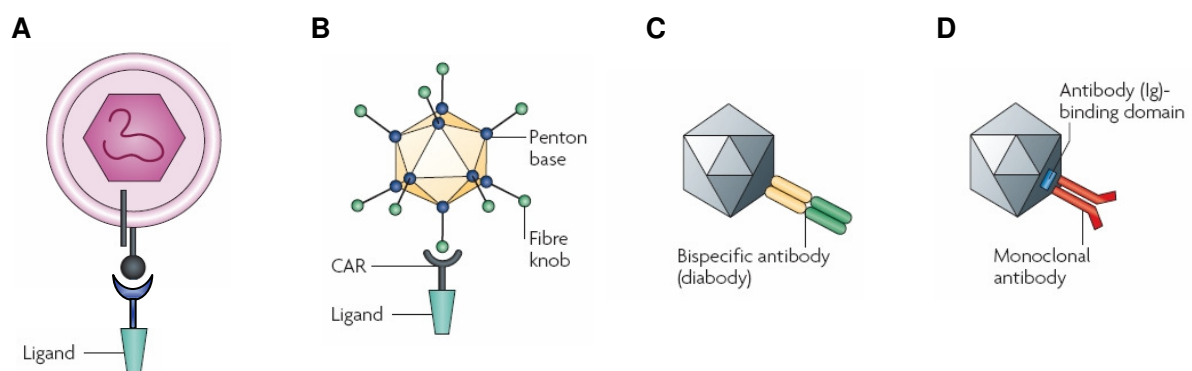
Figure 3: Vector targeting using adaptors

Adaptors consist of a receptor-ligand fusion protein that binds to the VAP of the viral vector (the Env protein of a retro-/lentiviral vector (**A**) or the fiber knob of an adenoviral vector (**B**)) and to the respective receptor on the target cell. AAV is attached to a bi-specific antibody that recognizes both, the AAV capsid and a cellular receptor (**C**). An antibody-binding domain is genetically incorporated into the AAV capsid to couple a monoclonal antibody to the vector (**D**). *Adapted by permission of Macmillan Publishers Ltd: Nature Reviews Genetics* [3]*, © 2007*

Coupling of targeting molecules is not limited to viral vectors but is also of great interest to the targeted delivery of non-viral vectors [55]. Similar to non-enveloped viruses, cationic polyplexes and lipoplexes can be taken up into the cell in endocytic or phagocytic vesicles [17]. Clathrin- and caveolin-mediated endocytosis as well as an entry process independent of clathrin and caveolin has been proposed for the internalization of non-viral vectors [56-58]. However, efficient gene delivery using non-viral vectors is impeded by the entrapment of DNA complexes in the endosomal compartment leading to degradation of the internalized DNA [18],[57]. An improvement in endosomal escape was achieved by the use of polyethylenimine (PEI), a cationic polymer that condenses DNA and offers an intrinsic mechanism enabling the release of endocytosed DNA into the cytoplasm [59]. Coupling of targeting ligands to DNA/PEI polyplexes led to further increase in efficiency and cell-type-

specific gene transfer [60-66]. These ligands can be small molecules (galactose, mannose or EGF) or peptides/proteins (transferrin or antibodies). Incorporation of EGF or transferrin into the DNA/PEI complex resulted in both receptor targeting and receptor-mediated endocytosis, enabling greatly enhanced gene delivery [60],[61],[67]. Specific antibodies for certain cell surface markers have also been used for targeting: antibodies against CD3 or ErbB2 enabled efficient gene delivery into human T-cell leukaemia cells (CD3$^+$) or ErbB2$^+$ human breast cancer cells [60],[68].

1.1.3 Genetic incorporation of targeting ligands

Although targeting approaches using adaptors achieved cell-type-specific targeting, there is the potential risk that the affinity of vector-adaptor complexes *in vivo* may not be sufficient to prevent dissociation of the adaptor-vector linkage which might result in side-effects [3],[1]. Thus, methods were developed for the genetic incorporation of targeting ligands into viral vectors. Genetic fusion of these ligands into the capsid or Env protein yields a stable modification that can direct the virion to its target cell [3].

Various targeting molecules such as short peptides and single-chain antibody fragments (scFv) have been inserted into retroviral Env proteins (Figure 4A). Short targeting peptides inserted into Env proteins have been shown to mediate targeted gene delivery without severely disrupting the envelope's function: upon insertion of RGD-containing motives, retroviral vectors could be targeted to human melanoma cells while the natural tropism of the vector was altered depending on the position of the inserted ligand [69]. Also the display of scFv on the surface of enveloped viruses was successfully accomplished by genetically fusing an antibody fragment to the surface component of Env glycoproteins. Retroviral vectors incorporating an anti-hapten antibody were shown to bind to hapten via the displayed antibody and vectors with an inserted low-density lipoprotein receptor (LDLR)-specific scFv could mediate a specific retroviral transduction of cells expressing LDLR [70],[71]. To reduce non-specific transduction of human cells, ecotropic MLV Env proteins have often been used as scaffold for the insertion of the scFv targeting domains [72]. In addition to peptides and single-chain antibodies, various ligands such as insulin-like growth factor I (IGF-1), EGF and erythropoietin (EPO) have been fused to Env proteins [73-76]. However, both, the incorporation of large scFv molecules and the insertion of ligands to the N-terminus of Env proteins, can interfere with the conformational changes required for Env proteins to mediate membrane fusion, resulting in low transduction efficiencies [75]. In particular, virus particles complexed with the targeted receptors were often sequestered on the cell surface or routed to degradative pathways after endocytosis [73],[76].

Most peptide modification approaches for Ad5 have focused on the fiber (Figure 4B). Insertion of small RGD-containing peptides targeting integrins, or the poly-lysine peptide

pK7, mediating attachment to heparan sulphates, yielded infectious viral vectors that bound to the respective targets [77]. Also the insertion of peptide epitopes into the HI loop of the Ad fiber has been investigated. Insertion of an RGD-containing peptide conferred targeted gene delivery to cells expressing high levels of integrins [78]. Further developments demonstrated that insertion of both RGD and pK7 peptides into the fiber provides an additive effect of both functionalities and that the insertion of targeting peptides can lead to an ablation of native tropism [79],[80]. The incorporation of scFv molecules into an Ad vector was initially impeded because of the different biosynthetic pathways that are used to produce the scFv (which is synthesized in the rough endoplasmic reticulum) and the Ad capsid proteins (which are synthesized in the cytosol) [81]. In addition, incorporation of such large proteins into the Ad fiber can impede proper folding (trimerization) of the fiber [3]. The use of cytosolically stabilized scFvs (intrabodies) and the generation of an artificial fiber allowed genetic coupling of the fiber and scFv in the Ad system, which additionally gave rise to the advantage of ablating the native tropism of Ad [82].

Several sites of the AAV capsid were shown to tolerate the insertion of peptides but only some of these sites have been examined for their suitability in AAV vector targeting [83-88] (Figure 4C). The first attempt used an scFv molecule fused to the N-terminus of VP2 to target CD34$^+$ cells but the overall transduction level remained low [89]. The incorporation of several smaller peptides, e.g. serpin receptor ligand, ApoE or an LH peptide, to the N-terminus of VP1 or VP2 yielded functional virions and could expand the tropism of AAV2 [83-85],[90],[91]. In two of these studies, the fusion of GFP to the N-terminus of VP2 gave rise to GFP-tagged viruses that have been used to visualize the infectious pathway of AAV [90],[91]. Genetic capsid modification by insertion of peptides into the common region of all three AAV capsid proteins (amino acid position 587 and 588) could successfully re-target AAV2 [86],[92]. These two positions have been used most frequently for the insertion of small peptides [86],[92-100], leading to superior ligand-mediated transduction of target cells by the capsid-modified AAV vectors. Insertions at the position 587 interfere with the binding of two (R585 and R588) of the five positively charged amino acids of the AAV2 HSPG-binding motif [101],[102], explaining the ablation of HSPG binding of some re-targeted vectors [54],[86],[93-95]. In some cases, binding was only partially affected or even restored, when ligands were inserted at amino acid position 587 [94],[95],[97],[100]. This loss or maintenance of HSPG binding was shown to depend on the nature of the inserted ligand sequence: Insertion of bulky or negatively charged peptides results in AAV2 capsid mutants unable to bind to HSPG due to sterical or charge interference. Insertion of positively charged peptides, however, can lead to an HSPG-binding phenotype by reconstituting a binding motif with one of the original arginines (R585 or R588) or independently of them [103].
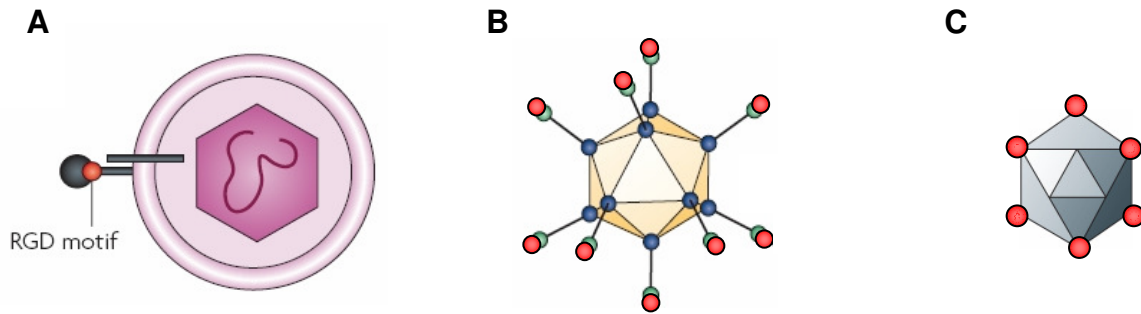
Figure 4: Genetic targeting

Small targeting ligands are genetically inserted into the Env protein of a retro-/lentiviral vector (**A**), into the fiber knob domain of adenoviral vectors (**B**) or into the capsid protein of AAV (**C**) to target the viral vectors to distinct cellular receptors. The incorporation of RGD-containing peptides, for example, is used to specifically target integrin receptors. *Adapted by permission of Macmillan Publishers Ltd: Nature Reviews Genetics* [3]*, © 2007*

1.1.4 AAV peptide display

Although rational modification techniques have generated viral vectors with novel gene delivery properties, the successful application of these approaches often requires detailed mechanistic knowledge of viral target proteins. Furthermore, the insertion of foreign peptides into the capsid structure may interfere with the stability of the viral particle or with the infectious process and by incorporation into the viral capsid, peptide ligands might be displayed in a non-functional conformation [1],[7]. A more basic restriction of this approach is the limited knowledge about cell-type-specific receptors and their natural ligands on clinically relevant tissues. The recent development of AAV peptide display libraries allows the selection of capsid mutants on various cell types [95],[96] (Figure 5). Two AAV peptide libraries have been developed consisting of mutants carrying 7-mer peptides with random sequence at amino acid position 587 [95] or 588 [96]. Perabo and colleagues performed five selection rounds with an AAV peptide library on MO7e, a megakaryocytic cell line, and on Mec1, which is derived from B-cell chronic lymphocytic leukemia (B-CLL) [95]. Both cell types are non-permissive for wtAAV2. In two separate selections, RGD-containing peptides (RGDAVGV and RGDTPTS) were obtained from the MO7e selections, whereas two different peptides were selected on Mec1 (GENQARS and RSNAVVP). rAAV vectors displaying the selected peptides on the capsid surface transduced their respective target cells with an up to 100-fold increased efficiency compared to wtAAV2, and ligand-mediated cell transduction was proven by peptide competition. Moreover, one of the mutants selected on Mec1 was able to transduce primary B-CLL cells (up to 54%) which are refractory to AAV2 infection. Müller and colleagues applied a similar approach for the selection of peptides able to mediate the transduction of human coronary artery endothelial cells [96]. Most of the

selected peptides fitted into the consensus sequence NSVRDL^G/$_S$ and NSVSSX^S/$_A$ and displayed remarkably higher transduction levels than AAV2 with unmodified capsid on the target cells. Furthermore, one of the peptides (NSSRDLG) enabled heart transduction after systemic application in mice, whereas only a weak transduction was observed with wtAAV2. Depending on the applied selection pressure and the use of viral progeny for further selection rounds, the AAV peptide display technology allows the selection of capsid mutants that own the characteristics of cell-type-specific cell entry and successful intracellular processing which both are essential for an efficient AAV targeting vector.
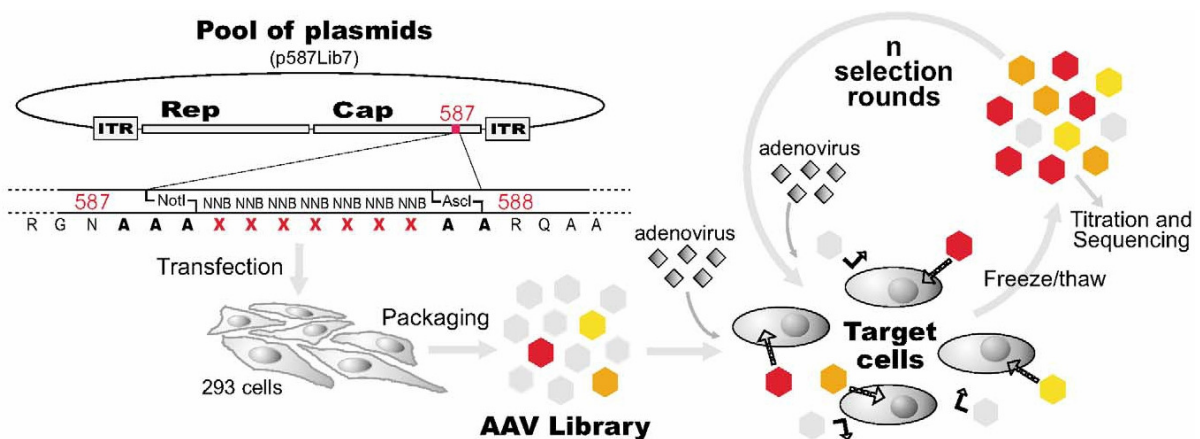
Figure 5: AAV peptide display

The picture schematically represents the construction of the library of AAV2 capsid-modified particles and the selection protocol for the isolation of targeted mutants. A pool of oligonucleotides with random sequence has been cloned into an AAV2-genome-encoding plasmid at the site corresponding to amino acid 587 of VP1. Following the standard AAV production protocol, a library of approximately 4×10^6 capsid-modified AAV2 clones was generated. For the selection of targeted mutants, target cells are co-infected with the pool of AAV2 mutants and adenovirus is applied to induce progeny production. Fourty-eight hours later, viral progeny is collected and used for the next selection round. *Figure kindly provided by Luca Perabo © 2003*

1.2 AAV and its infectious biology

As briefly mentioned above, rAAV vectors are based on AAV, which is classed into the family of *Parvoviridae*. This family is divided in two subfamilies: *Parvovirinae*, which infect vertebrates, and *Densovirinae*, which infect insects. *Parvovirinae* consist of the genera Parvoviruses, Amdoviruses, Bocaviruses, Erythroviruses and Dependoviruses, the latter of which AAV belongs to. As implicated by its name, AAV often occurs in association with other viruses, especially adenoviruses, and depends on the co-infection of a helper virus for

productive infection [7]. To date, 14 serotypes and multiple variants have been described, which were isolated either as contaminants of adenoviral preparations or from integrated proviral sequences found in rodents, non-human primates and human tissues [104-114].

All AAV serotypes contain a single-stranded DNA genome of approximately 5kb, which is packaged into an icosahedral, non-enveloped capsid and can be divided into three functional regions (Figure 6): two open reading frames (ORF; *rep* and *cap*) and the inverted terminal repeats (ITR) [115]. The ITRs at the 5'- and 3'-end of the AAV genome serve as origin of replication and play a key role in viral genome integration into the host genome as well as in the subsequent rescue of viral DNA from the integrated state [116-120]. The *rep* ORF codes for a family of multifunctional nonstructural proteins (Rep) that are involved in viral/vector genome replication, transcriptional control, integration and encapsidation of AAV genomes into preformed capsids [121-125]. The *cap* ORF codes for the three capsid proteins VP1, VP2 and VP3 [5],[126]. All capsid proteins share a common C-terminus, but differ in their N-terminus resulting in molecular weights of 90kDa (VP1), 72kDa (VP2) and 60kDa (VP3). Considering the functions of the capsid proteins, VP1 is essential for infectivity, whereas VP3 is sufficient for capsid formation [90]. VP2 is proposed to be neither necessary for capsid formation nor for production of infectious particles [90],[91].
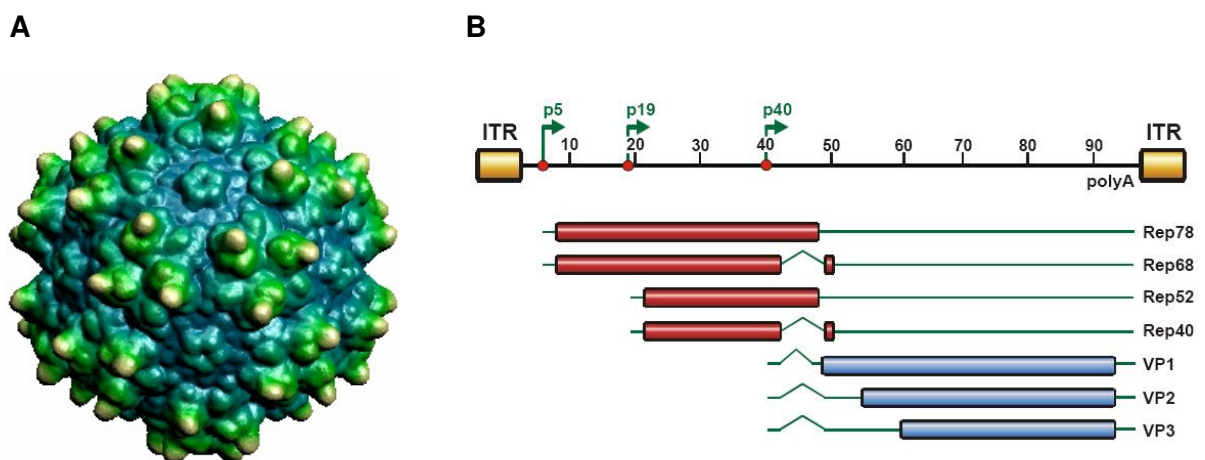
Figure 6: Capsid and genome structure of AAV2

A: The picture represents a surface rendering of the AAV2 capsid based on atomic coordinates. The colours are depth cued along a colour gradient: yellow at a larger radius, and greenish blue as the radius decreases. The view is down the two-fold axis (centre of the virus) with three-folds left and right of centre, five-folds above and below. *Capsid model kindly provided by Jorge Boucas © 2008*

B: The AAV genome contains of 4680 nucleotides (nts) divided into 100 map units (46.8 nts per unit). The AAV genome is flanked by inverted terminal repeats (ITRs), three viral promoters are positioned at units 5, 19 and 40 (p5, p19, p40) and the polyadenylation signal (polyA) at unit position 96. Open reading frames are shown as cylinders, untranslated regions as solid lines and introns as kinks. p5 and p19 regulate the four Rep proteins, which exist as spliced and unspliced isoforms. The p40

promoter controls the expression of the three different capsid proteins VP1, VP2 and VP3. *Scheme of AAV genome organization kindly provided by Nadja Huttner © 2003*

Like in every viral infection, AAV has to subsequently overcome numerous barriers – namely receptor binding, cell entry, intracellular trafficking, endosomal release, viral uncoating and nuclear entry – before it can deliver its genome into the nucleus for replication. The current knowledge of the AAV infectious biology is limited and the most detailed information is available for AAV serotype 2 (AAV2) (Figure 7). Single virus tracing technology revealed that AAV2 virions usually contact the cell membrane multiple times before internalization succeeds [127]. This characteristic most likely reflects the interaction of the capsids with HSPG, the primary receptor for AAV2 [6]. Also AAV3 is suggested to use HSPG as primary receptor, whereas the serotypes 1, 4, 5 and 6 bind to sialic acid [128],[129],[12]. N-linked sialic acids were identified as a primary receptor for AAV1, AAV5 and AAV6, while AAV4 binds to O-linked sialic acids. PDGFR was recently identified as a receptor for AAV5, and AAV8 was shown to bind to the laminin receptor (LamR) [130],[13]. LamR was also proposed to be involved in AAV2-, AAV3- and AAV9-mediated cell infection [130].

As mentioned in paragraph 1.1, AAV2 enters the cell in a two-step mechanism. Binding of AAV2 to its primary receptor HSPG is likely to induce a reversible structural rearrangement of the capsid required for the next step in viral entry, which is dependent on co-receptors [31]. The co-receptors FGFR-1, HGFR and laminin receptor may enhance the virus-cell contact, thereby facilitating the HSPG-induced structural rearrangement of the capsid [7], whereas integrins ($\alpha_v\beta_5$, $\alpha_5\beta_1$) are thought to mediate endocytosis of AAV2 [9],[131]. Integrin binding subsequently leads to the activation of the small GTPase Rac1 and phosphatidylinositol-3 kinase (PI3K) which results in cytoskeletal rearrangements that promote clathrin-dependent internalization of AAV2 as well as trafficking of AAV2 from the cell periphery towards the nucleus [9],[10],[132-134]. AAVs – at least serotype 5 – do not exclusively use clathrin-coated pits to enter the cell. Specifically, AAV5 is able to exploit both the clathrin-mediated pathway and caveolin-dependent internalization [14],[15].

Once internalized, AAV is trafficked mainly inside endosomes. Organelle separations, inhibitor and imaging studies revealed the presence of AAV2 particles in endosomal compartments [11],[127],[135-138]. These virus-containing vesicles were further shown to be transported along microfilaments and microtubules [9],[11],[136]. When and how AAV escapes from the endosome is still a matter of debate and may be cell type specific. For AAV2, evidence for viral release from early endosomes [11],[138], late endosomes [135],[136] or even perinuclear recycling endosomes [135] has been provided. In addition, AAV2 and AAV5 have been detected in the trans-Golgi network [14],[15],[137]. As described for other viruses [139], acidification of endosomes is necessary for viral gene expression

[11],[136],[137] and believed to trigger conformational changes of the viral capsid leading to exposure of previously hidden regions, which mediate endosomal escape and nuclear entry [140]. The N-terminus of VP1 contains a phospholipase A$_2$ (PLA$_2$) homology domain that is conserved among parvoviruses and becomes exposed during the AAV infection process [141],[142]. PLA$_2$ exhibits the catalytic activity of hydrolysing phospholipids into free fatty acids and lysophospholipids, which is thought to mediate endosomal escape of parvoviruses, including AAV2, by lipolytic pore formation [142],[143],[Stahnke et al., in revision].

When released from the endosome, the AAV capsid may be a target for ubiquitination and subsequent proteasomal degradation [144],[145]. Likewise, proteasome inhibitors enhanced cell transduction mediated by AAV1 to AAV5, AAV7 and AAV8 [136],[146-149]. In addition to inhibiting AAV degradation, proteasome inhibitors may affect viral genome translocation into or accumulation within the nucleus [150].

Viral particles start to accumulate in the perinuclear area between 15 and 30min post infection (p.i.) [11],[91],[127]. The majority of these virions still have intact viral capsids filled with viral genomes [91]. Furthermore, accumulation of viral particles in nuclear invaginations has been observed [91]. The question if viral uncoating happens before or after nuclear entry is still not answered. Several groups have described intact AAV particles in the nucleus, but data regarding the mechanism and efficiency of capsid import as well as their role in viral infection are controversial [9],[11],[91],[138],[151],[152]. However, Lux and colleagues revealed that nuclear entry of viral capsids is a rare event and that uncoating occurs before or during entry into the nucleus: at virus to cell ratios, at which viral genomes could be detected within the nucleus, signals of intact viral capsids were exclusively detected outside the nucleus [91]. Moreover, it is still a matter of debate whether AAV and/or AAV genomes enter the nucleus through the nuclear pore complex (NPC) or in a NPC-independent way [140],[152],[153].

Within the nucleus, the single-stranded AAV genome is converted into a transcriptionally active, double-stranded form. This genome conversion was shown to be a rate-limiting step in AAV infection, which is facilitated by adenoviral genes [154],[155]. Dependent on the presence or absence of a helper virus, AAV enters a lytic or latent life cycle. In the absence of helper functions, AAV enters a latent cycle and integrates at a specific locus known as AAVS1 on chromosome 19 (19q13.3-qter) [156],[157]. Prior to viral integration, second-strand synthesis and basal expression of the Rep proteins is activated [158],[159]. Rep proteins bind the viral genome at a Rep binding site located in the viral ITRs, and a homologous sequence in the AAVS1 locus, and mediate integration [160-162]. Integrated proviruses can be rescued by superinfection with a helper virus [163]. In the presence of a helper virus during AAV infection, induction of gene expression and replication proceed immediately.
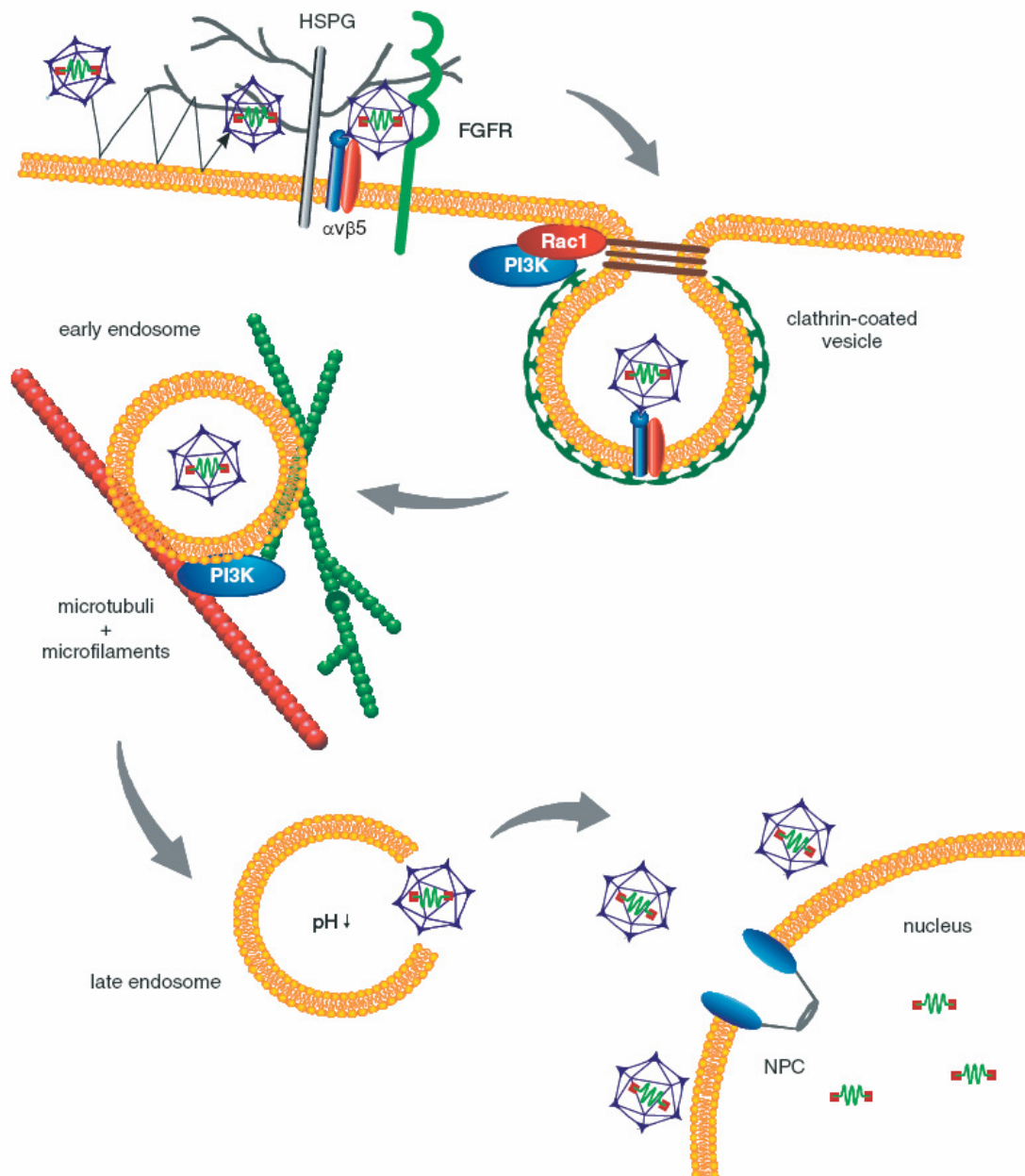
Figure 7: Current model of AAV2 infection in HeLa cells

AAV2 makes repeated contacts with the cell by binding to its negatively charged primary receptor heparan sulphate proteoglycan (HSPG) mediated by a cluster of basic amino acids in the AAV2 capsid. The attachment is enhanced by FGFR and/or HGFR binding. Subsequent binding to integrins leads to endocytosis via clathrin-coated pits. Integrin binding is assumed to activate the small GTP binding protein Rac1, which stimulates the PI3K pathway. The resulting rearrangement of the cytoskeleton allows trafficking of AAV2-containing endosomes. Acidification of the endosome may lead to conformational changes in the AAV2 capsid and its release. Uncoating and release of the viral genome takes place before or during nuclear entry. After transport of the AAV2 genome into the nucleus, the genome is replicated, integrated into the host genome or stays episomally. NPC: nuclear pore complex. *Picture kindly provided by Hildegard Büning © 2008*

1.3   Aim of the study

AAV targeting technologies hold promise to overcoming two major drawbacks in viral gene delivery, namely transduction of AAV-refractory cell types and avoidance of non-target cell transduction. Ligand-mediated cell transduction by AAV targeting vectors can achieve both re-targeting to target cells of interest and de-targeting from the natural tropism depending of the inserted peptide. Besides the fact that capsid modification leads to a change of viral tropism, to date, little is known about consequences of peptide insertions on the virus-host interplay. However, to optimize efficiency and safety of AAV targeting vectors, a detailed understanding of the vector-cell interaction is pivotal. Since the peptide ligands inserted into the viral capsid mediate target cell transduction, differences in the intracellular processing of the targeting vectors in comparison to non-targeted, unmodified AAV vectors are anticipated. This work aimed to clarify, how targeting non-natural receptors by the insertion of peptides into the AAV capsid influences the vector-cell interplay. Knowing that peptide insertions at amino acid position 587 in the AAV capsid can either disrupt, conserve or restore the ability to bind to HSPG which determines the *in vivo* tropism of AAV targeting vectors [103], HSPG-binder and HSPG-non-binder mutants ought to be selected by AAV peptide display. The generated AAV peptide insertion mutants should serve as tools for the analysis of cell entry and intracellular processes like proteasomal degradation and transgene expression in comparison to unmodified rAAV2. To elucidate distinct steps of the vector-cell interaction, different techniques were to be applied, e.g. inhibitor studies to analyze the cell entry mechanism, qPCR to quantify uptake and transcription of vector genomes and subcellular fractionation to monitor the intracellular distribution of vector particles. With these means, this study should lead to an improvement in the basic knowledge of cell transduction by AAV peptide insertion mutants, which is necessary for their use in targeted gene delivery *in vivo*.

2 Materials and Methods

2.1 Materials

2.1.1 Chemicals, solutions and enzymes

Product	Company
4′,6-Diamidino-2-phenylindol (DAPI)	Sigma-Aldrich, Taufkirchen, Germany
Agar-Agar	Roth, Karlsruhe, Germany
Agarose	Invitrogen, Karlsruhe, Germany
Ammonium Chloride	Merck, Darmstadt, Germany
Ampicillin	Sigma-Aldrich, Taufkirchen, Germany
APS	Invitrogen, Karlsruhe, Germany
Aqua bidest. (Ampuwa)	Fresenius Kabi, Homburg, Germany
Bafilomycin	Sigma-Aldrich, Taufkirchen, Germany
Bovine Serum Albumine	AppliChem, Darmstadt, Germany
Calcium Chloride	Sigma-Aldrich, Taufkirchen, Germany
Chlorpromazine	Sigma-Aldrich, Taufkirchen, Germany
Dimethyl sulfoxide (DMSO)	Riedel-de Haën, Seelze, Germany
DNA restriction endonucleases	MBI Fermentas, St. Leon-Rot, Germany; New England Biolabs, Frankfurt, Germany
DMEM Medium + GlutaMAX^{TM}-I	Invitrogen, Karlsruhe, Germany
EDTA	Roth, Karlsruhe, Germany
Ethanol	Roth, Karlsruhe, Germany
Ethidium Bromide	Roth, Karlsruhe, Germany
Gelatine	Sigma-Aldrich, Taufkirchen, Germany
Genistein	Sigma-Aldrich, Taufkirchen, Germany
Glycerol	Roth, Karlsruhe, Germany
Heparin	B. Braun Melsungen AG, Germany
HEPES	Roth, Karlsruhe, Germany
Iodixanol	Sigma-Aldrich, Taufkirchen, Germany
Isopropanol	Roth, Karlsruhe, Germany
Magnesium Chloride	Roth, Karlsruhe, Germany
MassRuler DNA Ladder Mix	MBI Fermentas, St. Leon-Rot, Germany
MG-132	Sigma-Aldrich, Taufkirchen, Germany
NP-40	Sigma-Aldrich, Taufkirchen, Germany
PBS	Invitrogen, Karlsruhe, Germany
Penicillin/Streptomycin	Invitrogen, Karlsruhe, Germany
Peptone/Tryptone	Roth, Karlsruhe, Germany
PIPES	Sigma-Aldrich, Taufkirchen, Germany
Phusion^{TM} DNA Polymerase	Finnzymes, Keilaranta, Finland

RPMI-1640 medium + GlutaMAX™-I	Invitrogen, Karlsruhe, Germany
Precision Plus Protein Gel Color Standards	Bio-Rad Laboratories GmbH, München, Germany
Sodium Dodecyl Sulfate (SDS)	Merck, Darmstadt, Germany
Sodium Phosphate	Roth, Karlsruhe, Germany
Streptavidin peroxidase conjugate	Dianova, Hamburg, Germany
T4 DNA Ligase	MBI Fermentas, St. Leon-Rot, Germany
TEMED	Sigma-Aldrich, Taufkirchen, Germany
TMB	Sigma-Aldrich, Taufkirchen, Germany
Transferrin from human serum, Alexa Fluor® 488 conjugate	Invitrogen Molecular Probes, Karlsruhe, Germany
Tris	Merck, Darmstadt, Germany
Triton X 100	Sigma-Aldrich, Taufkirchen, Germany
Trypsin-EDTA	Invitrogen, Karlsruhe, Germany
Tween 20	Merck, Darmstadt, Germany
Vectashield VC-H-1400	Vector Laboratories, Inc., Burlingame, USA
Western Lightning™ Chemiluminescence Reagent Plus	PerkinElmer Life Sciences, Boston, USA

All other chemicals were bought from Sigma-Aldrich (Taufkirchen, Germany), Merck (Darmstadt, Germany) or Carl Roth GmbH & Co. (Karlsruhe, Germany).

2.1.2 Standard kits

Product	Company
BigDye® Terminator v3.1 Cycle Sequencing Kit	Applied Biosystems, Foster City, USA
DNeasy® Blood & Tissue Kit	Qiagen, Hilden, Germany
EndoFree® Plasmid Kits	Qiagen, Hilden, Germany
Gel Extraction Kit	Qiagen, Hilden, Germany
LightCycler® 480 SYBR Green Master	Roche, Mannheim, Germany
LightCycler® FastStart DNA Master SYBR Green I	Roche, Mannheim, Germany
RNase-free DNase Set	Qiagen, Hilden, Germany
RNeasy® Tissue Kit	Qiagen, Hilden, Germany
PCR Purification Kit	Qiagen, Hilden, Germany
Qproteome Cell Compartment Kit	Qiagen, Hilden, Germany
SuperScript™ III First-Strand Synthesis SuperMix for qRT-PCR	Invitrogen, Karlsruhe, Germany

2.1.3 Plasmids

peGFP-VP2.2: Plasmid encoding a fusion protein of eGFP and AAV2 VP2; Kanamycin-resistance; plasmid kindly provided by K. Lux

peGFP-VP2.2-"XN587": Plasmid encoding a fusion protein of eGFP and AAV2 VP2 carrying a targeting insertion at position 587. "XN587" represents the targeting insertion A2 (ASASNSVRSDAA), B1 (ASANGIRRFDAA), C2 (ASANGIRSFDAA) or D5 (ASAKGTKAPKAA). Kanamycin-resistance; plasmids were generated in this PhD work.

pGFP: EGFP cDNA controlled by the human cytomegalovirus (CMV) promoter and hygromycin resistance gene controlled by the thimidine kinase promoter flanked by the AAV2 ITRs; Ampicillin-resistance [164]

pLuci: Luciferase gene controlled by the CMV promoter, flanked by one intact ITR and one ITR containing a mutated terminal resolution site. The plasmid is packaged as pseudo-double-stranded genome. Ampicillin-resistance; plasmid kindly provided by S. Quadt-Humme

pmCherry-VP2.2: Plasmid encoding a fusion protein of mCherry and AAV2 VP2; Kanamycin-resistance; plasmid kindly provided by S. Stahnke

pRC: AAV based helper plasmid containing the AAV2 Rep and Cap open reading frame (ORF) but lacking the viral ITRs; Ampicillin-resistance [86]

pRC99: AAV based helper plasmid containing the AAV2 Rep and Cap ORF but lacking the viral ITRs, containing MluI and AscI cloning sites flanking the amino acid position 587; Ampicillin-resistance [93]

pRC99-"XN587": AAV based helper plasmid containing the AAV2 Rep and Cap ORF carrying a targeting insertion at position 587 but lacking the viral ITRs. Ampicillin-resistance; plasmids were generated in this PhD work.

pRC"Kotin": AAV based helper plasmid containing the AAV2 Rep and Cap ORF but lacking the viral ITRs, containing SnaBI and BsiWI cloning sites within the Cap ORF; Ampicillin-resistance; plasmid kindly provided by A. Girod

pRC VP2 k.o.: Plasmid encoding Rep-Proteins and capsid proteins VP1 and VP3. Ampicillin-resistance; plasmid kindly provided by K. Lux

pRC VP2 k.o.-"XN587": Plasmid encoding Rep-Proteins and capsid proteins VP1 and VP3 carrying a targeting insertion at position 587. Ampicillin-resistance; plasmids were generated in this PhD work.

pRGD-4C-587: AAV based helper plasmid containing the AAV2 Rep and Cap ORF like pRC; the RGD4C peptide – ACDCRGDCFCA – is inserted at position N587; Ampicillin-resistance [87]

pXX6-80: Adenoviral helper plasmid encoding for VA, E2A and E4, kindly provided by J. Samulski (University of North Carolina, Chapel Hill, USA); Ampicillin-resistance [165]

2.1.4 Primers

All primers have been purchased from Invitrogen (Karlsruhe, Germany).

Sequencing primer

4066_rev	5' – ATGTCCGTCCGTGTGTGG – 3'

Primers for qPCR

AlasI_fw	5' – CAATCAATTACCCTACGGTG – 3'
AlasI_rev	5' – CAAAATGCAGTGGCCT – 3'
GFP_fw	5' – GCTACCCCGACCACATGAAG – 3'
GFP_rev	5' – GCTCATGCCGAGAGTGATCC – 3'
Luci_fw	5' – CGTGCTGGACTCCTTCATCA – 3'
Luci_rev	5' – TTGCGGACAATCTGGACGAC – 3'
Plat_fw	5' – ACCTAGACTGGATTCGTG – 3'
Plat_rev	5' – AGAGGCTAGTGTGCAT – 3'
wt_fw	5' – GGTACGACGACGATTGCC – 3'
wt_rev	5' – ATGTCCGTCCGTGTGTGG – 3'

Primers for amplification of selected clones

BsiWI_fw	5' – TACCAGCTCCCGTACGTCCTCGGC – 3'
NewSnaBI_rev	5' – CGCCATGCTACTTATCTACG – 3'

2.1.5 Single-stranded oligonucleotides

All single-stranded oligonucleotides were 5'-phosphorylated and purchased from Metabion (Martinsried, Germany).

A2_sense: 5' – C GCG TCC GCG TCT AAC TCG GTG CGA TCG GAC GCG G – 3'
A2_antisense: 5' – CG CGC CGC GTC CGA TCG CAC CGA GTT AGA CGC GGA – 3'
B1_sense: 5' – C GCG TCC GCG AAC GGG ATC CGG AGG TTT GAC GCG G – 3'
B1_antisense: 5' – CG CGC CGC GTC AAA CCT CCG GAT CCC GTT CGC GGA – 3'
C2_sense: 5' – C GCG TCC GCG AAC GGG ATC CGG AGC TTC GAC GCG G – 3'
C2_antisense: 5' – CG CGC CGC GTC GAA GCT CCG GAT CCC GTT CGC GGA – 3'
D5_sense: 5' – C GCG TCC GCG AAG GGC ACC AAG GCG CCC AAG GCG G – 3'
D5_antisense: 5' – CG CGC CGC CTT GGG CGC CTT GGT GCC CTT CGC GGA – 3'

2.1.6 Antibodies

2.1.6.1 Primary antibodies

name	antigen	generated in	clonality	manufacturer
A20	AAV intact capsid	mouse	polyclonal	hybridoma supernatant kindly provided by J. Kleinschmidt, DKFZ Heidelberg, Germany
anti-AKT	AKT	rabbit	polyclonal	Cell Signaling Technologies Inc., Danvers, USA
anti-Lamin B	Lamin B	goat	polyclonal	Santa Cruz Biotechnology Inc., Santa Cruz, USA
anti-Rab5	Rab5	mouse	monoclonal	Santa Cruz Biotechnology Inc., Santa Cruz, USA
B1	C-terminus of VP1, VP2, VP3	mouse	monoclonal	hybridoma supernatant kindly provided by J. Kleinschmidt, DKFZ Heidelberg, Germany

2.1.6.2 Secondary antibodies

Donkey anti-goat IgG-HRP (Santa Cruz Biotechnology Inc., Santa Cruz, USA)

Donkey anti-mouse IgG-HRP (Jackson ImmunoResearch Ltd., Suffolk, UK)

Donkey anti-rabbit IgG-HRP (Jackson ImmunoResearch Ltd., Suffolk, UK)

Donkey anti-goat Cy5 (Dianova, Hamburg, Germany)

Rabbit anti-mouse IgG-biotin (Dianova, Hamburg, Germany)

2.1.7 Bacteria strain

Escherichia coli:

For chemical transformation, the *E. coli* strain DH5α was used.

Genotype: F-, *lac*1-, *rec*A1, *end*A1, *hsd*R17, (*lac*ZYA-*arg*F), U169, F80d*lac*Z_M15, *sup*E44, *thi*-1, *gyr*A96, *rel*A1 [166]

2.1.8 Eukaryotic cell lines

BLM: Human melanoma cells; kindly provided by C. Mauch, Cologne

HEK293: Human embryonic kidney cells, transformed with Ad5 DNA and containing the adenoviral genes *E1a* and *E1b*, American Type Culture Collection (ATCC) CRL-1573 [167]

HeLa: Human epithelial cervix adenocarcinoma cells; ATCC CCL-2 [168]

HepG2: Human epithelial hepatocellular carcinoma cells; ATCC HB-8065 [169]

K-562: Human chronic myelogenous leukemia cells; ATCC CCL-243 [170]

2.1.9 Laboratory equipment and disposables

Product	Company
Balance Adventurer Pro	Ohaus, NJ, USA
Biomax Light Film	Kodak, Stuttgart, Germany
Capillary Light Cycler	Roche, Mannheim, Germany
Cell Culture Plastic Ware	TPP AG, Trasadingen, Switzerland
Centrifuge Z 216 MK	Hermle, Wehingen, Germany
Centrifuge Z 233 M-2	Hermle, Wehingen, Germany
Centrifuge Z 383 K	Hermle, Wehingen, Germany
Centrifuge 5415 D	Eppendorf, Hamburg, Germany
Cell scrapers	Corning Incorporated
CO_2 Incubator MCO-20AIC	Sanyo, München, Germany
Cover slips 10mm	Roth, Karlsruhe, Germany
FACS Calibur	Becton Dickinson, Heidelberg, Germany
FACS tubes	Becton Dickinson, Heidelberg, Germany
General laboratory ware	VWR, Darmstadt, Germany
Heater/Magnetic stirrer Heidolph MR 3001	Heidolph Instruments, Schwabach, Germany
Hera -80ºC freezer	Heraeus/Thermo Fisher Scientific, Germany
HiTrap Heparin Affinity Columns (1ml)	Amersham /GE Healthcare, Freiburg, Germany
Incubator Shaker Multitron Standard	Infors HT, Bottmingen-Basel, Switzerland
Laminar Air Flow BioWizard Golden Line	Kojair, Vilppula, Finland
Laminar Air Flow BioWizard Xtra	Kojair, Vilppula, Finland
LightCycler 480 II	Roche, Mannheim, Germany
Light Cycler plates and foils	Roche, Mannheim, Germany
LightCycler Capillaries	Roche, Mannheim, Germany
LightCycler carousel centrifuge	Roche, Mannheim, Germany
Microscope Olympus CKX41	Olympus, Hamburg, Germany
Mini Sub GT Gel Electrophoresis Unit	BioRad, München, Germany
Mini Trans-Blot Electrophoretic Transfer Cell	BioRad, München, Germany
Nitrocellulose membrane (Hybond ECL)	Amersham/GE Healthcare, Freiburg, Germany
Parafilm	Pechinery Plastic Packaging, Chicago, USA
Pharmacia GeneQuant spectrophotometer	Pharmacia/GE Healthcare, Freiburg, Germany
pH Meter Seven Easy	Mettler-Toledo, Schwerzenbach, Switzerland
Pipettes and Filtertips	Sarstedt, Nümbrecht, Germany
Power Supply	Renner, Dannstadt, Germany
Pump P-1	Amersham/GE Healthcare, Freiburg, Germany
Reaction tubes (1.5ml, 2ml)	Eppendorf, Hamburg, Germany

Reaction tubes (15ml, 50ml)	Sarstedt, Nümbrecht, Germany; Becton Dickinson, Heidelberg, Germany
Scalpels	Feather Safety Razor Co. Ltd., Japan
Sorvall T-865 rotor	Thermo Fisher Scientific, Germany
Sorvall Ultracentrifuge OTD Combi	Thermo Fisher Scientific, Germany
Syringes and Needles	B. Braun Melsungen, Melsungen, Germany
Thermomixer Comfort	Eppendorf, Hamburg, Germany
Ultracentrifuge tubes	Kendro/Thermo Fisher Scientific, Germany
Vortex Genie 2	Scientific Industries, NY, USA
Waterbath Medingen W6	Medingen, Freital, Germany
Whatman filter paper	Schleicher&Schuell, Dassel, Germany

2.1.10 Data treating software

Adobe Photoshop CS4, Chromas Lite, Clone Manager, IrfanView, LightCycler 480 Software 1.5, Microsoft Excel, RelQuant, WinMDI, Zotero, specific software for the respective instruments

2.2 Methods

2.2.1 Bacteria culture

2.2.1.1 Cultivation of bacteria

Bacteria were grown in LB medium at 37°C over night while vigorously shaking. For growing bacteria on plates, 15g/l Agar was added to LB medium for solidification. For transformed bacteria with resistance to Ampicillin or Kanamycin, 100mg/l Ampicillin or 50mg/l Kanamycin was added to the medium.

LB medium: 10g Peptone/Tryptone

5g Yeast extract

10g NaCl

15g agar (for plates)

ad 1l distilled H_2O

2.2.1.2 Preparation of chemically competent bacteria

The bacteria strain DH5α was grown at 37°C on vigorous shaking (200rpm) over night in 8 ml of LB medium. Ten hours later, 4ml of this culture were transferred into 400ml of LB medium and bacteria were grown to an optical density (OD_{590}) of 0.4. Cultured bacteria were divided in two parts and incubated on ice for 10min followed by centrifugation at 1600xg for 7 min at 4°C. Each pellet was carefully resuspended in 40ml ice-cold sterilized $CaCl_2$ solution followed by centrifugation at 1100xg for 5min at 4°C. Pellets were resuspended as described before and incubated on ice for 30min followed by centrifugation at 1100xg for 5min at 4°C. Each pellet was carefully resuspended in 8ml ice-cold $CaCl_2$ solution. After pooling the two parts, 100µl aliquots of the chemically competent bacteria were immediately shock-frozen in liquid N_2 and stored at –80°C.

$CaCl_2$ solution: 60mM $CaCl_2$

10mM PIPES (pH 7.0)

15% Glycerol (v/v)

2.2.1.3 Transformation of bacteria

Competent bacteria were slowly thawn on ice. After adding 100µl of competent bacteria to the transforming DNA (100–500ng) carrying Ampicillin or Kanamycin resistance, the suspension was mixed and incubated on ice for 30min. Then, the suspension was incubated for 45sec at 42ºC followed by an incubation on ice for 2min. One ml of LB medium was added and the mixture shaken at 200rpm and 37ºC for 30-60min. Bacteria were distributed

on LB agar plates already containing Ampicillin (100µg/ml) or Kanamycin (50µg/ml). Plates were incubated over night at 37ºC. The next day, a single colony was picked from the plate, grown as described before and analyzed.

2.2.2 Working with nucleic acids

2.2.2.1 Plasmid amplification and extraction

For plasmid amplification and extraction, the Qiagen EndoFree Plasmid Mega Kit was used according to the manufacturer's instructions.

2.2.2.2 DNA and RNA quantification

DNA and RNA samples were diluted in H_2O before they were measured in a Pharmacia GeneQuant spectrophotometer. Samples were measured at a wavelength of 260nm and 280nm. Purity of the nucleic acid preparation is given by the ratio Abs 260nm / Abs 280nm. DNA of high purity has a ratio of 1.8, lower values point to contaminations with proteins and aromatic substances, whereas higher ratios indicate possible contaminations with RNA.

2.2.2.3 Restriction enzyme digest

Digestion with restriction enzymes was performed according to the manufacturer's instructions in a final volume of 20µl containing 1µg of DNA, 1-10 units of restriction enzyme per 1µg DNA and 1x buffer.

2.2.2.4 Agarose gel electrophoresis and gel extraction

Restriction enzyme digests as well as PCR products were analyzed by agarose gel electrophoresis to verify the size of the fragments or PCR products.

1x TBE buffer was boiled with the desired amount of agarose (0.7% to 2%, depending on fragment size) and mixed with the DNA intercalating substance ethidium bromide (0.1µg per 1ml gel volume). Electrophoresis was performed at 80V and 200mA in 1x TBE buffer.

TBE Buffer (10x):   540g Tris base
                     275g boric acid
                     200ml 0.5M EDTA pH 8.0
                     ad 5l H_2O

Extraction of DNA fragments or PCR products from agarose gels was performed using the Qiagen Gel Extraction Kit according to the manufacturer's instructions.

2.2.2.5   DNA extraction from animal cells

DNA was extracted from animal cells using the Qiagen DNeasy Blood & Tissue Kit following the protocol for "Purification of Total DNA from Animal Blood or Cells" according to the manufacturer's instructions and eluted in 100µl 10mM Tris/HCl pH 8.5.

2.2.2.6   RNA extraction from animal cells and DNase I digest

RNA was extracted from animal cells using the Qiagen RNeasy Mini Kit following the protocol for "Purification of Total RNA from Animal Cells" according to the manufacturer's instructions and eluted in 30µl sterile H_2O.

The "On-column DNase Digestion with the RNase-free DNase Set" (Qiagen) was included in the RNA extraction protocol according to the manufacturer's instructions.

2.2.2.7   cDNA synthesis

cDNA synthesis from 8µl total RNA (2.2.2.6) was performed using the SuperScript^TM III First-Strand Synthesis SuperMix for qRT-PCR (Invitrogen) according to the manufacturer's instructions.

2.2.2.8   Polymerase chain reaction (PCR)

Viral DNA obtained after the third selection round (2.2.6.2) was amplified for subsequent cloning into the AAV helper plasmid pRC"Kotin". Using the primers BsiWI_fw and NewSnaBI_rev and the below described reaction conditions, a 1.2kb fragment surrounding the targeting insertion at amino acid position 587 (corresponding to nucleotides 6018-6020 in the Cap ORF) from nt 5311 to nt 6532 was amplified.

PCR reaction mix:
      5µl template DNA
      2µl dNTPs (10mM)
      10µl 5xPhusion reaction buffer
      2µl BsiWI_fw (10µM)
      2µl New SnaBI_rev (10µM)
      0.5µl Phusion^TM DNA Polymerase
      ad 50µl H_2O

PCR cycling program:

Denaturation	30 sec	98°C
Denaturation	10 sec	98°C
Annealing	30 sec	56°C
Elongation	40 sec	72°C
Final elongation	10 min	72°C
Final hold	hold	4°C

The Denaturation, Annealing and Elongation steps are repeated 35x.

2.2.2.9   Quantitative PCR (qPCR)

Quantitative PCR was performed to determine either the genomic titer of rAAV vector stocks (absolute quantification) or the amount of DNA or cDNA in a sample (relative quantification of target versus reference gene). In case of absolute quantification, absolute standards were included in the qPCR reaction. For relative quantification, a calibrator standard curve was generated for normalization of target versus reference value. For reasons of accuracy, the calibrator standard curve was prepared by serial dilution (1:5, 1:10, 1:50, 1:100) of the sample with the highest expected amount of target gene. Relative quantification was carried out using the RelQuant software for Capillary LightCycler or the LightCycler® 480 Software 1.5 for LightCycler® 480 II.

The Light Cycler System (LightCycler® 480 II or Capillary LightCycler, both from Roche) and the appropriate kit (LightCycler® 480 SYBR Green Master for LightCycler® 480 II, LightCycler® FastStart DNA Master SYBR Green I for Capillary LightCycler) was chosen depending on amount of samples and type of analysis.

2µl of DNA or cDNA was put per reaction. For determination of genomic titer of AAV vector preparations, 2µl of the extracted DNA was analyzed.

Pipetting scheme using LightCycler® Fast Start DNA Master SYBR Green I:

2µl template DNA

1µl Primer fw (20µM)

1µl Primer rev (20µM)

4µl Mix (including FastStart Taq DNA Polymerase, reaction buffer, dNTP mix, SYBR Green I dye and $MgCl_2$)

ad 20µl H_2O

Pipetting scheme using LightCycler® 480 SYBR Green Master:

>2µl template DNA
>
>1µl Primer fw (20µM)
>
>1µl Primer rev (20µM)
>
>10µl Mix (including FastStart Taq DNA Polymerase, reaction buffer, dNTP mix, SYBR Green I dye and MgCl$_2$)
>
>ad 20µl H$_2$O

Using the below-mentioned qPCR cycling program, genomic titers were determined for rAAV vector preparations carrying either GFP or Luciferase as transgene. The same program was used to analyze transduced cells with regard to vector DNA or vector transcripts (GFP), the single-copy gene Plat (exon priming on genomic DNA) and the single-copy transcript AlasI (exon priming on cDNA). Specificity of PCR products was assured by melting peak analysis.

qPCR cycling program:

Program	Cycles	Analysis Mode	Target (°C)	Acquisition Mode	Hold (hh:mm:ss)	Ramp Rate (°C/s)	Acquisitions (per °C)
Denaturation	1	None	95	None	00:05:00	4.4	
Amplification	40	Quantification	95	None	00:00:15	4.4	
			60	None	00:00:10	2.2	
			72	Single	00:00:20	4.4	
Melting	1	Melting Curve	95	None	00:00:01	4.4	
			68	None	00:00:15	2.2	
			95	Continous			5
Cooling	1	None	40	None	00:00:30	2.2	

Genomic titers of the AAV peptide display library and the progeny of each selection round were determined using the wild-type AAV (wtAAV) qPCR cycling program.

wtAAV qPCR cycling program:

Program	Cycles	Analysis Mode	Target (°C)	Acquisition Mode	Hold (hh:mm:ss)	Ramp Rate (°C/s)	Acquisitions (per °C)
Denaturation	1	None	95	None	00:15:00	4.4	
Amplification	40	Quantification	95	None	00:00:10	4.4	
			60	None	00:00:03	2.2	
			72	Single	00:00:35	4.4	
Melting	1	Melting Curve	95	None	00:00:01	4.4	
			68	None	00:00:10	2.2	
			95	Continous			5
Cooling	1	None	40	None	00:00:30	2.2	

2.2.2.10   Sequencing

Sequencing of single DNA clones was carried out in an ABI 3730 Sequencer at the Cologne Center for Genomics, University of Cologne, Germany. For the sequencing reaction, the BigDye® Terminator v3.1 Cycle Sequencing Kit (Applied Biosystems) was used.

Sequencing reaction mix:

    200ng template DNA
    0.5µl 10xBuffer
    0.5µl Primer 4066 (10pmol/µl)
    1µl BigDye v3.1
    ad 5µl H_2O

PCR cycling program:

Denaturation	2 min	94°C	
Denaturation	20 sec	94°C	
Annealing	30 sec	50°C	25x
Elongation	4 min	60°C	
Final elongation	4 min	60°C	
Final hold	hold	4°C	

2.2.2.11   Molecular Cloning

2.2.2.11.1 Cloning amplified viral DNA

100ng of vector backbone (pRC"Kotin" plasmid, digested with SnaBI and BsiWI and dephosphorylated) was mixed with a 5-fold excess of insert (purified PCR product (2.2.2.8), digested with SnaBI and BsiWI). The amount of insert was calculated using the equation weight$_{fragment}$[ng] = 5 x weight$_{vector}$[ng] x length$_{fragment}$[bp] / length$_{vector}$[bp]. T4 ligation mix containing reaction buffer and 5 Weiss units of T4 DNA Ligase was added. The reaction mixture was incubated at 16°C over night and transformed into chemically competent bacteria (2.2.1.3). Sequencing of bacterial clones was performed using Primer 4066 (Qiagen Sequencing Services, Hilden, Germany) after picking single colonies of the plated cultures.

2.2.2.11.2 Re-cloning viral insertion sequences

The plasmids pRC99-A2, pRC99-B1, pRC99-C2 and pRC99-D5 were generated by sticky-end ligation of double-stranded oligonucleotides containing the respective sequences of A2, B1, C2 and D5 (2.1.5) into pRC99 vector backbone (previously digested with MluI and AscI and dephosphorylated). Briefly, annealing of 50µg sense oligonucleotide and 50µg antisense oligonucleotide was performed in 150mM NaCl and 10mM Tris/HCl pH 7.4. Initial heating of

the reaction mix for 3min at 95°C was followed by cooling down over night to allow nucleic acid hybridization. The resulting double-stranded oligonucleotide displayed 5' and 3' sticky ends complementary to the cohesive ends of the MluI- and AscI-cut pRC99 backbone. Ligation and transformation into chemically competent bacteria was performed as described before (2.2.1.3, 2.2.2.11.1).

2.2.2.11.3 Cloning GFP-tagged rAAV peptide insertion mutants

An 800 bp fragment surrounding the specific peptide insertions of the vectors A2, B1, C2 and D5 at amino acid (aa) position 587 (corresponding to nt 6020 in the Cap ORF) from nt 5311 to 6063 was cut from the pRC99 plasmids using BsiWI and XcmI. The fragments were cloned into peGFP-VP2.2 and pRC VP2 k.o. (both previously cut with BsiWI and XcmI and dephosphorylated) in order to generate vectors displaying the peptide ligand in the common VP3 region of all three capsid proteins and, in addition, having a genetically fused GFP-tag at the N-terminus of VP2. Ligation and transformation into chemically competent bacteria was performed as described before (2.2.1.3, 2.2.2.11.1).

2.2.3 Working with proteins

2.2.3.1   Protein extraction from HeLa cells

$1x10^6$ cells – previously washed with 1x PBS and trypsinized – were pelleted at 500xg for 5min. The supernatant was discarded, the pellet was washed with 1x PBS and centrifuged again. As before, the supernatant was discarded, the pellet was resuspeded in 200µl ice-cold RIPA buffer and incubated on ice for 30min. Then, the lysate was centrifuged at 16000xg for 30min at 4°C. The supernatant containing the extracted proteins was transferred to a clean tube and stored at –80°C.

RIPA buffer: 0.5% DOC
                    0.1% SDS
                    150mM NaCl
                    50mM Tris pH 8.0
                    1% NP-40

2.2.3.2   Acetone precipitation of proteins

To concentrate and desalt protein samples, four volumes of ice-cold acetone were added to the sample followed by 15min incubation on ice and centrifugation at 12000xg for 10min at 4°C. The supernatant was discarded and the pellet air-dried. Then, the pellet was resuspended in 100-200µl 1x PBS and stored at –80°C.

2.2.3.3   Western Blot

Western blot analysis was performed on protein extracts from whole cells or subcellular fractions or on iodixanol gradient purified vector preparations.

Laemmli buffer was added to the samples followed by incubation at 95ºC for 5min. 20µl of each subcellular fraction and whole cell extract or 5×10^{10} vector capsids were loaded. A 5% stacking gel was used, whereas the percentage of the running gel was chosen according to the size of the proteins that should be detected. Electrophoresis was performed at 80-100V in 1x running buffer.

After protein separation by SDS-PAGE the proteins were transferred to a nitrocellulose membrane (Hybond-ECL (Amersham Bioscience)) using a "BioRad Mini Trans-Blot Electrophoretic Transfer Cell" according to the manufacturer's instructions. Blotting was performed over night at 20mA.

After blotting, the membrane was blocked for 60min using 5% milk powder and 0.1% Tween 20 in 1x PBS shaking at room temperature. The blocking solution was substituted with the primary antibody in a suitable dilution (B1 (1:10), anti-Akt (1:1000), anti-Lamin B (1:500), anti-Rab5 (1:1000)) and left for 60min shaking at room temperature. After three washing steps with 0.1% Tween 20 in 1x PBS shaking for 5min at room temperature, the solution on the membrane was replaced by the secondary antibody (anti-mouse IgG-HRP diluted 1:2000-1:5000 in blocking buffer, anti-goat IgG-HRP and anti-rabbit IgG-HRP 1:2000) and left for 60min shaking at room temperature. After three washing steps like before, 0.125ml/cm^2 membrane of substrate solution for the peroxidase-conjugated secondary antibody (Western Lightning™ Chemiluminescence Reagent Plus (PerkinElmer)) was added to the membrane. After removing the substrate solution, a radiographic film was exposed to the membrane and subsequently the film was developed.

Laemmli buffer (6x): 60mM Tris pH 6.8

                9.3mg/ml DTT (Dithiothreitol)

                12% SDS

                47% Glycerol (v/v)

                0.6mg/ml Bromophenol Blue

Running buffer: 25mM Tris Base

                192mM Glycin

                0.1% SDS

Transfer buffer pH 8.3:   0.30% Tris Base

1.44% Glycin

0.02% SDS

5% stacking gel (2ml):   1.4ml distilled water

0.33ml acrylamide stock solution, 30% (w/v)

0.25ml 1.0M Tris (pH 6.8)

0.02ml 10% sodium dodecyl sulfate (SDS)

0.02ml 10% ammonium persulfate (APS)

2μl N,N,N,N-Tetramethylethylenediamine (TEMED)

8% resolving gel (5 ml):   2.3ml distilled water

1.3ml acrylamide stock solution, 30% (w/v)

1.3ml 1.5M Tris (pH 8.8)

0.05ml 10% SDS

0.05ml 10% APS

3μl TEMED

12% resolving gel (5 ml):   1.6ml distilled water

2.0ml acrylamide stock solution, 30% (w/v)

1.3ml 1.5M Tris (pH 8.8)

0.05ml 10% SDS

0.05ml 10% APS

2μl TEMED

2.2.3.4   ELISA

To determine the capsid titer of rAAV vector preparations, an ELISA was performed using the anti-capsid antibody A20.

AAV capsid standard and samples (diluted in 100μl 1x PBS) and 100μl 1x PBS (negative control) were pipetted separately into a 96-well plate. Eight serial dilutions were prepared of all samples to obtain concentrations in a linear range. The plate was sealed with parafilm and incubated over night at 4°C.

The next day, the contents of the plate were discarded, each well was filled with 200μl washing buffer, incubated for 5sec and emptied again. This washing step was repeated nine times. Afterwards, the wells were incubated with 200μl blocking buffer for 1h at room temperature. Then, wells were incubated with 100μl of anti-capsid antibody A20 (diluted 1:10 in blocking buffer) for 1h at room temperature. Three washing steps were repeated as

described above. The secondary antibody (anti-mouse IgG-biotin, diluted 1:25000 in blocking buffer) was pipetted into each well and incubated for 1h at room temperature. Another three washing steps were performed as described before and 100µl of streptavidin peroxidase conjugate (diluted 1:500 in blocking buffer) were pipetted into each well and incubated for 1h at room temperature. After another three washing steps and two additional washing steps with 200µl of distilled water, 100µl of substrate solution were added into each well. Incubation was performed for 5-15min at room temperature. Colour reaction was then stopped by adding 50µl of 1M H_2SO_4 into each well and the intensity of the colour reaction was measured at 450 nm using a photometer.

Washing buffer: 0.05% Tween 20 in 1x PBS

Blocking Buffer: washing buffer containing 3% BSA and 5% sucrose

Substrate solution: 1mg TMB (3,3', 5,5'-Tetramethylbenzidine)
100µl DMSO
10ml 0.1M NaOAc pH 6.2
1µl 30% H_2O_2 (added just before use)

2.2.4 Eukaryotic cell culture

2.2.4.1 Cultivation of cells

HeLa, HEK293 and HepG2 were maintained in Dulbecco`s modified Eagle`s medium (DMEM) with GlutaMAX^{TM}-I, supplemented with 10% fetal calf serum, 100 U/ml penicillin, 100 mg/ml streptomycin. BLM and K-562 were maintained in RPMI-1640 medium with GlutaMAX^{TM}-I, supplemented with 10% fetal calf serum, 100U/ml penicillin, 100mg/ml streptomycin. All cell lines were maintained in a humidified incubator with 5% CO_2 at 37°C.

2.2.4.2 Drug treatment

Chlorpromazine (10µg/ml final concentration) or Genistein (200µM final concentration) was used to inhibit clathrin- or caveolin-mediated endocytosis. Bafilomycin A_1 (100nM final concentration) is a specific inhibitor of the vacuolar ATPase and was used to inhibit endosomal maturation. MG-132 (carbobenzoxy-Leu-Leu-leucinal, 10µM final concentration) was used to inhibit the 26S proteasome. All drugs were added to cells 30min prior to transduction and remained present until transduction was stopped by washing or trypsin treatment.

2.2.4.3   Trypsin treatment

Cells were washed with PBS, then trypsin (0.5g/l) was added in an amount that covered the bottom of the plate or flask, followed by an incubation at 37ºC (time depending on the cell line). When the cells detached from the plate, reaction was stopped by adding medium containing 10% FCS.

2.2.4.4   Counting, seeding and passaging

After washing and trypsin treatment, cells were either passaged or seeded. For passaging, cells were diluted 1:10 in a new flask containing fresh medium pre-warmed to 37°C. Slight agitation of the flask should ensure homogenous distribution of the cells. Prior to seeding, cells were counted. 10µl of diluted cells were transferred into a "Neubauer" chamber. The number of cells in each of the four squares (n) was counted and an average was built for more precise determination. The amount of cells in 1ml equals n x 10^4 x dilution factor. Cells were suspended in fresh medium, pre-warmed to 37°C, and homogenously distributed.

2.2.4.5   Freezing and thawing cells

Cells were trypsinized and pelleted at 500xg before resuspending them in freezing solution containing 90% FCS and 10% DMSO. Approximately $1x10^6$ cells per 1ml suspension were added to each freezing vial. Immediately, the suspension was put on ice and then transferred to -80°C in an isopropanol containing freezing carrousel. The next day, cells were transferred to liquid nitrogen.

For thawing cells, the freezing vial was taken out of the liquid nitrogen tank and transported on ice. Carefully, the suspension was thawed in a water bath at 37°C and the cells were transferred into a 50ml plastic tube containing pre-warmed medium before pelleting the cells at 500xg for 5min at room temperature in order to remove toxic DMSO. After resuspension in fresh medium, the cells were plated in culture dishes.

2.2.4.6   DAPI staining

HeLa cells seeded on 12mm coverslips inside 24-well plates were washed twice with 1x PBS. 4′,6-Diamidino-2-phenylindol (DAPI) was dissolved in sterile H_2O at a concentration of 1mg/ml. DAPI-solution was diluted to a final concentration 1µg/ml in methanol and distributed on the cells. Cells were incubated in the dark for 10-15min, then DAPI-solution was removed and cells were washed twice with 1x PBS. After embedding the cover slips in Vectashield mounting medium, samples were analyzed at a wavelength of 360nm using a fluorescence microscope.

2.2.5 Vector production and purification

2.2.5.1 AAV vector packaging

AAV particles were produced in HEK293 cells by the adenovirus-free production method using pXX6-80 to supplement the adenoviral helper functions [165].

Briefly, 7.5×10^6 HEK293 cells were seeded in $15cm^2$ cell culture plates. Twenty-four hours later, at an approximate confluence of 80%, medium was exchanged. Two hours afterwards, co-transfection was performed using the calcium phosphate method. Depending on the desired vector type, the following plasmids were used per $15 cm^2$ cell culture plate:

For rAAV2 and rAAV peptide insertion mutants:

7.5µg AAV helper plasmid (pRC, pRC99-A2, pRC99-B1, pRC99-C2 or pRC99-D5)

7.5µg pGFP

22.5µg pXX6-80

For GFP-tagged rAAV peptide insertion mutants:

7.5µg pRC VP2 k.o.-A2 (or pVP2k.o.-B1, pVP2k.o.-C2, pVP2k.o.-D5)

7.5µg peGFP VP2.2-A2 (or peGFP VP2.2-B1, peGFP VP2.2-C2, peGFP VP2.2-D5)

7.5µg pLuci

22.5µg pXX6-80

For each plate, 1ml $CaCl_2$ (250mM) was mixed with the plasmid DNA, then 1ml HBS buffer (50mM HEPES, 280mM NaCl, 1.5mM NaP) was dropped onto the solution, incubated for 2min and pipetted onto the plate while cautiously mixing with the medium. After 24h incubation at 37°C/ 5% CO_2, medium was exchanged with DMEM containing only 2% FCS to reduce further cell division activity. The transfected cells were harvested and pelleted by low-speed centrifugation on the following day (48h post transfection). The pellet was resuspended in lysis buffer (150mM NaCl, 50mM Tris-HCl (pH 8.5)) and the cellular and nuclear membranes were destroyed by repeated freeze and thaw cycles. To abolish genomic and plasmid DNA or RNA contaminants in the vector preparation, the suspension was treated with 50U/ml Benzonase for 30min at 37°C. Then, the suspension was centrifuged at 3220xg for 30min at 4°C. The supernatant was taken off carefully and centrifuged again as mentioned before.

2.2.5.2 Iodixanol gradient purification

Discontinuous iodixanol gradient centrifugation was used to remove cellular debris. Full capsids were concentrated in the 40% phase of the iodixanol gradient. Vector suspension was inserted into an ultracentrifugation tube. The different phases of the iodixanol gradient -

starting with 15% - were sub-layered using a syringe connected to an Amersham Biosciences Pump P-1. 8ml, 6ml, 5ml and 6ml of the respective solutions were applied to a 35ml ultracentrifugation tube. The tube was filled with PBS/MgCl$_2$ (1mM)/KCl (2.5mM), closed and centrifuged at 63000rpm for 2h at 4°C (Sorvall Ultracentrifuge OTD Combi). Subsequently, the 40% iodixanol phase was harvested.

	15%	25%	40%	60%
10x PBS	5ml	5ml	5ml	-
1M MgCl$_2$	50µl	50µl	50µl	50µl
2.5M KCl	50µl	50µl	50µl	50µl
5M NaCl	10ml	-	-	-
Optiprep	12.5ml	20ml	33.3ml	50ml
0.5% Phenolred	75µl	75µl	-	25µl
H$_2$O	ad 50ml	ad 50ml	ad 50ml	ad 50ml

2.2.5.3   Vector titration

For extraction of the vector genome from viral particles, the DNeasy Blood & Tissue Kit (QIAGEN) was used according to the protocol for "Isolation of Total DNA from Cultured Animal Cells". Starting with 10µl of the vector preparation mixed with 190µl PBS, DNA was finally eluted in 200µl 10mM Tris/HCl pH 8.5.

The genomic titer was then determined by qPCR as described before (2.2.2.9). To quantify the amount of vector genomes within the extracted DNA, defined dilutions ($1x10^8$ to $1x10^5$ genomic particles (g.p.)/µl) of the respective transgene-encoding plasmid were prepared and used as absolute standards in the qPCR.

2.2.6   Selection of rAAV peptide insertion mutants

2.2.6.1   Heparin affinity chromatography

Prior to selection, the coupled AAV peptide display library was divided into an HSPG-binding and HSPG-non-binding fraction by heparin affinity chromatography. Using the Amersham Biosciences Pump P-1, a HiTrap Heparin Affinity Column was equilibrated with 1x PBS/ MgCl$_2$ (1mM)/ KCl (2.5mM) (abbrev. PBS M/K). Two ml of AAV peptide display library were diluted 1:3.5 with PBS M/K and applied to the column. The flow-through was collected and applied again after washing the column with PBS M/K. The flow-through was collected again and designated "HSPG-non-binder library". After another washing with PBS M/K the Heparin-bound particles were eluted with PBS M/K containing 1M NaCl. The eluate was designated "HSPG-binder library". Subsequently, both fractions were concentrated by discontinuous iodixanol gradient centrifugation and the genomic titer was determined as described before (2.2.5.2, 2.2.5.3).

2.2.6.2   Selection of rAAV peptide insertion mutants on K-562 cells

Selection procedure was carried out according to a protocol established in our laboratory [171]. $7.5x10^6$ K-562 cells were seeded in $75cm^2$ flasks and transduced with 10^3 genomic particles of HSPG-non-binder library. Separately, $7.5x10^6$ K-562 cells were transduced with 10^3 genomic particles of HSPG-binder library. Two hours post transduction, AAV was removed; cells were washed twice with PBS, resuspended in RPMI-1640 and superinfected with 10µl of wild-type adenovirus type 5 (wtAd5). Two hours post infection, wtAd5 was removed from the cells and cells were washed like before. Cells were maintained in RPMI-1640 for 48h at 37°C. Fourty-eight hours post infection, cells were harvested, resuspended in 300µl lysis buffer (150mM NaCl, 50mM Tris-HCl (pH 8.5)) and viral progeny was obtained by three cycles of freeze and thaw. Adenovirus was heat-inactivated at 60°C for 30min. After each selection round, the genomic titer of these preparations was monitored by qPCR using the wtAAV protocol (2.2.2.9) and the preparations were used for further selection rounds. Selection pressure was raised by reducing the initial amount of virus applied to the cells from 1000g.p./cell in the first selection round to 10g.p./cell in the second selection round to 1g.p./cell in the third selection round.

2.2.7   Cell transduction by rAAV vectors

2.2.7.1   Quantification of vector entry efficiency

Twenty-four hours prior to transduction, cells were seeded sub-confluently in 12-well plates. Cells in one well were counted before cells were incubated with rAAV2 or rAAV peptide insertion mutants in 500µl of medium. To allow vector binding, 60min incubation on ice was performed before cells were shifted to 37°C and 5% CO_2. Cells were harvested at different points in time. The supernatant was removed and cells were washed with 1x PBS. Then, cells were extensively treated with trypsin to ensure the removal of membrane-bound vector particles and to detach cells from the plate as previously described [9],[10],[172]. Cells were pelleted at 500xg for 5min, washed twice with 1x PBS and total DNA was isolated as described before (2.2.2.5). Relative quantification of vector genomes (GFP) and reference gene (Plat) was performed by qPCR as previously depicted (2.2.2.9).

2.2.7.2   Quantification of vector genome transcripts

Twenty-four hours prior to transduction, cells were seeded sub-confluently in 12-well plates. Cells in one well were counted before cells were incubated with rAAV2 or rAAV peptide insertion mutants as described above (2.2.7.1). One hour p.t., medium was changed to DMEM containing 3% anti-capsid antibody A20 in order to prevent so far unbound vector particles from binding to the cell. At different points in time, cells were harvested by removing

the supernatant, washing twice with 1x PBS and lysing the cells in buffer ATL (component of the Qiagen RNeasy Mini Kit) containing 1% β-mercaptoethanol. Total RNA was extracted and cDNA was synthesized as described before (2.2.2.6, 2.2.2.7). Relative quantification of vector genome transcripts (GFP) and reference transcript (AlasI) was performed by qPCR as previously depicted (2.2.2.9).

2.2.7.3 Cell transduction assay

Twenty-four hours prior to transduction, cells were seeded sub-confluently in 12-well plates. Cells in one well were counted before cells were incubated with rAAV2 or rAAV peptide insertion mutants as described above (2.2.7.1). In case of Chlorpromazine, Bafilomycin or Genistein treatment, transduction was stopped after 2h by washing with 1x PBS, trypsin treatment and re-seeding the transduced cells in fresh medium. Cells treated with MG-132 were washed with 1x PBS 4h p.t. and fresh medium was added. If the experiment was performed with adjusted intracellular vector particles, with the exception of MG-132 treatment, medium was changed to DMEM containing 3% anti-capsid antibody A20 1h p.t. to avoid further cell entry of vector particles. Twenty-four hours p.t., cells were harvested, washed and resuspended in 1x PBS. Since the vectors used for transduction carried GFP as a transgene, the percentage of transduced, GFP-expressing cells was determined by flow cytometry using a BD FACS Calibur system. According to the wavelength of GFP, samples were measured in the FITC channel. A minimum of 5000 cells was counted for each sample. Background fluorescence was set to 1%.

2.2.7.4 Heparin competition assay

Twenty-four hours prior to transduction, cells were seeded sub-confluently in 12-well plates. Cells in one well were counted and rAAV vectors were incubated with concentrations between 0.02 IU/ml and 400 IU/ml of soluble Heparin (25000IU/ml) in 500µl of medium for 30min at room temperature. Then, the mixture was applied to the cells. Twenty-four hours p.t., cells were harvested, washed and resuspended in 1x PBS. The percentage of GFP-expressing cells was determined by flow cytometry as described before (2.2.7.3).

2.2.7.5 Quantification of vector genomes in subcellular fractions

Twenty-four hours prior to transduction, HeLa cells were seeded sub-confluently in 10 cm^2 cell culture plates. Cells in one plate were counted before cells were incubated with rAAV2 or rAAV peptide insertion mutants as described above (2.2.7.1). One hour p.t., medium was changed to DMEM containing 3% anti-capsid antibody A20 in order to prevent so far unbound vector particles from binding to the cell. Two hours p.t., cells were harvested. The supernatant was removed and cells were washed with 1x PBS. Then, cells were extensively

treated with trypsin to remove membrane-bound vector particles and to detach cells from the plate. Cells were pelleted at 500xg for 5min and washed twice with 1x PBS. Then, subcellular fractionation was performed using the Qproteome Cell Compartment Kit (QIAGEN) according to the protocol for "Subcellular Fractionation of Cultured Cell Sampes". Briefly, cells were resuspended in cytosol extraction buffer. After centrifugation, the supernatant was collected as the cytosolic fraction. The pellet was resuspended in membrane extraction buffer to separate the membrane fraction in the supernatant. The pellet was further resuspended in nuclear extraction buffer. Benzonase treatment was not performed like in the manufacturer's protocol to maintain non-denaturating conditions for free vector genomes inside the nucleus. After centrifugation, the supernatant was collected as the nuclear fraction. The fractions were divided for further analysis of DNA and protein. 200µl of the cytosolic, membrane and nuclear fraction were used to extract DNA as described before (2.2.2.5). Prior to DNA extraction, 2µg of pLuci plasmid DNA was added to each fraction to monitor the accuracy of downstream procedures. Relative quantification of vector genomes (GFP) and reference gene (Luciferase) was performed by qPCR as previously depicted (2.2.2.9). To determine the purity of fractionation, proteins were concentrated from the fractions put aside for protein analysis using acetone precipitation (2.2.3.2). Subsequently, proteins from the cytosolic, membrane and nuclear fractions or from total HeLa cell lysat were analyzed by SDS-PAGE and western blot (2.2.3.3).

2.2.7.6 Immunoflourescence assay of fluorescent-protein-tagged rAAV vectors

Twenty-four hours prior to transduction, $4x10^4$ HeLa cells were seeded onto 12mm coverslips inside 24-well plates. Cells in one well were counted before cells were incubated with $5x10^6$ capsids/cell of the respective fluorescent-protein-tagged vectors. To allow vector binding, 60min incubation on ice was performed before cells were shifted to 37°C and 5% CO_2. Four hours p.t., cells were washed twice with 1x PBS and fixed for 15min with 3% PFA in 1x PBS at room temperature. To quench remaining PFA, cells were washed with 50mM NH_4Cl in 1x PBS and incubated with 50mM NH_4Cl in 1x PBS for 30min at room temperature. Then, cells were washed twice with 1x PBS and permeabilized with 0.2% Triton X 100 in 1x PBS for 5min at room temperature. After four washing steps with 1x PBS, samples were incubated with 0.2% gelatine in 1x PBS for 10min at room temperature to prevent unspecific binding of antibody. Incubation with the primary antibody (anti-Lamin B, diluted 1:50 in 0.2% gelatine in 1x PBS) was carried out for 1h at room temperature. After washing and blocking as described before, cells were incubated at room temperature for 1h with the secondary antibody (anti-goat Cy5, diluted 1:50 in 0.2% gelatine in 1x PBS). Cells were washed again with 1x PBS, then, the cover slips were embedded in Vectashield mounting medium (Alexis) and examined using a confocal microscope (OLYMPUS FluoView FV1000).

2.2.8 Statistical analysis

To test for statistical significance, unpaired Student's t-test was performed. Two means or two groups of samples were defined as "significantly" different, if P was smaller than 0.05. In this case, the probability that the difference between to means or two groups of samples is due to chance is smaller than 5% and the probability that two means or two groups of samples are in fact "significantly" different is higher than 95%. Three gradations were used in this work to illustrate the magnitude of significance: ***:P<0.0005; **:P<0.005; *:P<0.05.

3 Results

3.1 Selection of AAV peptide insertion mutants on K-562 cells

A previous study revealed that AAV peptide display carried out on HeLa cells results primarily in the selection of HSPG-binder mutants [Dissertation D. Goldnau, 2006]. In order to perform the proposed analysis, however, HSPG-binder and HSPG-non-binder mutants were required. Therefore, a cell line expressing only low levels of HSPG, the human chronic myelogenous leukemia cell line K-562 [92] was chosen as target for AAV peptide display selections.

Prior to selection, the AAV peptide display library was coupled (PCT/EP2008/004366). This step is necessary to match the genotype with the phenotype of viral particles in the library. To carry out separate selections with a pool of AAV mutants, which are able to bind to HSPG, and a pool of AAV mutants enriched for non-HSPG-binding mutants, the coupled AAV display library was divided into a HSPG-binder and a HSPG-non-binder fraction by heparin affinity chromatography prior to selection (2.2.6.1). The genomic titers of the HSPG-binder and HSPG-non-binder library were determined by qPCR and are indicated in Table 1.

Three selection rounds on K-562 cells were performed with increasing selective pressure (2.2.6.2). Briefly, in the first selection round, K-562 cells were infected with 10^3 genomic particles (g.p.)/cell of HSPG-non-binder library and of HSPG-binder library, respectively. Helper virus fuction was provided by super infection with adenovirus 2h post AAV infection. Viral progeny was harvested, the genomic titer was measured by qPCR and the viral preparation was subjected to the next selection round. The second and third selection rounds were carried out exactly as described above with the exception that selection pressure was raised by reducing the virus to cell ratio from 1000 g.p./cell to 1 g.p./cell in the third selection round. As summarized in Table 1, viral progeny was produced in all three selection rounds. During the first selection round, progeny production with the HSPG-binder library was higher than with the HSPG-non-binder library (187-fold and 48-fold, respectively). The highest yield in viral progeny was obtained for both libraries in the second selection round, in which the selective pressure had been strongly raised (960-fold with HSPG-binder library, 1280-fold with HSPG-non-binder library). Comparing the viral yield again after the third selection round, the HSPG-binder library was more effective than the HSPG-non-binder library (307-fold and 240-fold, respectively).

Table 1: Overview of the selection procedure

Selection round	library	Genomic titer per µl	Number of cells	g.p./cell	Total viral particles („ancestors")	Total viral particles (progeny)	Progeny production (x-fold)
0	NB	3.7×10^7					
	B	1.8×10^9					
1	NB	1.2×10^9	7.5×10^6	1000	7.5×10^9	3.6×10^{11}	48
	B	4.7×10^9	7.5×10^6	1000	7.5×10^9	1.4×10^{12}	187
2	NB	3.2×10^8	7.5×10^6	10	7.5×10^7	9.6×10^{10}	1280
	B	2.4×10^8	7.5×10^6	10	7.5×10^7	7.2×10^{10}	960
3	NB	6.1×10^6	7.5×10^6	1	7.5×10^6	1.8×10^9	240
	B	7.6×10^6	7.5×10^6	1	7.5×10^6	2.3×10^9	307

Genomic titers of the initial HSPG-non-binder (NB) and HSPG-binder library (B) were determined prior to the first selection round (0). According to the number of cells and desired g.p./cell, the total amount of viral particles ("ancestors") for the selection was calculated. The total amount of viral particles (progeny) was calculated from the genomic titer and the total volume (300µl) of viral progeny after each selection round. The relative progeny production is represented by the ratio of total viral progeny over total viral "ancestors".

After the third selection round viral DNA was amplified for subsequent cloning into the AAV helper plasmid pRC"Kotin" (2.2.2.8). 1.2kb were amplified surrounding the peptide insertion at amino acid position 587 (2.2.2.11.1). Fifty single viral clones were sequenced out of which 21 readable sequences were obtained (Table 2). Several motives were apparently enriched by the selection: The sequence SNSVRSD was found in 29% of all sequences and was present in both HSPG-non-binder and HSPG-binder pool. Furthermore, sequences starting with NGI were prominent and found in both pools. RGD-containing sequences were exclusively observed in the HSPG-non-binder pool, whereas lysine-rich, positively charged sequences were mostly found in the HSPG-binder pool.

Table 2: Sequences in HSPG-non-binder and HSPG-binder pool after the third selection round

pool	mutant	sequence	net charge
HSPG-non-binder (NB)	NB-A2, NB-A3, NB-H3, NB-6	SNSV**RS**D	neutral
	NB-H1	SDSV**RS**E	neutral
	NB-B1	NGI**RR**F**D**	**+**
	NB-C2, NB-E3	NGI**R**SF**D**	neutral
	NB-D1	**R**GD**S**LSA	neutral
	NB-E2	**R**GD**S**LSG	neutral
	NB-D2	**R**GD**S**GIG	neutral

	NB-G2	**R**GD**S**LIG	neutral
	NB-E1	PA**D**NGTG	**-**
	NB-H2	**K**GV**R**SF**D**	**+**
HSPG-binder (B)	B-A5, B-H5	SNSV**R**S**D**	neutral
	B-E4	NGI**R**SF**D**	neutral
	B-F4	NGIGSL**D**	**-**
	B-B2	TGTTAL**K**	**+**
	B-C5	TGS**KE**L**K**	**+**
	B-D5	**K**GT**K**AP**K**	**+++**

Sequences are given in one letter code. Normal letters represent neutral amino acids, bold letters represent charged amino acids. Net charge of the sequence is indicated in the far right column.

A total of four sequences out of both pools were chosen for further analysis in comparison to rAAV2: SNSVRSD (NB-A2), NGIRRFD (NB-B1), NGIRSFD (NB-C2) and KGTKAPK (B-D5). NB-A2 was chosen due to its abundance in the pool of sequences, NB-B1 and NB-C2 because they differ in only one amino acid and thereby in overall charge. B-D5 was picked because of its high positive charge which is likely to confer HSPG-binding ability to the mutant. In this work, the four mutants chosen will be referred to as A2, B1, C2 and D5.

Single-stranded, 5'-phosphorylated oligonucleotides of the four insertion sequences N-terminally flanked by the amino acids ASA and C-terminally flanked by the amino acids AA were used for subsequent cloning into the AAV helper plasmid pRC99. Annealing of single-stranded oligonucleotides led to double-stranded oligonucleotides possessing MluI and AscI sticky-ends for ligation into pRC99 (2.2.2.11.2).

The four mutants A2, B1, C2 and D5 in pRC99 as well as rAAV2 were packaged with single-stranded vector genome conformation encoding for the reporter gene GFP to further investigate their characteristics (2.2.5.1). Genomic titers were determined by qPCR (2.2.2.9) and capsid titer by A20 ELISA (2.2.3.4). The capsid to genomic ratio was calculated to compare packaging efficiency [101] (Table 3). Packaging efficiency varied slightly between the different vector preparations but all rAAV peptide insertion mutants were packaged with an efficiency of <50, which is indicative of a wild-type AAV2 phenotype according to Kern and colleagues [101].

Table 3: Characterization of vector preparations

vector	sequence in 587	net charge	genomic titer per µl	capsid titer per µl	capsid to genomic ratio
rAAV2	/	/	1.28×10^9	1.41×10^{10}	11
A2	SNSV**RS**D	neutral	3.06×10^8	7.39×10^9	24
B1	NGI**RR**F**D**	**+**	6.59×10^8	1.21×10^{10}	18
C2	NGI**R**SF**D**	neutral	3.15×10^8	6.03×10^9	19
D5	**K**GT**K**AP**K**	**+++**	1.18×10^8	1.23×10^9	10

Titers were determined by qPCR and A20 ELISA, respectively. Capsid to genomic ratio indicates packaging efficiency.

3.2   Characterization of rAAV peptide insertion mutants regarding cell entry

To study rAAV peptide insertion mutants in comparison to rAAV2 with respect to their cell interaction, HeLa rather than K-562 were chosen as target cells since HeLa cells are highly permissive for AAV2, and the key steps in AAV2 infectious biology have been characterized on HeLa cells [9], [135], [136], [151]. To test if the selected rAAV peptide insertion mutants are capable of transducing HeLa cells, cells were incubated with 5×10^3 g.p./cell of the insertion mutants and rAAV2 for 24h at 37°C. Then, the percentage of GFP-expressing cells was measured by flow-cytometry (Figure 8, grey bars). rAAV2 showed the highest transduction efficiency (86.8%), followed by B1 with 61.9%. For A2 and C2, transduction efficiencies of 55.1% and 48.1%, respectively, were observed. D5 showed the lowest transduction efficiency (34.2%). Since HeLa cells were successfully transduced by all four AAV peptide insertion mutants, the selection performed on K-562 cells in fact gave rise to tools that could subsequently be analyzed on a rAAV2-permissive cell line.

3.2.1   Analysis of primary receptor binding ability by Heparin competition

The first crucial step in a viral infection is to overcome the cellular membrane. rAAV2 makes its first contact with the cell by binding to its primary receptor HSPG [6]. In order to analyze whether the four rAAV peptide insertion mutants also bind to HSPG, a Heparin competition assay was carried out. Heparin is structurally closely related to heparan sulphate and can therefore be designated as a soluble analogue of HSPG. Hence, Heparin can bind to the viral capsid of AAV2, suppressing its ability to bind to HSPG on the cell surface in a competitive way [6].

To assess the ability of the four rAAV peptide insertion mutants to bind to HSPG, 5×10^3 g.p./cell of the insertion mutants and rAAV2 were incubated for 30min with 20 IU/ml Heparin and subsequently transferred onto HeLa cells. Twenty-four hours later, the percentage of transduced cells was determined by flow cytometry (Figure 8). Cell transduction by rAAV2 and D5 was blocked by the addition of Heparin (1.7% and 0.7% residual transduction), while B1 transduction was notably less affected (26.2% residual transduction). In contrast, addition of Heparin did not interfere with A2- and C2-mediated transduction. In line with our previous observation [103], when comparing the net charge of the inserted ligand to the outcome of the Heparin competition assay, it can be concluded that rAAV mutants displaying a positively charged peptide insertion (B1 and D5) bind to Heparin, and consequently to HSPG, while the rAAV mutants with neutral insertions (A2 and C2) transduce HeLa cells HSPG-independently.
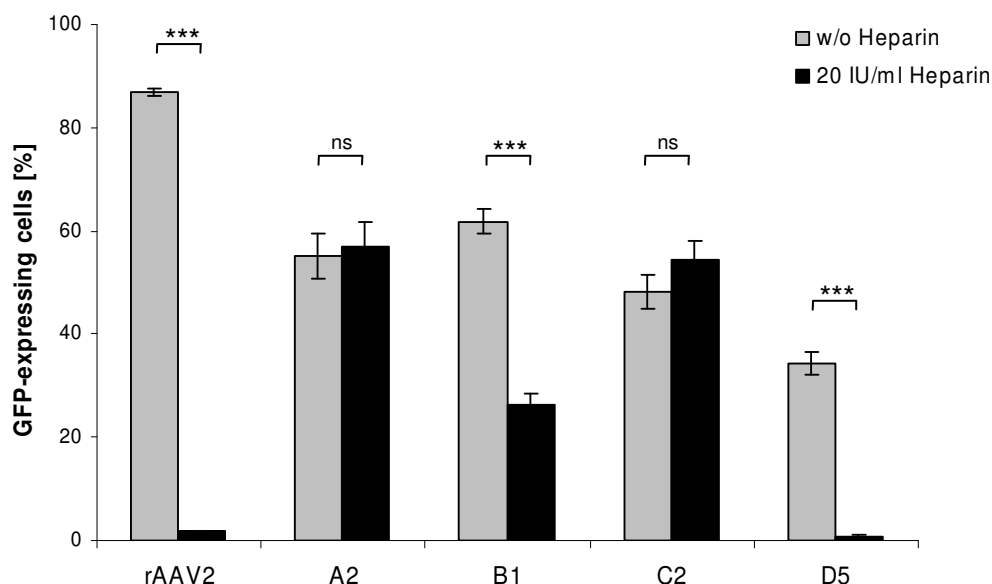
Figure 8: Transduction efficiencies of rAAV2 and rAAV peptide insertion mutants in the presence or absence of soluble Heparin

20 IU/ml soluble Heparin was incubated with 5×10^3 g.p./cell of rAAV vectors in medium for 30min at room temperature. The vector-heparin suspension or 5×10^3 g.p./cell of rAAV vectors without Heparin were added to HeLa cells and incubated at 37°C in a humidified CO_2 incubator. GFP-expression was measured by flow cytometry 24h p.t. Values represent the mean of three independent experiments, error bars show s.e.m. To define statistical significance between transduction of untreated and Heparin-treated samples, Student's t-test was performed. ***:$P<0.0005$; ns: not significant.

To further characterize the interplay of B1 and D5 – the insertion mutants displaying a positively charged peptide in 587 – with HSPG, equal amounts of genomic particles of B1

and D5 (5×10^3 g.p./cell) were incubated with increasing Heparin concentrations and subsequently incubated with HeLa cells. rAAV2 was used as a control. Twenty-four hours later, the percentage of transduced cells was determined by flow cytometry (Figure 9). The Heparin titration revealed different dose-responses of inhibition for all three vectors, hence, they differed in the half maximal inhibitory concentration (IC_{50}) of Heparin, implying that the three vectors exhibit different affinities to Heparin: rAAV2 showed an IC_{50} of approximately 0.8 IU/ml, while the IC_{50} of D5 was 10 times lower (0.08 IU/ml). For B1, even at the highest Heparin concentration, only a maximum of 60% inhibition and an IC_{50} of approximately 30 IU/ml were observed. The higher IC_{50} of B1 explained its higher residual transduction at 20 IU/ml Heparin compared to the complete inhibition of rAAV2 and D5 at the same Heparin concentration.
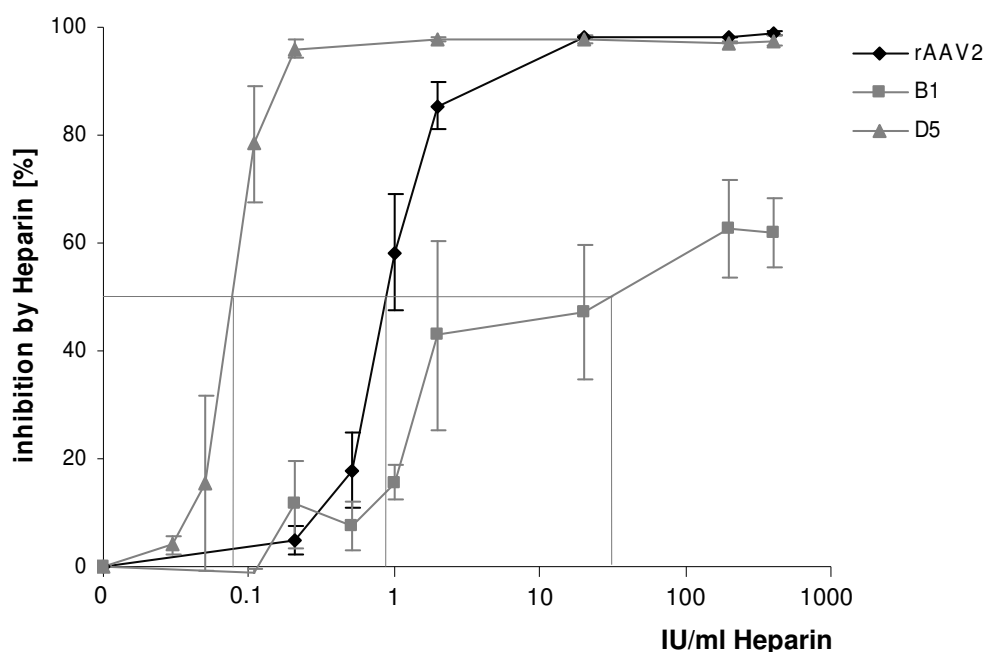
Figure 9: Inhibition of cell transduction by HSPG-binder vectors in the presence of increasing concentrations of Heparin

Heparin at the indicated concentrations was incubated with 5×10^3 g.p./cell of rAAV2 and HSPG-binder mutants in medium for 30min at room temperature. The vector-Heparin suspension or 5×10^3 g.p./cell of rAAV vectors without Heparin were added to HeLa cells and incubated at 37°C in a humidified CO_2 incubator. GFP-expression was measured by flow cytometry 24h p.t. Values represent the mean of three independent experiments; error bars show s.e.m. Fine grey lines indicate Heparin concentration at IC_{50}.

3.2.2 Inhibition of clathrin-mediated endocytosis by Chlorpromazine

The most prominent entry pathway taken by viruses is clathrin-mediated endocytosis [173]. Also AAV2 is endocytosed from the cell surface in a clathrin-dependent process after binding to receptors on the host cell plasma membrane [9-11]. To monitor, whether any of the peptide insertion mutants is internalized in a clathrin-dependent way, inhibitor studies with Chlorpromazine (CPZ) were carried out. CPZ is a substance leading to mis-assembly of clathrin lattices on endosomes and loss of coated pits from the cell surface by inhibiting the assembly of the clathrin adaptor protein AP2 [174]. To determine the effect of CPZ on cell transduction by the insertion mutants and rAAV2, HeLa cells were incubated with a final concentration of 10µg/ml CPZ for 30min at 37°C. The peptide insertion mutants and rAAV2 were added in two different genomic particle numbers per cell: $5x10^3$ and $2x10^3$. After 1h incubation on ice to allow vector binding, tranduction was performed for 2h at 37°C in the presence or absence of CPZ. Transduction was stopped by trypsin treatment, cells were re-seeded in fresh medium and transduction efficiency was measured by flow cytometry 24h p.t. (Figure 10A). In addition, CPZ-treated and untreated HeLa cells seeded on 12mm cover slips were incubated with 0.5mg/ml transferrin-Alexa Fluor® 488-conjugate to control the effectiveness of CPZ treatment, since transferrin is known to be taken up via clathrin-mediated endocytosis [175]. After 1h incubation on ice and 2h at 37°C, cells were stained with DAPI and analyzed by fluorescence microscopy (Figure 10B and C). With $5x10^3$ g.p./cell, transduction efficiencies of rAAV2 and of the insertion mutants A2, B1 and C2 were significantly inhibited by the addition of CPZ, while no interference with D5-mediated transduction was observed (light grey and black bars). In contrast to the particle to cell ratio of $5x10^3$ g.p./cell, transduction of HeLa cells with $2x10^3$ g.p./cell of B1 was not significantly inhibited by CPZ, whereas transduction by rAAV2, A2 and C2 was significantly reduced. D5 was again not affected by CPZ treatment (white and dark grey bars). The strongest inhibition by CPZ was observed for the HSPG-non-binder mutants: 67.6% and 72.0% inhibition for A2 and C2, respectively, with $5x10^3$ g.p./cell; 62.4% and 64.9% inhibition for A2 and C2, respectively, with $2x10^3$ g.p./cell. rAAV2-mediated transduction was inhibited to about the same extent in both genomic particle numbers: 29.3% inhibition with $5x10^3$ g.p./cell and 33.1% inhibition with $2x10^3$ g.p./cell. B1 was only sensitive to CPZ with $5x10^3$ g.p./cell: 39.2% inhibition was observed in this case, while no significant change in transduction efficiency was seen for B1 with $2x10^3$ g.p./cell. The transduction efficiency of D5 was not significantly reduced by CPZ, irrespective of the genomic particle number.
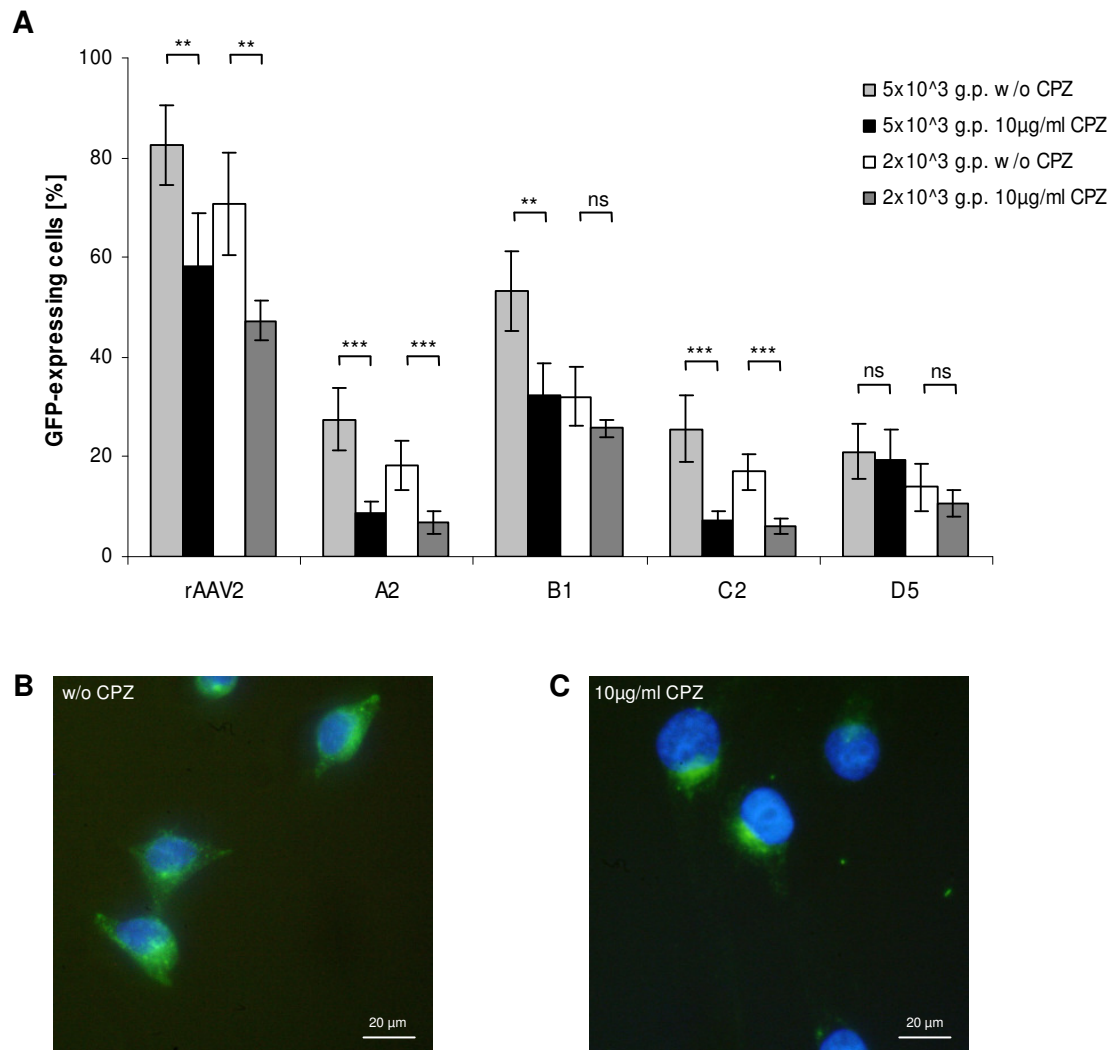
Figure 10: Transduction efficiencies in the presence or absence of Chlorpromazine

A: HeLa cells were incubated with or without 10µg/ml Chlorpromazine (CPZ) for 30min at 37°C prior to transduction. $5x10^3$ g.p./cell (light grey and black bars) or $2x10^3$ g.p./cell (white and dark grey bars) of rAAV vectors were added. One hour incubation on ice was followed by 2h at 37°C in a humidified CO_2 incubator. Transduction was stopped by trypsin treatment and re-seeding the cells in fresh medium. GFP-expression was measured by flow cytometry 24h p.t. Values represent the mean of six independent experiments, error bars show s.e.m. To define statistical significance between transduction of untreated and drug-treated samples, Student's t-test was performed. ***:P<0.0005; **:P<0.005; ns: not significant.

B and **C:** HeLa cells seeded on 12mm cover slips were incubated with or without 10µg/ml Chlorpromazine (CPZ) for 30min at 37°C. 0.5mg/ml Transferrin-Alexa Fluor® 488-conjugate in medium was added and incubated for 1h on ice. After 2h at 37°C, cells were washed, stained with DAPI and analyzed by fluorescence microscopy. Merged images of pictures obtained by excitation at 360nm and 500nm are shown. Scale bars indicate 20µm. **B:** w/o CPZ, **C:** 10µg/ml CPZ

3.2.3 Inhibition of caveolar endocytosis by Genistein

As outlined above, rAAV2 is taken up by clathrin-mediated endocytosis. Similarly, the uptake of A2, C2 and B1 at a high particle number (5×10^3g.p./cell) seemed to rely on clathrin-coated pit formation. The entry route of D5 and B1 with 2×10^3g.p./cell, at which no inibition by CPZ was observed, remained unclear. Therefore, inhibitor studies with Genistein were performed. Genistein blocks caveolae-mediated internalization through inhibition of protein tyrosine kinases [176]. Caveolar endocytosis was described as another popular entry route used by members of the virus families *Picornaviridae* and *Polyomaviridae*, e.g. SV40 and coxsackie B virus, and was recently shown to be an alternative entry pathway of AAV5 into HeLa cells [14],[15],[173]. To monitor the consequence of Genistein treatment on cell transduction by rAAV vectors, HeLa cells were incubated with a final concentration of 200µM Genistein for 30min at 37°C. 2×10^3g.p./cell of rAAV2 and the insertion mutants were added and incubated for 1h on ice. rAAV5, packaged with single-stranded GFP, was included in the analysis (vector kindly provided by N. Schuhmann). Subsequently, transduction was carried out for 2h at 37°C in the presence or absence of Genistein. Transduction was stopped by trypsin treatment, cells were re-seeded in fresh medium and transduction efficiency was measured by flow cytometry 24h p.t. (Figure 11). rAAV5 was the only vector inhibited by Genistein (39.6% inhibition), rAAV2 transduction was unaffected by Genistein, while for the peptide insertion mutants an increase in transduction was observed upon Genistein treatment.
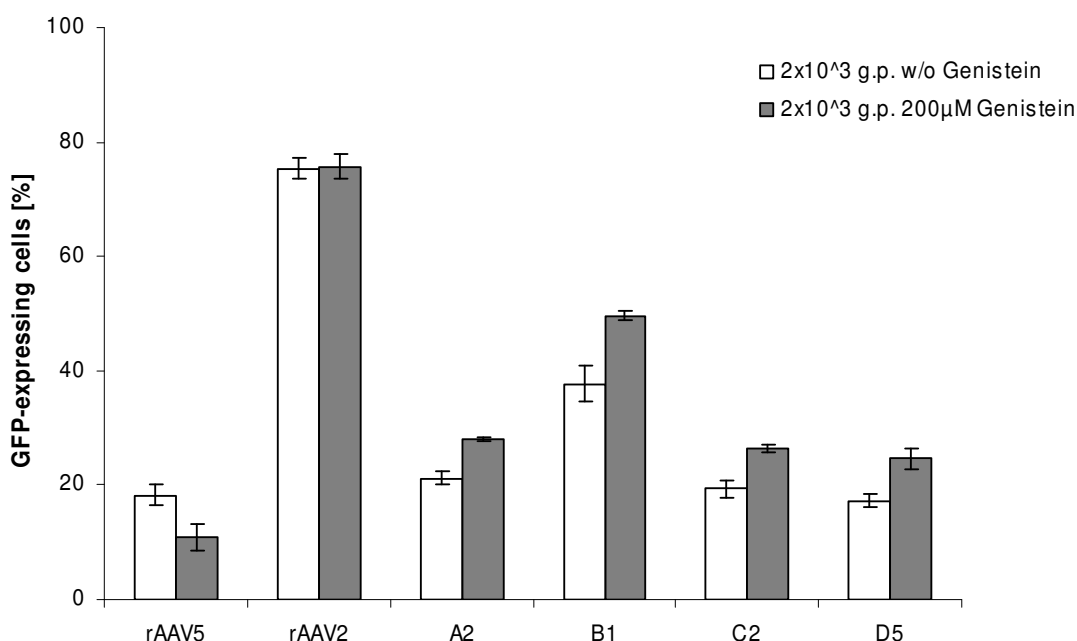
Figure 11: Transduction efficiencies in the presence or absence of Genistein

HeLa cells were incubated with or without 200µM Genistein for 30min at 37°C prior to transduction. $2x10^3$ g.p./cell of rAAV vectors were added. One hour vector binding on ice was followed by 2h at 37°C in a humidified CO_2 incubator. Transduction was stopped by trypsin treatment and re-seeding the cells in fresh medium. GFP-expression was measured by flow cytometry 24h p.t. Values represent the mean of three independent experiments, error bars show s.e.m.

3.2.4 Combining Heparin competition and inhibition of clathrin-mediated endocytosis by Chlorpromazine

As shown in paragraph 3.2.2, cell transduction efficiency of rAAV2 and the HSPG-binder mutant B1 were significantly inhibited by Chlorpromazine. To analyze, whether the vectors can use either pathway for cell entry, a combined treatment with Heparin at the IC_{50} and CPZ was carried out. Aiming to inhibit transduction by rAAV2 about 50%, $5x10^3$ g.p./cell of rAAV2 were incubated with 0.8 IU/ml soluble Heparin for 30min. For 50% inhibition of B1-mediated transduction, 30 IU/ml Heparin were incubated with $5x10^3$ g.p./cell of B1 for 30min (IC_{50} values were chosen according to Figure 9). HeLa cells were treated with CPZ as described before (3.2.2). The vector-Heparin suspensions were either transferred onto untreated HeLa cells or HeLa cells pre-treated with CPZ. In case of pre-treatment with CPZ, the drug was added to the vector-Heparin suspension in a final concentration of 10µg/ml. After 1h incubation on ice, tranduction was performed for 2h at 37°C. Transduction was stopped by trypsin treatment, cells were re-seeded in fresh medium and transduction efficiency was measured by flow cytometry 24h p.t. (Figure 12). In the presence of CPZ, residual transduction efficiencies of 61.5% and 57.4% were observed for rAAV2 and B1, respectively, while Heparin reduced transduction efficiencies to 37.5% and 54.8% in case of rAAV2 and B1, respectively. The combined treatment with Heparin and CPZ resulted in a further decrease of transduction for both vectors: rAAV2 and B1 were inhibited to residual transduction efficiencies of 18.9% and 22.2%, respectively.
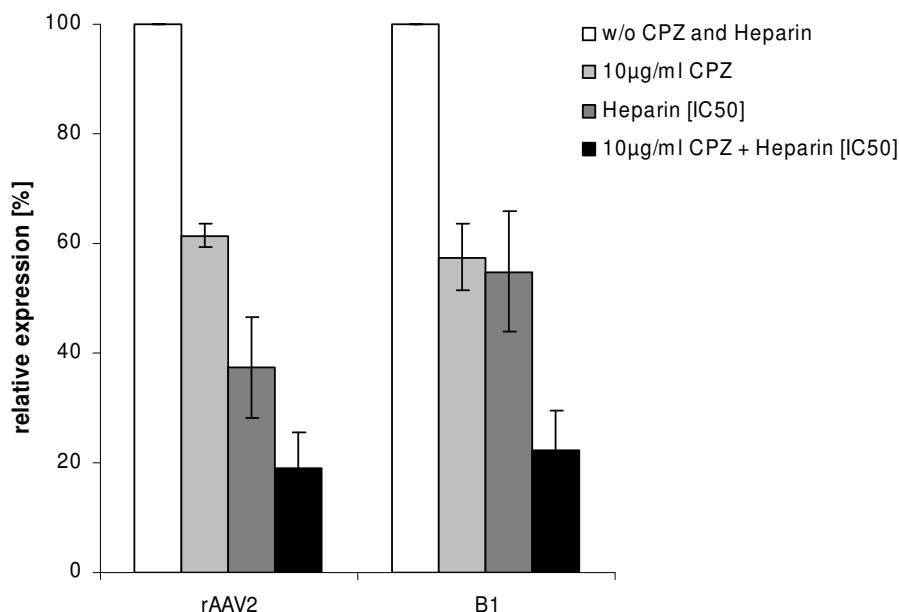
Figure 12: Transduction efficiencies in the presence of Chlorpromazine, Heparin, Chlorpromazine and Heparin or in the absence of the substances

HeLa cells were incubated with or without 10μg/ml Chlorpromazine (CPZ) for 30min at 37°C prior to transduction (drug-untreated: white and dark-grey bars; CPZ-treated: light-grey and black bars). $5x10^3$ g.p./cell of rAAV2 and B1 were added (white and light-grey bars). Heparin at the inhibitory concentration 50 [IC_{50}] of each vector (rAAV2: 0.8IU/ml; B1: 30IU/ml) was incubated with $5x10^3$ g.p./cell of the respective vector in medium for 30min at room temperature. The vector-Heparin suspension was added to either HeLa cells pre-treated with CPZ (black bars) or untreated HeLa cells (dark-grey bars). In case of pre-treatment with CPZ (black bars), the drug was added to the vector-Heparin suspension in a final concentration of 10μg/ml. One hour incubation on ice was followed by 2h at 37°C in a humidified CO_2 incubator. Transduction was stopped by trypsin treatment and re-seeding the cells in fresh medium. GFP-expression was measured by flow cytometry 24h p.t. Transduction efficiencies without CPZ or Heparin treatment were set to 100%. Values represent the mean of three independent experiments, error bars show s.e.m.

3.2.5 Determination of cell entry efficiency

Having studied the cell entry mode of rAAV2 and the peptide insertion mutants, the impact of the cell entry mode on entry efficiency into different cell types was analyzed. In order to be independent of the accomplishment of all further steps in viral infection, cell entry efficiency was determined by qPCR of intracellular vector particles. Besides HeLa cells, HEK293, BLM and HepG2 cells were assayed. Cells were incubated with $5x10^3$ g.p./cell of rAAV2 and the insertion mutants for 1h on ice followed by 4h incubation at 37°C. Cells were harvested by trypsin treatment to remove membrane-bound vector particles [9],[10],[172] and washed

before total DNA was extracted. To determine intracellular vector genomes, qPCR was performed for vector DNA (GFP) and the human single-copy gene Plat. Melting peak analysis was accomplished to proof specificity of PCR products. Normalization of target gene (GFP) to reference gene (Plat) was carried out and the normalized target/reference ratios of rAAV2 were set to 1 (Figure 13). rAAV2, B1 and D5, which are all able to bind to HSPG, entered HeLa cells with a significantly higher efficiency than the HSPG-non-binder mutants A2 and C2. Similarly, entry efficiency of rAAV2 and the HSPG-binder mutants B1 and D5 was significantly higher in case of HEK293, BLM and HepG2 cells compared to A2 and C2 pointing towards a positive correlation of HSPG-binding ability and cell entry efficiency.
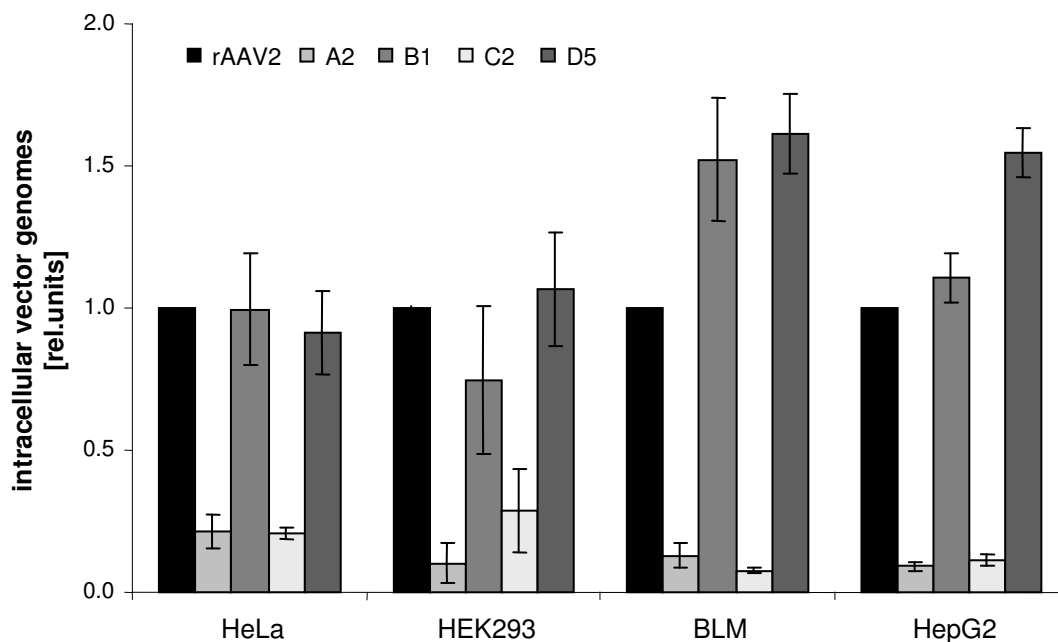
Figure 13: Cell entry efficiencies of rAAV vectors into different cell lines

HeLa, HEK293, BLM and HepG2 cells were incubated with 5×10^3 g.p./cell of rAAV vectors for 1h on ice to allow vector binding and subsequently shifted to 37°C and 5% CO_2. Cells were harvested by trypsin treatment 4h p.t. and total DNA was isolated. Intracellular vector genomes (GFP) and the single-copy gene Plat were determined by qPCR. Normalization to Plat was performed and the normalized target/reference ratios of rAAV2 at 4h were set to 1. Values represent the mean of three independent experiments, error bars show s.e.m. Student's t-test was performed for each cell line, revealing a significant difference ($P<0.0001$) between HSPG-binders (rAAV2, B1 and D5) as one group and HSPG-non-binders (A2 and C2) as a second group.

To monitor the course of cell entry of rAAV2 and the peptide insertion mutants into HeLa cells, intracellular vector genomes were determined at several points in time. HeLa cells were incubated with $5x10^3$ g.p./cell of rAAV2 and the insertion mutants for 1h on ice to allow vector binding followed by incubation at 37°C. Cells were harvested at 15min, 30min, 60min, 2h and 4h p.t. by trypsin treatment to ensure removal of membrane-bound vector particles. Cells were washed and total DNA was extracted. qPCR was performed for vector DNA and Plat (single-copy gene). The normalized target/reference ratios of rAAV2 at 4h p.t. were set to 1 (Figure 14A). rAAV2 and the HSPG-binder mutants B1 and D5 showed similar cell entry rates (black lines, filled symbols). For the HSPG-non-binder mutants A2 and C2, a less efficient cell entry than that of the HSPG-binder mutants and rAAV2 was observed (grey lines, open symbols). One hour p.t., significantly more intracellular vector genomes were detected for the HSPG-binder mutants and rAAV2 compared to the HSPG-non-binder mutants (P=0.0003). Between 1h and 4h p.t., further particles of all vectors were internalized but the cell entry efficiency of the HSPG-non-binder mutants remained significantly lower than that of the HSPG-binder mutants and rAAV2.

To find out, if an HSPG-non-binder vector known to bind to cellular integrins exhibits a similar cell entry rate to the HSPG-non-binder mutants A2 and C2, the course of cell entry was monitored for rAAV-RGD4C587 in comparison to rAAV2 [87]. This rAAV mutant carrying an RDG4C insertion peptide at position 587 was previously shown to bind to soluble $\alpha_v\beta_3$ and $\alpha_v\beta_5$ integrins and to transduce HeLa cells independent of HSPG via integrins [87],[177],[178]. Transduction of HeLa cells with $5x10^3$ g.p./cell of RGD4C587 and rAAV2, DNA extraction, qPCR and normalization was performed exactly as described above (Figure 14B). Compared to rAAV2, the course of cell entry of RGD4C587 was significantly less efficient (P=0.0004 at 1h p.t.; P<0.0001 at 4h p.t.), whereas cell entry rates of RGD4C587 and the HSPG-non-binder mutants A2 and C2 were similar at all points in time (Figure 14A vs. B).
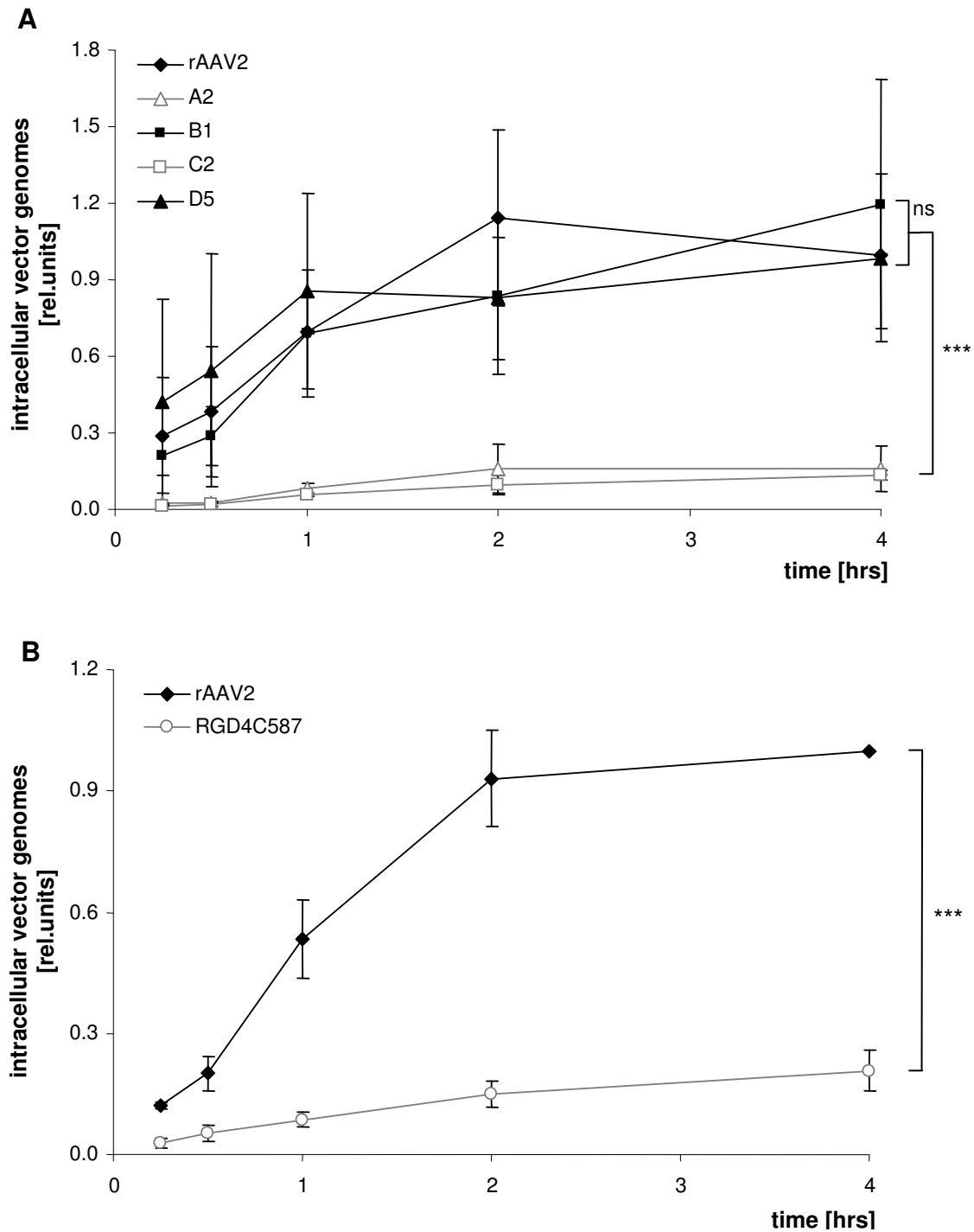
Figure 14: Cell entry efficiencies of rAAV2 and rAAV peptide insertion mutants

HeLa cells were incubated with $5x10^3$ g.p./cell of rAAV vectors for 1h on ice to allow vector binding and subsequently shifted to 37°C and 5% CO_2. Cells were harvested by trypsin treatment at the indicated time points and total DNA was isolated. Intracellular vector genomes (GFP) and the single-copy gene Plat were determined by qPCR. Normalization to Plat was performed and the normalized target/reference ratios of rAAV2 at 4h were set to 1. Values represent the mean of three independent experiments; error bars show s.e.m.

A: Student's t-test revealed a significant difference (***:$P<0.0005$) between HSPG-binders (rAAV2, B1 and D5) as one group and HSPG-non-binders (A2 and C2) as a second group at 4h p.t.

B: Student's t-test revealed a significant difference (***:$P<0.0005$) between rAAV2 and RGD-4C at 4h p.t.

3.3 Genetic fluorescence labelling of rAAV peptide insertion mutants

Fluorescent proteins like GFP have been extensively used as fusion proteins to study intracellular trafficking and localization of proteins and viral particles [179],[180]. Previous studies showed that AAV2 incorporates the N-terminal fusion protein of GFP and VP2, thereby allowing a labelling of AAV2 particles [90],[91]. Further analyses carried out in our group revealed that additional fluorophores like CFP, dsRed and mCherry are tolerated in this position [Dissertation S. Stahnke, 2008]. Here, the peptide insertion mutants A2, B1, C2 and D5 were labeled with GFP and compared to a mCherry-tagged rAAV2, since no antibody is available to distinguish between rAAV2 and the peptide insertion mutants. In order to generate vectors displaying the peptide insertion in all VP3 copies and, in addition, having a genetically fused GFP-tag at the N-terminus of VP2, the peptide insertions of the mutants A2, B1, C2 and D5 were cloned into peGFP-VP2.2 and pRC VP2 k.o. (2.2.2.11.3). These plasmids were used to package GFP-tagged insertion mutants. In parallel, a mCherry-tagged rAAV2 was packaged as a control. All vectors were packaged with Luciferase as transgene (2.2.5.1). Genomic titers were determined by qPCR (2.2.2.9), capsid titer by A20 ELISA (2.2.3.4) and the capsid to genomic ratio was calculated to compare packaging efficiency (Table 4). According to Kern and colleagues, wildtype packaging phenotype was observed for GFP-A2 and mCherry-rAAV2 with capsid to genomic ratios <50, whereas higher ratios were obtained in case of GFP-B1, GFP-C2 and GFP-D5, indicating reduced packaging efficiency [101].

Table 4: Characterization of vector preparations: mCherry-tagged rAAV2 and GFP-tagged peptide insertion mutants

vector	genomic titer per µl	capsid titer per µl	capsid to genomic ratio
mCherry-rAAV2	1.86×10^8	9.2×10^9	49.5
GFP-A2	1.96×10^8	6.86×10^9	35
GFP-B1	1.25×10^8	6.68×10^9	53.5
GFP-C2	1.58×10^8	1.4×10^{10}	87.5
GFP-D5	5.32×10^7	3.3×10^9	62

Titers were determined by qPCR and A20 ELISA, respectively. Capsid to genomic ratio indicates packaging efficiency.

Western blot analysis of purified vector preparations was carried out to proof the incorporation of GFP or mCherry into the capsid of the respective vectors. 5×10^{10} capsids of mCherry-tagged rAAV2, the GFP-tagged insertion mutants and rAAV2 with unmodified capsid were separated by SDS-PAGE and blotted on nitrocellulose membrane. The three AAV capsid proteins were detected by B1 antibody that binds to the C-terminus of all capsid proteins. As depicted in Figure 15, a band of 100kDa was detected in case of all fluorescent-protein-tagged rAAV vectors (the weaker bands of GFP-tagged A2 and GFP-tagged B1 probably result from an overestimation of the respective capsid titers). This size corresponded to the fusion protein of VP2 (72kDa) and GFP or mCherry (both 27kDa). For unlabelled rAAV2, VP1 (90kDa), VP2 and VP3 (60kDa) were detected at a ratio of approximately 1:1:10.
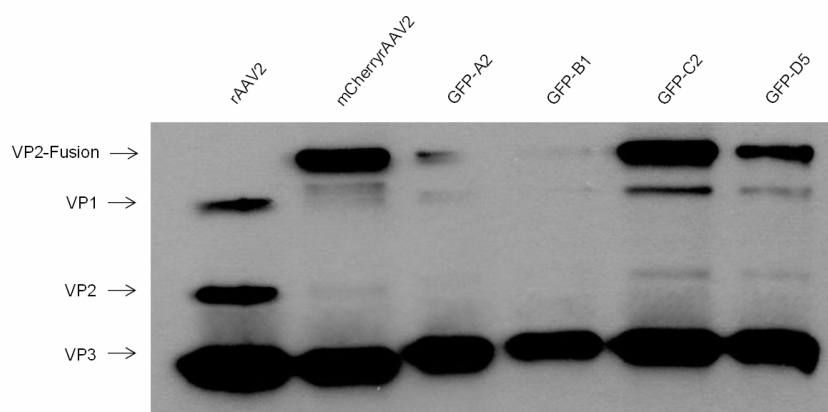
Figure 15: Western blot analysis of GFP-tagged insertion mutants and mCherry-tagged rAAV2
5×10^{10} capsids of unmodified rAAV2 (wt), the GFP-tagged insertion mutants (GFP-A2, GFP-B1, GFP-C2, GFP-D5) and mCherry-tagged rAAV2 were separated by SDS-PAGE using an 8% dissolving gel. After western blotting, the three capsid proteins were detected by B1, detecting the C-terminus of all three AAV capsid proteins (secondary antibody: Donkey anti-mouse IgG-HRP).

To determine if the GFP-tagged insertion mutants were suited for intracellular visualization, HeLa cells were transduced with 5×10^6 capsids/cell. This capsid to cell ratio has previously been used to visualize GFP-tagged vectors inside transduced cells by fluorescence microscopy [91]. To promote binding of mCherry-tagged rAAV2 and the GFP-tagged insertion mutants, HeLa cells were incubated with the vectors for 1h on ice, followed by 4h at 37°C. Transduction was stopped by washing and fixing the cells, followed by staining the nuclear lamina with anti-Lamin B. In Figure 16, multi-plane images obtained by confocal microscopy are shown. In case of mCherry-tagged rAAV2 and all GFP-tagged insertion mutants, fluorescence signals were detected inside transduced cells.
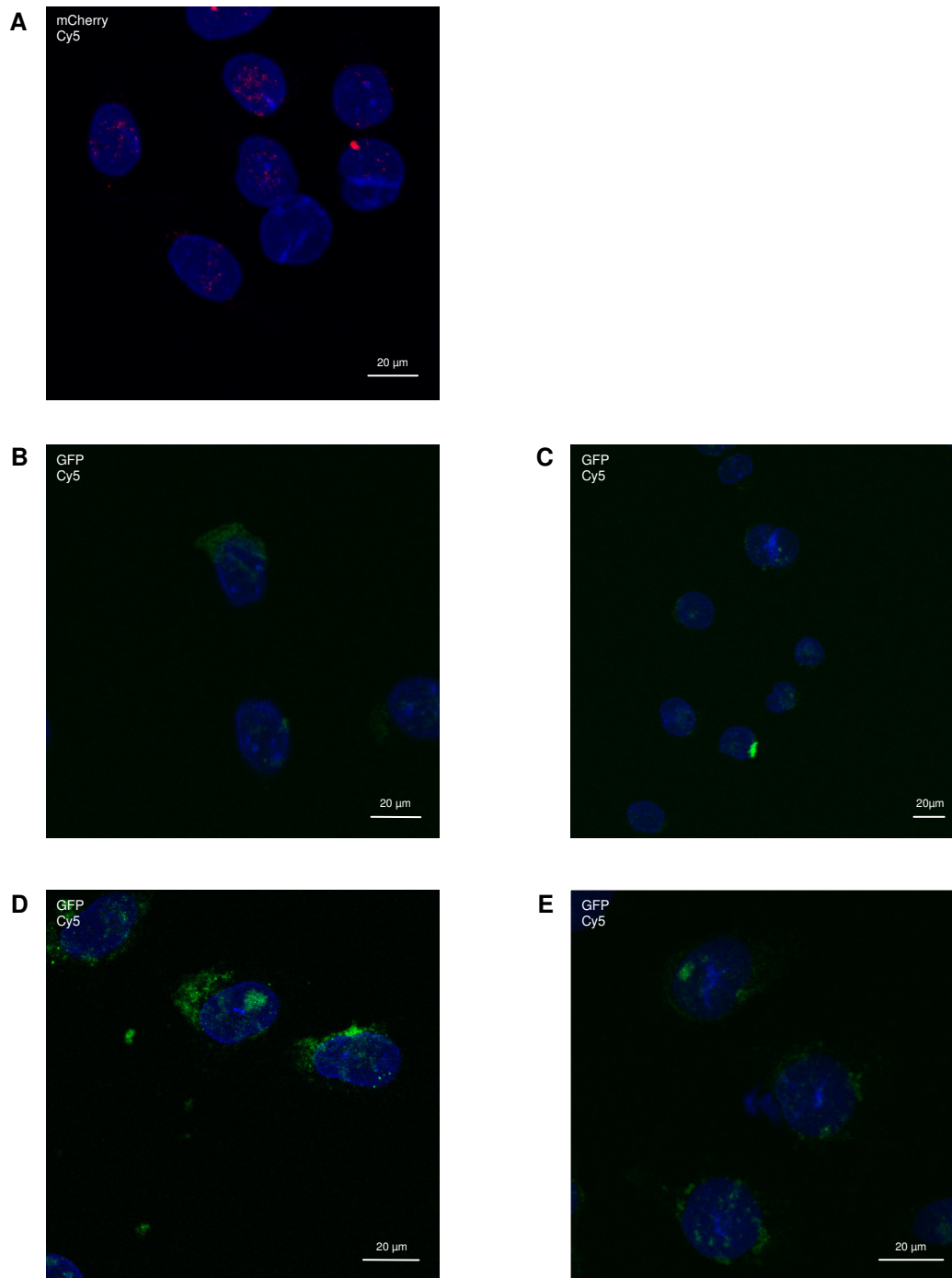
Figure 16: Evaluation of GFP-tagged peptide insertion mutants and mCherry-tagged rAAV2

HeLa cells were incubated with 5×10^6 capsids/cell of the respective fluorescent-protein-tagged vectors for 1h on ice and subsequently shifted to 37°C and 5% CO_2. Four hours p.t., cells were washed and fixed. After permeabilization of the cells, nuclear lamina was stained with anti-Lamin B (secondary antibody: donkey anti-goat Cy5). Pictures show multi-plane images of HeLa cells transduced with mCherry-tagged rAAV2 (**A**), GFP-tagged A2 (**B**), GFP-tagged B1 (**C**), GFP-tagged C2 (**D**) and GFP-tagged D5 (**E**). Fluorescent dyes are indicated, scale bars represent 20µm.

To analyze whether rAAV2 and the insertion mutants localize to the same intracellular region, co-transduction studies with mCherry-tagged rAAV2 were conducted exemplarily for the HSPG-binder mutant B1 and the HSPG-non-binder mutant C2. Single transductions with mCherry-tagged rAAV2, GFP-tagged B1 and GFP-tagged C2 were carried out for comparison. As described above, 1h incubation on ice was followed by 4h at 37°C. Then, transduced cells were washed, fixed and the nuclear lamina was stained with anti-Lamin B. Figure 17 shows pictures representing one slice (1µm) of a z-stack obtained by confocal microscopy. mCherry-tagged rAAV2 (A) as well as GFP-tagged B1 (B) and GFP-tagged C2 (C) localized to the perinuclear area in single transductions. Co-transductions with mCherry-tagged rAAV2 and GFP-tagged B1 (D-F) as well as mCherry-tagged rAAV2 and GFP-tagged C2 (G-I) revealed a perinuclear localization of rAAV2 and the peptide insertion mutants, since the signals coming from mCherry and GFP were detected in the same, 1µm thin image plane.
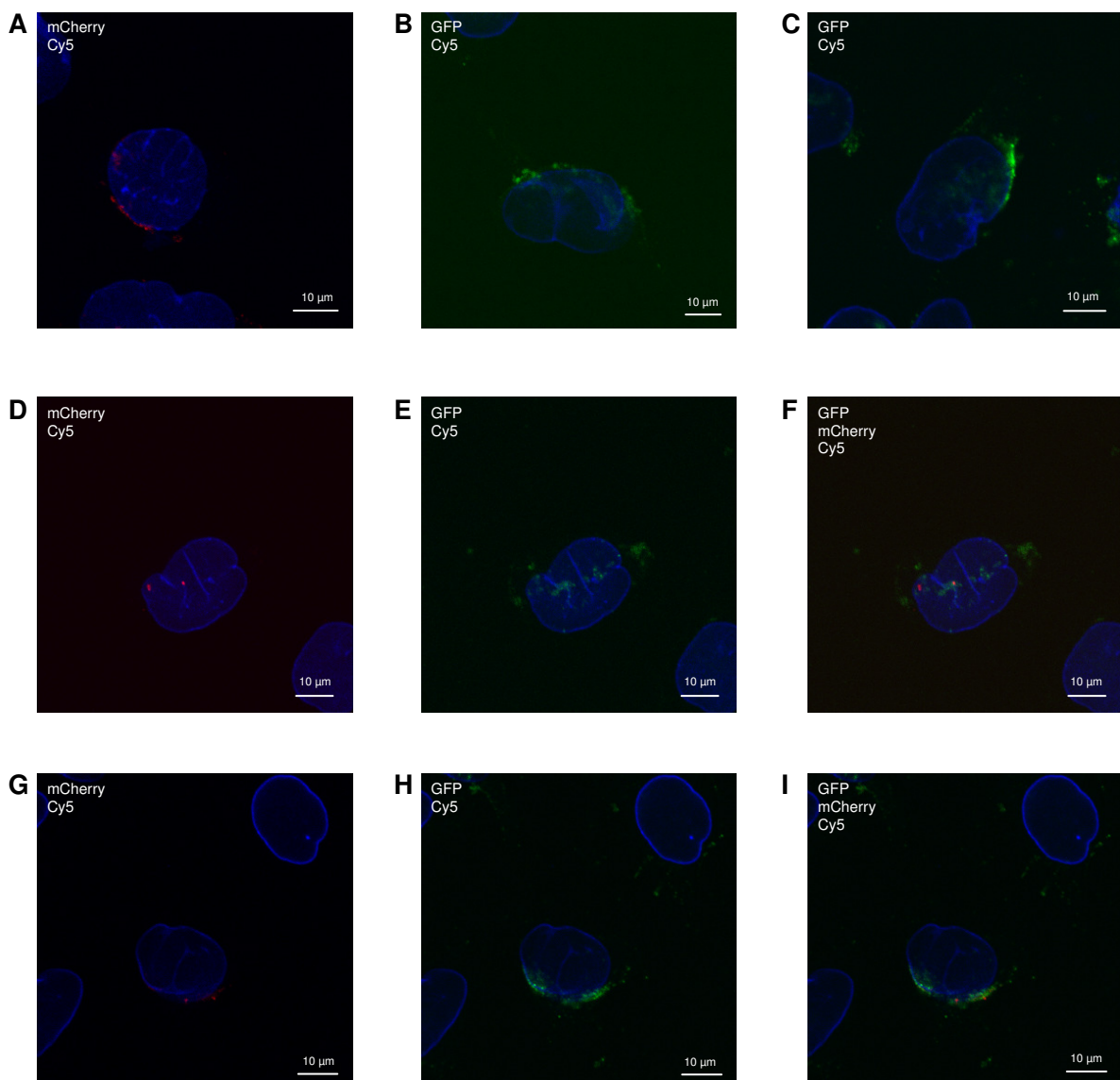
Figure 17: Intracellular localization of GFP-tagged B1, GFP-tagged C2 and mCherry-tagged rAAV2 after single or co-transduction

HeLa cells were incubated with 5×10^6 capsids/cell of mCherry-tagged rAAV2, GFP-tagged B1 and GFP-tagged C2 for 1h on ice and subsequently shifted to 37°C and 5% CO_2. For co-transduction, HeLa cells were incubated with 5×10^6 capsids/cell of mCherry-tagged rAAV2 and 5×10^6 capsids/cell of GFP-tagged B1 or 5×10^6 capsids/cell of mCherry-tagged rAAV2 and 5×10^6 capsids/cell of GFP-tagged C2. Four hours p.t., cells were washed and fixed. After permeabilization of the cells, nuclear lamina was stained with anti-Lamin B (secondary antibody: donkey anti-goat Cy5). Pictures show single-plane images representing one slice (1μm) of a z-stack. **A-C:** Transduction by mCherry-tagged rAAV2, GFP-tagged B1 and GFP-tagged C2; **D-F:** Co-transduction by mCherry-tagged rAAV2 and GFP-tagged B1; **G-I:** Co-transduction by mCherry-tagged rAAV2 and GFP-tagged C2. Fluorescent dyes are indicated, scale bars represent 10μm.

3.4 Characterization of rAAV peptide insertion mutants with respect to intracellular events

3.4.1 Adjustment of intracellular vector particles

The HSPG-non-binder mutants A2 and C2 entered cells significantly less efficient than rAAV2 and the HSPG-binder mutants B1 and D5 (3.2.5). Hence, to compare intracellular events such as intracellular trafficking and transgene expression, an adjustment of intracellular vector particles was necessary [181]. Similar to the studies on re-targeted adenoviral vectors, intracellular vector particles of the HSPG-non-binder mutants A2 and C2 were adjusted to those of rAAV2. Based on the relative numbers of intracellular vector genomes determined 1h p.t. (Figure 14), the genomic particle to cell ratio of A2 and C2, compared to rAAV2, was increased assuming that thereby the number of A2 and C2 that successfully enter the cell can be increased (Table 5). In details, compared to rAAV2, A2 and C2 showed 8.22 times and 12.48 times less intracellular vector genomes, respectively. Hence, to obtain comparable amounts of intracellular vector particles for all rAAV vectors, 8.22 times more genomic particles per cell of A2 and 12.48 times more genomic particles per cell of C2 have to be applied compared to the genomic particles per cell of rAAV2. Since the entry efficiencies of B1 and D5 were not significantly different from rAAV2, no adjustment should be necessary.

Table 5: Calculation of intracellular genomic particles (i.g.p.) based on cell entry efficiency 1h post transduction

vector	genomic particles	intracellular vector genomes 1h p.t. [rel.units]	multiplier	intracellular genomic particles
rAAV2	5×10^3	0.699	/	5×10^3
A2	5×10^3	0.085	8.22	$8.22 \times 5 \times 10^3$
B1	5×10^3	0.690	1	$1 \times 5 \times 10^3$
C2	5×10^3	0.056	12.48	$12.48 \times 5 \times 10^3$
D5	5×10^3	0.854	1	$1 \times 5 \times 10^3$

Based on cell entry efficiency 1h p.t., the multiplier between intracellular vector genomes of HSPG-non-binder mutants (A2, C2) and intracellular vector genomes of rAAV2 was calculated in order to obtain comparable amounts of intracellular genomic particles. Since the entry efficiencies of B1 and D5 are not significantly different from rAAV2, the factor in this case is 1.

In order to proof whether the above decribed assumption results in the desired adjustment of intracellular particles, HeLa cells were incubated with 5×10^3 g.p./cell of rAAV2, B1 and D5, $8.22 \times 5 \times 10^3$ g.p./cell of A2 and $12.48 \times 5 \times 10^3$ g.p./cell of C2, which should correspond to 5×10^3 intracellular genomic particles (i.g.p.)/cell. In addition, HeLa cells were incubated with 2×10^2 i.g.p./cell of the rAAV vectors to test if the calculation for adjustment of intracellular particles is transferable to a lower particle to cell ratio. After 1h incubation on ice to allow vector attachment, transduction was performed for 1h at 37°C. Thereafter, cells were harvested by trypsin treatment to remove membrane-bound vector particles and cells were washed prior to DNA isolation. To determine intracellular vector genomes, qPCR was performed for vector DNA and Plat (single-copy gene). Normalization to Plat was carried out and the normalized target/reference ratios of rAAV2 were set to 1 (Figure 18). Without adjustment of intracellular particles, intracellular vector genomes of A2 and C2 1h p.t. were significantly different from rAAV2, whereas B1 and D5 were not significantly different from rAAV2 (Figure 18A). Compared to the initial situation, in case of 5×10^3 i.g.p./cell, no significant difference was observed between intracellular vector genomes of rAAV2 and any of the insertion mutants (Figure 18B). Also the adjustment to 2×10^2 i.g.p./cell revealed that none of the insertion mutants show a significant difference in intracellular vector genomes compared to rAAV2 (Figure 18C).
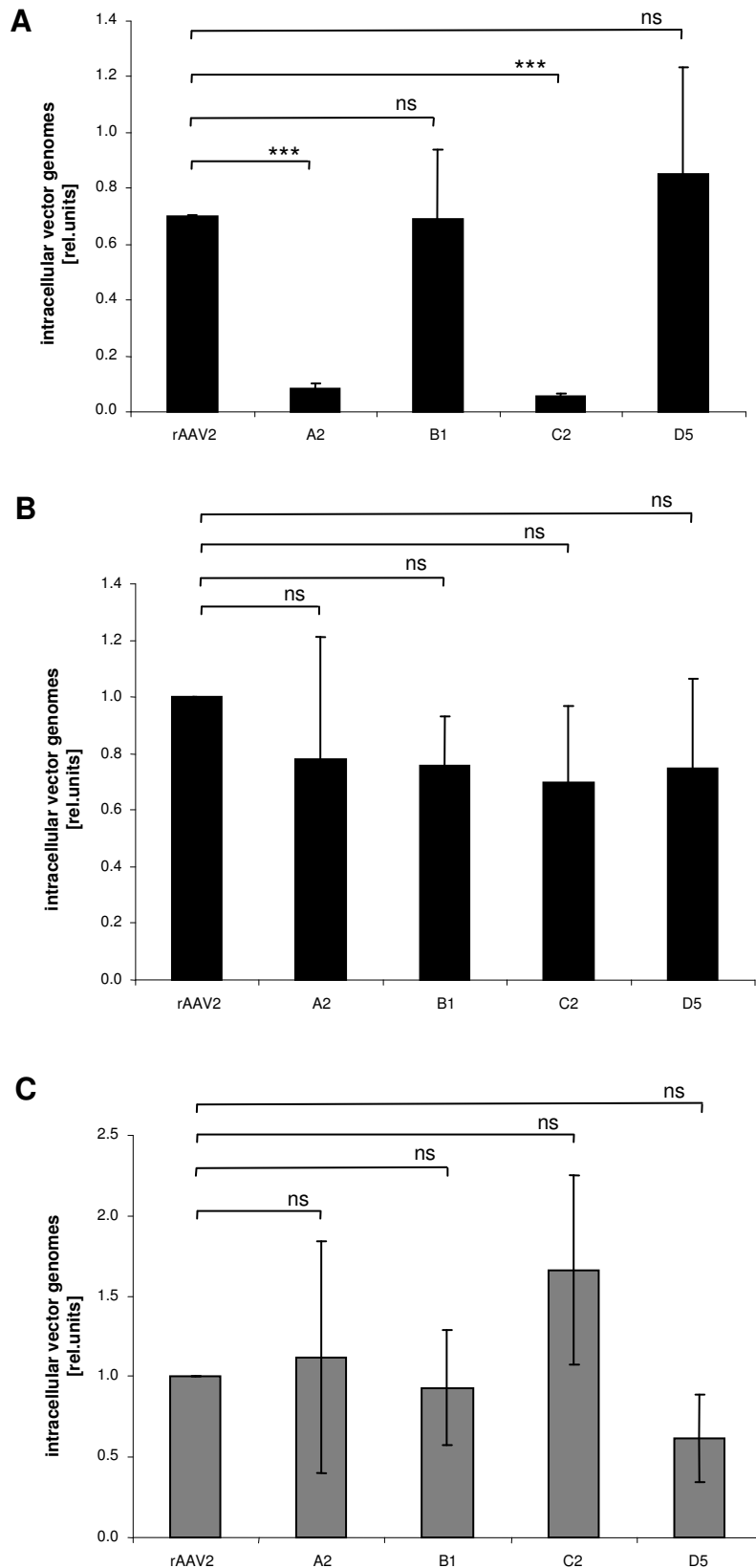
Figure 18: Adjustment of intracellular vector particles

$5x10^3$ g.p./cell of rAAV vectors (**A**), rAAVs adjusted to $5x10^3$ i.g.p./cell (**B**) or to $2x10^2$ i.g.p./cell (**C**) were incubated with HeLa cells for 1h on ice to allow vector binding and subsequently shifted to 37°C and 5% CO_2. Cells were harvested by trypsin treatment 1h p.t. and total DNA was isolated.

Intracellular vector genomes (GFP) and the single-copy gene Plat were determined by qPCR. Normalization to Plat was performed and the normalized target/reference ratios of rAAV2 were set to 1 (B, C). **A**: data 1h p.t. from Figure 14. Values represent the mean of three (**A**), five (**B**) or four (**C**) independent experiments; error bars show s.e.m. To define statistical significance between rAAV2 and the four insertion mutants, Student's t-test was performed. ***:P<0.0005; ns: not significant.

3.4.2 Transduction efficiencies of rAAV vectors with adjusted intracellular particles

In paragraph 3.2, transduction efficiencies of rAAV2 and the peptide insertion mutants was determined irrespective of different entry efficiencies of HSPG-binders and HSPG-non-binders. Here, transduction efficiencies were monitored with adjusted intracellular vector particles. HeLa cells were incubated with 5×10^3 i.g.p./cell or 2×10^2 i.g.p./cell of rAAV2 and the insertion mutants for 1h on ice to promote vector binding followed by incubation at 37°C. One hour p.t., medium was exchanged to medium containing 3% anti-capsid antibody A20 in order to prevent so far unbound vector particles from binding to the cell and subsequent internalization. Transduction efficiency was measured by flow cytometry 24h p.t. (Figure 19). With 5×10^3 i.g.p./cell, rAAV2 transduced HeLa cells significantly more efficient (87%) than the HSPG-non-binder mutants A2 and C2, which showed similar transduction efficiencies (75.8% and 77.8%, respectively). Transduction efficiency of the HSPG-binder mutant B1 (68.5%) was significantly lower compared to rAAV2, but no statistical difference was detected between the three insertion mutants B1, A2 and C2. For the HSPG-binder mutant D5, the lowest transduction efficiency was observed (27%), which is significantly different from all other vectors (Figure 19, Table 6). With 2×10^2 i.g.p./cell, rAAV2 as well as the HSPG-non-binder mutants A2 and C2 transduced HeLa cells with similar efficiencies: 25.1%, 17.1% and 21% in case of rAAV2, A2 and C2, respectively. The HSPG-binder mutants B1 and D5 showed significantly lower transduction efficiencies (7.8% and 2.9%, respectively) compared to rAAV2, A2 and C2. Furthermore, the poor transduction by D5 was revealed to be significantly different from B1 (Figure 19, Table 6).
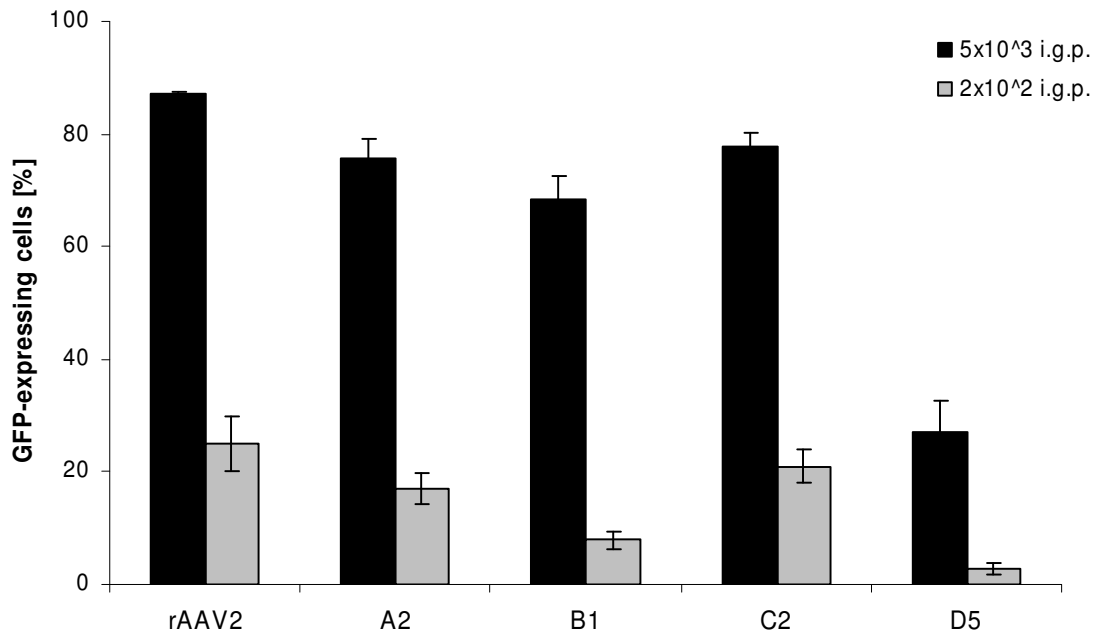
Figure 19: Transduction efficiencies of rAAV vectors with adjusted intracellular genomic particles

HeLa cells were incubated with 5×10^3 i.g.p./cell (black bars) or 2×10^2 i.g.p./cell (grey bars) of rAAV vectors for 1h on ice to allow vector binding and subsequently shifted to 37 °C and 5% CO_2. One hour p.t., medium containing 3% A20 was added. GFP-expression was measured by flow cytometry 24h p.t. Values represent the mean of three independent experiments, error bars show s.e.m. For statistical analysis, see Table 6.

Table 6: Statistical analysis for transduction efficiencies of rAAV vectors with adjusted intracellular genomic particles

A	5×10^3 i.g.p./cell						
	P (vectors vs rAAV2)	P (A2 vs C2)	P (A2 vs B1)	P (C2 vs B1)	P (A2 vs D5)	P (C2 vs D5)	P (B1 vs D5)
rAAV2	/						
A2	0.02	0.59	0.19		0.0007		
B1	0.0065		0.19	0.084			0.0017
C2	0.012	0.59		0.084		0.0004	
D5	0.0002				0.0007	0.0004	0.0017

B	2×10^2 i.g.p./cell						
	P (vectors vs rAAV2)	P (A2 vs C2)	P (A2 vs B1)	P (C2 vs B1)	P (A2 vs D5)	P (C2 vs D5)	P (B1 vs D5)
rAAV2	/						
A2	0.14	0.31	0.02		0.0045		
B1	0.011		0.02	0.0079			0.033
C2	0.39	0.31		0.0079		0.0018	
D5	0.004				0.0045	0.0018	0.033

A: Student's t-test revealed significant differences between rAAV2 and all four rAAV peptide insertion mutants. A2 and C2 are not significantly different from each other and not significantly different from B1, but they are significantly different from D5. Furthermore, B1 is significantly different from D5.

B: Student's t-test revealed significant differences between rAAV2, B1 and D5. A2 and C2 are not significantly different from rAAV2 and from each other but they are significantly different from B1 and D5. Moreover, B1 is significantly different from D5.

3.4.3 Proteasome inhibition by MG-132

Proteasome inhibitors are small molecule compounds that are able to specifically inhibit the activity of the proteasome. Most widely used are peptide aldehyds like carbobenzoxy-leu-leu-leucinal (MG-132) which primarily inhibit the chymotrypsin-like activity of the proteasome [182]. Proteasome inhibitors have been previously shown to enhance AAV transduction in different cell types [136],[146],[144]. To analyze if the peptide insertion mutants and rAAV2 are targets of proteasomal degradation, HeLa cells were incubated with a final concentration of 10μM MG-132 for 30min at 37°C. 2×10^2 i.g.p./cell of the insertion mutants and rAAV2 were added. After 1h incubation on ice to allow vector binding, tranduction was performed for 4h at 37°C in the presence or absence of MG-132. Transduction was stopped by washing and addition of fresh medium. Transduction efficiency was measured by flow cytometry 24h p.t. (Figure 20). MG-132 treatment resulted in a significant enhancement of transduction in case of all vectors, albeit to slightly varying degree. Cell transduction by rAAV2 was increased by 1.4-fold upon MG-132 treatment, while for the insertion mutants, a slightly stronger enhancement was detected. Cell transduction by B1 was doubled, whereas D5 showed 1.7-fold higher transduction efficiency in the presence of MG-132. A2 and C2 were enhanced 1.8-fold and 1.6-fold, respectively.
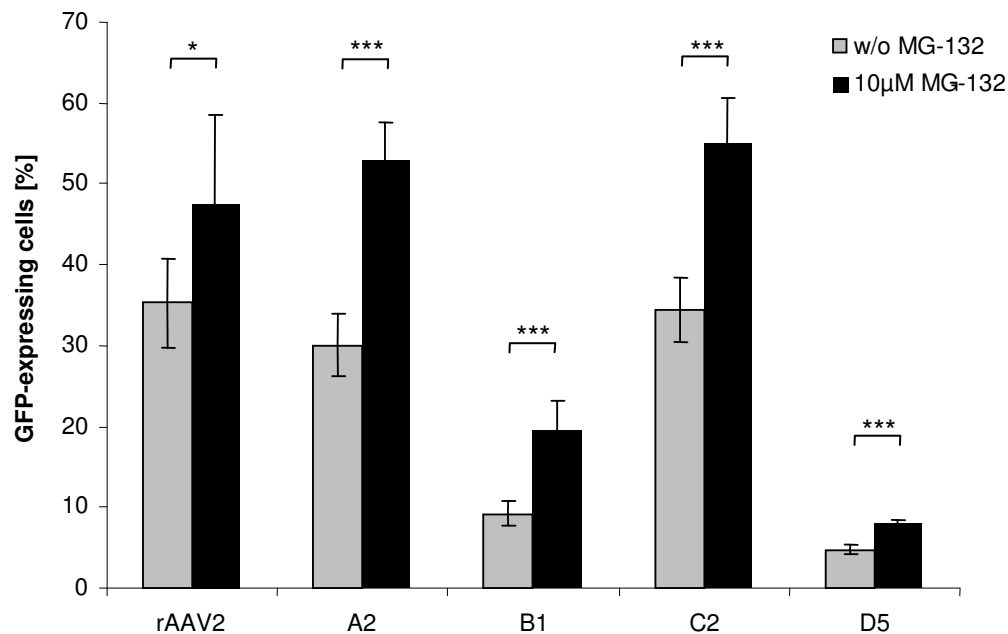
Figure 20: Transduction efficiencies in the presence or absence of MG-132

HeLa cells were incubated with or without 10µM MG-132 for 30min at 37°C prior to transduction. 2×10^2 i.g.p./cell of rAAV vectors were added. One hour incubation on ice was followed by 4h at 37°C in a humidified CO_2 incubator. Transduction was stopped by removing the medium, washing the cells with PBS and addition of fresh medium. GFP-expression was measured by flow cytometry 24h p.t. Values represent the mean of three independent experiments; error bars show s.e.m. To define statistical significance between transduction of untreated and drug-treated samples, Student's t-test was performed. ***:$P<0.0005$; *:$P<0.05$.

3.4.4 Quantification of vector genome transcripts

Transduction efficiencies with adjusted intracellular vector particles obtained by flow cytometry revealed that the HSPG-non-binder mutants A2 and C2 were superior to the HSPG-binder mutant D5 and – depending on the particle to cell ratio – also to B1, and reached similar transduction efficiencies as rAAV2 in a low particle to cell ratio (3.4.2). Vector uncoating was previously reported to limit the efficiency of transduction of hepatocytes mediated by AAV2 [183]. To analyze whether the weak cell transduction observed for B1 in a low particle to cell ratio and for D5 irrespective of the particle to cell ratio was due to an impaired vector uncoating, the onset of transgene expression – indicating a successful vector uncoating and delivery of vector genomes to the nucleus – was measured by quantifying vector genome transcripts at early points in HeLa cell transduction via qRT-PCR. Therefore, HeLa cells were incubated with 5×10^3 i.g.p./cell or 2×10^2 i.g.p./cell of rAAV2 and the insertion mutants for 1h on ice to allow vector attachment followed by incubation at 37°C. One hour

p.t., medium was exchanged to medium containing 3% anti-capsid antibody A20 in order to prevent so far unbound vector particles from binding to the cell and subsequent internalization. Cells were harvested at 1h, 2h, 2.5h, 3h and 4h p.t. by lysis in β-mercaptoethanol containing lysis buffer. Total RNA was extracted from the samples and cDNA was synthesized. To determine transcripts of vector genomes, qPCR was performed on cDNA for vector transcripts (GFP) and the human single-copy transcript AlasI. Melting peak analysis was accomplished to proof specificity of PCR products. Normalization to AlasI was carried out and the normalized target/reference ratios of rAAV2 at 3h p.t. were set to 1 (Figure 21). One hour p.t., irrespective of the particle number, vector genome transcripts were detectable for all rAAV vectors, and from 2h p.t. onwards, transcript levels of all vectors increased (Figure 21A and B). Notably, already 2h p.t., more vector genome transcripts of rAAV2, A2, B1 and C2 were detected compared to D5. Similar to the results obtained by flow cytometry, with 5×10^3 i.g.p./cell, 4h p.t., rAAV2 showed the highest level of vector genome transcripts followed by the insertion mutants A2, B1 and C2. No significant difference was observed between rAAV2, A2, B1 and C2, whereas for D5, significantly fewer vector genome transcripts were detected 4h p.t. (Figure 21A). With 2×10^2 i.g.p./cell, the highest levels of vector genome transcripts were observed for rAAV2, A2 and C2 4h p.t., which were not significantly different. The HSPG-binder mutants B1 and D5 showed significantly lower vector genome transcript levels. Furthermore, significantly fewer vector genome transcripts were detected for D5, compared to B1 (Figure 21B).
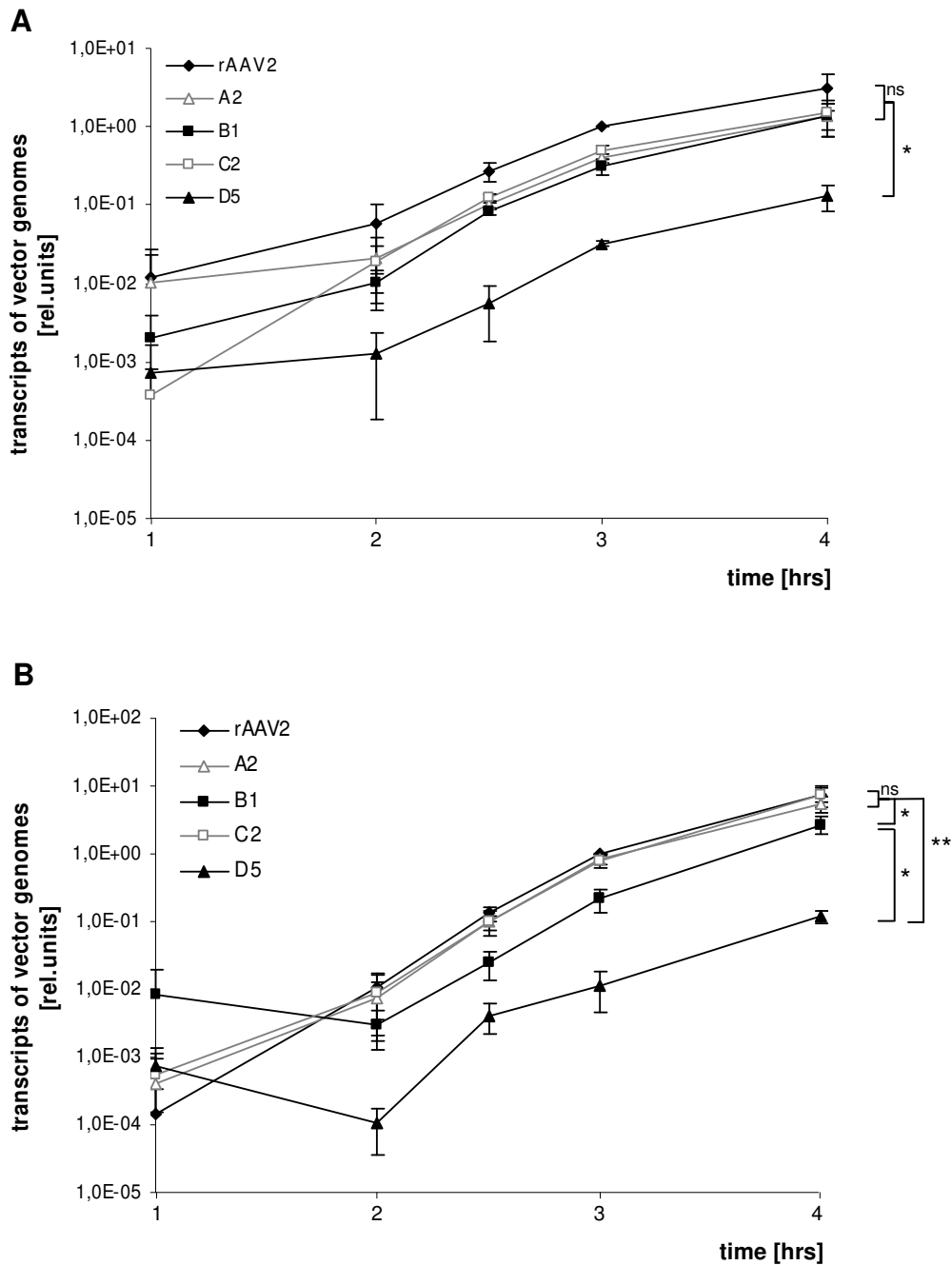
Figure 21: Quantification of vector genome transcripts depending on time

HeLa cells were incubated with 5×10^3 i.g.p./cell (**A**) or 2×10^2 i.g.p./cell (**B**) of rAAV vectors for 1h on ice followed by incubation at 37°C and 5% CO_2. One hour p.t., medium containing 3% A20 was added. Cells were harvested at indicated time points and total RNA was isolated. After cDNA synthesis, transcripts of vector genomes (GFP) and the single-copy transcript AlasI were analyzed by qPCR. Normalization to AlasI was performed and the normalized target/reference ratios of rAAV2 at 3h were set to 1 and untransduced negative control was subtracted from the samples. Values represent the mean of three independent experiments; error bars show s.e.m.

A: Student's t-test revealed that rAAV2, A2, B1 and C2 are not significantly different from each other but significantly different from D5 at 4h p.t.

B: Student's t-test revealed that rAAV2, A2 and C2 are not significantly different from each other but significantly different from B1 as well as from D5 at 4h p.t. Moreover, B1 is significantly different from D5. **:P<0.005; *:P<0.05; ns: not significant.

3.4.5   Subcellular distribution of rAAV vectors

As shown in paragraph 3.2.2, both B1 at a low particle to cell ratio and D5 were insensitive to treatment with CPZ, while rAAV2 was significantly inhibited by CPZ. Analysis of transduction efficiency and quantification of vector genome transcripts revealed that the HSPG-binder mutants B1 and D5 had both significantly lower transduction and transcript levels than rAAV2 in case of cell transduction with 2×10^2 g.p. (3.4.2, 3.4.4). To assess whether the cell entry mode also influences the intracellular routing of rAAV vectors, the subcellular distribution of vector genomes was compared between rAAV2 and the HSPG-binder mutants B1 and D5. Since visualization of fluorescent-protein-tagged rAAV vectors is technically not possible with a lower particle to cell ratio than 5×10^6 capsids per cell (corresponding to about 10^5 g.p./cell), the Qiagen Qproteome Cell Compartment Kit was used for cell fractionation in order to quantify vector genomes in the cytosol, membranes and nuclei (2.2.7.5). HeLa cells were incubated with 2×10^2 g.p./cell of rAAV2 and the HSPG-binder mutants B1 and D5 for 1h on ice followed by incubation at 37°C. To prevent so far unbound vector particles from binding to the cell and subsequent internalization, medium was exchanged to medium containing 3% anti-capsid antibody A20 at 1h p.t. Two hours p.t., cells were harvested by extensive trypsin treatment to ensure the removement of unbound vector particles. Cells were washed and divided into cytosolic, membrane and nuclear fractions. After fractionation, DNA was extracted from equal volumes of the cytosolic, membrane and nuclear fraction. Prior to DNA extraction, Luciferase plasmid DNA was added to each fraction to monitor the accuracy of downstream procedures. To analyze vector genomes in subcellular fractions, qPCR was carried out for vector genomes (GFP) and reference gene (Luciferase). Normalization of target (GFP) to reference gene (Luciferase) was performed. In case of all three vectors, the majority of vector genomes were found in the membrane and nuclear fractions, whereas few vector genomes were observed in the cytosolic fraction (Table 7).

Table 7: Subcellular distribution of rAAV vector genomes 2h post transduction

	Distribution [%]		
	Cytosol	Membranes	Nuclei
rAAV2	7.84 ± 2.32	36.63 ± 6.95	55.53 ± 7.08
B1	5.18 ± 0.36	72.03 ± 4.63	22.8 ± 4.56
D5	5.55 ± 0.12	73.7 ± 0.63	20.76 ± 0.62

Values represent the mean of three independent experiments ± s.e.m.

To compare the efficiency of intracellular routing of rAAV2 and the HSPG-binder mutants B1 and D5, the ratio of vector genomes in membranes to vector genomes in nuclei was calculated (Figure 22A). The higher the ratio, the more vector genomes are detected in the membrane fraction. For B1 and D5, significantly higher ratios were determined compared to rAAV2, demonstrating that 2h p.t., a higher proportion of vector genomes of the HSPG-binder mutants B1 and D5 was present inside membrane-coated cellular compartments (0.7, 3.4 and 3.6 for rAAV2, B1 and D5, respectively). For rAAV2, the ratio of vector genomes in membranes to vector genomes in nuclei was smaller than one, indicating that more vector genomes were present in nuclei than inside membrane-coated cellular compartments.
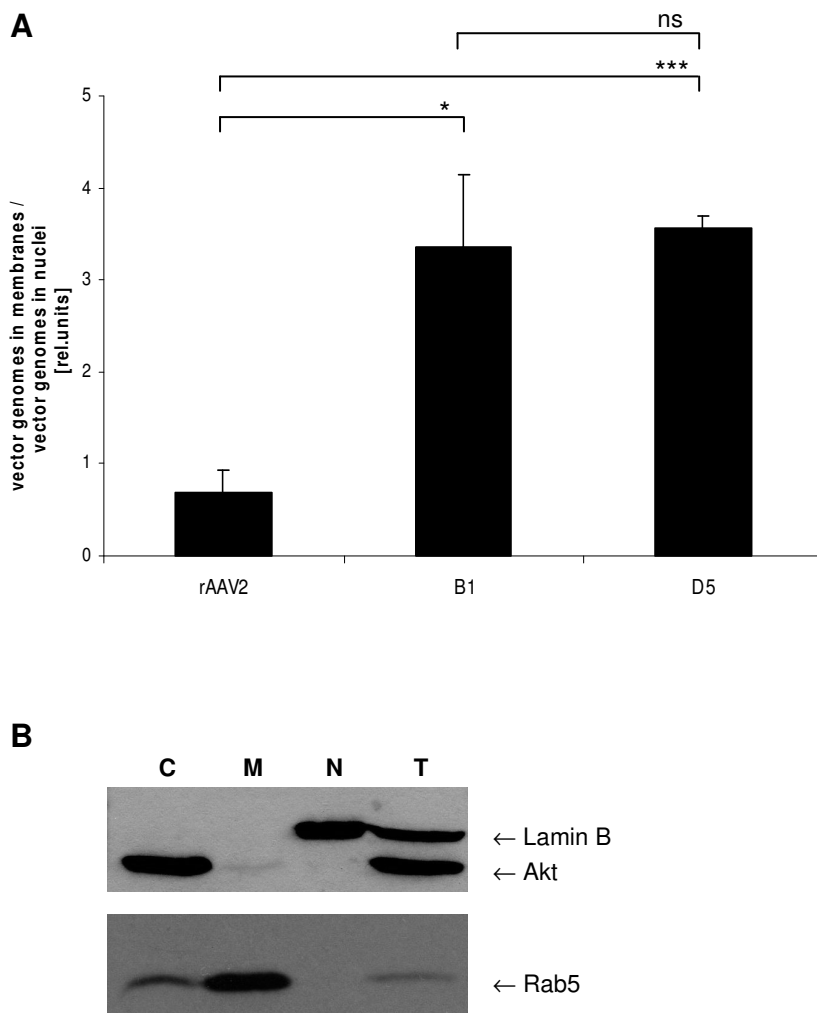
Figure 22: Subcellular distribution of rAAV2 and HSPG-binder mutants in cellular membranes and nuclei

A: HeLa cells were incubated with 2×10^2 g.p./cell of rAAV vectors for 1h on ice to allow vector binding. Cells were subsequently shifted to 37°C and 1h p.t., medium containing 3% A20 was added. Two hours p.t., cells were fractionated into cytoplasm, membranes and nuclei. Total DNA was isolated from

each of the fractions previously spiked with Luciferase plasmid DNA and vector genomes (GFP) normalized to Luciferase (plasmid DNA) were determined by qPCR. Bars indicate the ratio of vector genomes in membranes over vector genomes in nuclei at 2h p.t. Values represent the mean of three independent experiments; error bars show s.e.m. Student's t-test revealed a significant difference between rAAV2 and B1 as well as between rAAV2 and D5. ***:P<0.0005; *:P<0.05; ns: not significant. **B:** Proteins extracted from the cytosolic (C), membrane (M) and nuclear fractions (N) or from total cell lysat (T) were separated by SDS-PAGE. After western blotting, cytosolic and nuclear proteins were detected by anti-Akt and anti-Lamin B (upper part), proteins in cellular membranes by anti-Rab5 (lower part).

To determine the purity of fractionation, equal volumes of protein from the cytosolic, membrane and nuclear fractions or protein extracted from total HeLa cell lysat were analyzed by western blot (Figure 22B). Cytosolic proteins were detected by anti-Akt antibody, proteins in the membrane fraction by anti-Rab5 antibody and nuclear proteins by anti-Lamin B antibody. The upper blot shows detection by anti-Akt and anti-Lamin B, on the lower blot, detection by anti-Rab5 is depicted. Proteins were specifically detected in their corresponding fraction as well as in protein extract from total cell lysat with the exception of a weak band detected by Rab5 in the cytosolic fraction.

3.4.6 Inhibition of endosomal maturation by Bafilomycin

As shown in the previous paragraph, the HSPG-binder mutants B1 and D5 were mainly present in the membrane fraction of HeLa cells at 2h p.t., while for rAAV2, a higher proportion of vector genomes was observed in the nucleus at the same point in time. To monitor, whether rAAV2 and the insertion mutants B1 and D5 all rely on endosomal processing through early and late endosomes, inhibitor studies with Bafilomycin A1 were carried out. Bafilomycin is a specific inhibitor of the vacuolar ATPase in late endosomes and has been shown to block transport from early to late endosomes in HeLa cells [184]. To determine the effect of Bafilomycin on cell transduction by rAAV vectors, HeLa cells were incubated with a final concentration of 100nM Bafilomycin for 30min at 37℃. 5x10^3 g.p./cell of rAAV2 and the HSPG-binder mutants B1 and D5 were added. After 1h incubation on ice to allow vector binding, transduction was performed for 2h at 37℃ in the presence or absence of Bafilomycin. Then, transduction was stopped by trypsin treatment, cells were re-seeded in fresh medium and transduction efficiency was measured by flow cytometry 24h p.t. (Figure 23). In case of all three rAAV vectors, transduction was significantly reduced by the addition of Bafilomycin. rAAV2 showed 79.3% inhibition, while for B1 and D5, respectively, 91.2% and 95.3% inhibition of transduction was observed.
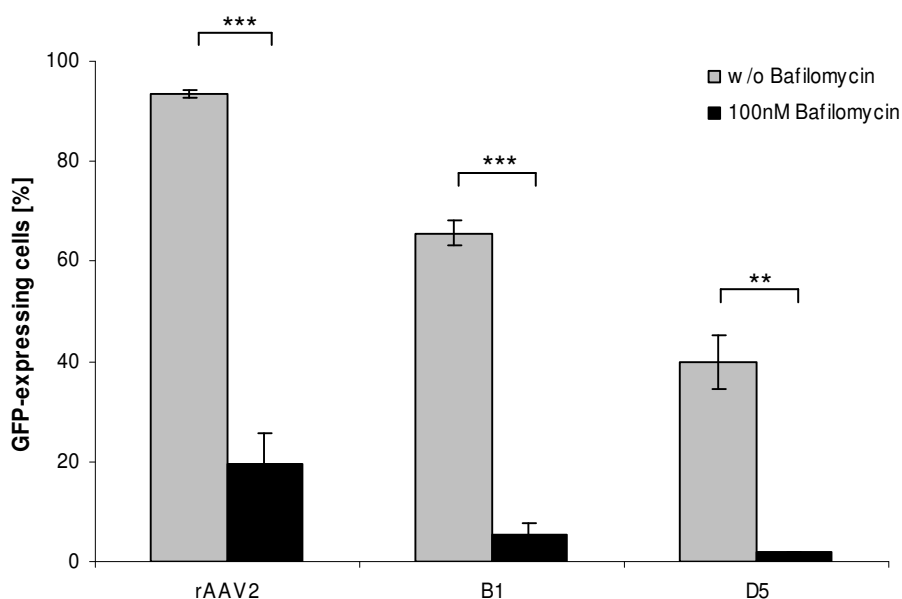
Figure 23: Transduction efficiencies of rAAV2 and HSPG-binder mutants in the presence or absence of Bafilomycin

HeLa cells were incubated with or without 100nM Bafilomycin for 30min at 37°C prior to transduction. 5×10^3 g.p./cell of rAAV2 and HSPG-binder mutants were added. One hour incubation on ice was followed by 2h at 37°C in a humidified CO_2 incubator. Transduction was stopped by trypsin treatment and re-seeding the cells in fresh medium. GFP-expression was measured by flow cytometry 24h p.t. Values represent the mean of three independent experiments; error bars show s.e.m. To define statistical significance between transduction of untreated and drug-treated samples, Student's t-test was performed. ***:P<0.0005; **:P<0.005.

4 Discussion

In vivo gene therapeutic approaches depend on efficient and specific gene transfer vehicles in order to lower the vector dose to be applied, to achieve therapeutic levels of transgene expression and to minimize the risk of off-target transduction and toxic side effects. Adeno-associated viral (AAV) vectors are among the leading gene therapy vector systems. However, like other vector systems, the broad tissue tropism and the accumulation of viral vector particles in the liver are obstacles for their *in vivo* application [7]. AAV vector targeting approaches have recently been developed to overcome these limitations. These approaches aim to redirect AAV from its natural tropism towards a desired target cell. Several small peptides genetically inserted into the AAV2 capsid at position 587 have been shown to mediate cell transduction independently of the AAV2 primary receptor heparan sulphate proteoglycan (HSPG), which is an important improvement regarding the restriction of vector tropism [54],[86],[93-95]. Furthermore, AAV display libraries with random peptide insertions at either 587 or 588 were applied to select capsid insertion mutants superior to AAV2 or natural AAV serotypes in transduction of the desired target cells or tissues *in vitro* and *in vivo* [95],[96],[185]. To date, little is known about the mechanisms of cell transduction that rely on a novel ligand-receptor interaction mediated by rAAV targeting vectors. This study provides not only insights into the uptake process of rAAV peptide insertion mutants, but also into the consequences for transgene expression.

4.1 Vector-cell interactions at the plasma membrane

Separate AAV display selections with an HSPG-binder library and an HSPG-non-binder library led to insertion mutants differing in sequence and net charge of the inserted ligand. The four mutants chosen for further analysis, namely A2, B1, C2 and D5, were packaged with an efficiency that indicates wildtype phenotype according to Kern and colleagues [101], revealing that that neither insertion interfered with capsid assembly or packaging.

As observed previously, HeLa cells, which are highly permissive for rAAV2, were less efficiently transduced by most AAV targeting vectors [103]. In line, the four selected rAAV peptide insertion mutants were able to transduce HeLa cells, but rAAV2 clearly outperformed the mutants with respect to transduction efficiency.

Efficient rAAV2-mediated cell transduction depends on primary receptor binding, since the ablation of the HSPG-binding motif by point mutations resulted in a loss of infectivity [101],[102],[87]. Targeting vectors with an insertion at amino acid position 453, which does not disrupt the HSPG-binding motif, achieved ligand-mediated cell transduction only if the HSPG-binding motif was ablated [87]. In this study, peptide insertion mutants displaying

peptides in 587 were used. Characterization of the insertion mutants concerning primary receptor binding revealed that two insertion mutants identified in the HSPG-non-binder pool, A2 and C2, were able to transduce HeLa cells independent of HSPG, while the insertion mutants B1 and D5 – like rAAV2 – were competed by the addition of Heparin. Moreover, those mutants that are independent of HSPG carry neutral insertions, while the HSPG-binder mutants possess positively charged insertion peptides. As previously reported, peptide insertions at amino acid position 587 interfere with the AAV2 HSPG-binding motif by separating two important arginine residues (R585 and R588) of this motif [101-103]. In accordance with a model postulated by our group [103], neutral peptide insertions which are not likely to bind to HSPG consequently mediate HSPG-independent cell transduction, whereas arginine-containing peptides can restore primary receptor binding ability, which seems to be the case for the HSPG-binder mutant B1. A Heparin titration further revealed a dramatic difference in dose-response relationship among the HSPG-binder vectors: D5, possessing three positive charges in the inserted sequence, showed a 10-times lower IC_{50} than rAAV2 indicating a notably higher affinity to HSPG. Presumably, in case of D5, HSPG-binding is mediated by electrostatic attraction of the positively charged ligand and the negatively charged cell surface proteoglycan. On the contrary, B1 was only partially affected by the addition of Heparin suggesting a lower affinity to HSPG of this insertion mutant.

Attachment of AAV2 to HSPG results in a conformational change of the AAV2 capsid, which in turn leads to binding of the virus to its co-receptors [8],[131],[186]. AAV2 co-receptors, such as $\alpha_v\beta_5$ and $\alpha_5\beta_1$ integrins, subsequently mediate endocytosis via clathrin-coated pits [9-11]. As yet, besides Heparin or peptide competitions, the uptake mechanism of rAAV targeting vectors has not been analyzed, but receptor-mediated endocytosis was suggested for vectors targeting integrins or CD13 [86],[92],[94],[87]. In this study, two entry pathways discussed for AAV – clathrin- and caveolae-mediated endocytosis [9-11],[14],[15] – were assessed by inhibitor studies. Correct formation of clathrin-coated pits was impeded by the addition of Chlorpromazine (CPZ) and resulted in a significant inhibition of transduction by rAAV2 and the two HSPG-non-binder mutants A2 and C2, strongly suggesting clathrin-mediated uptake. In contrast, D5 – the high sensitivity HSPG-binder mutant – was not affected by CPZ treatment, pointing towards a different cell entry pathway. B1 was significantly inhibited by the addition of CPZ if the vector was applied in a high particle to cell ratio, while in a low particle to cell ratio, CPZ did not influence transduction efficiency. Obviously, in case of B1, vector dose was determining the uptake mechanism of the targeting vector. Maybe, the affinity of B1 to its receptor is not sufficient to achieve proper binding and numerous vector particles increase the probability for receptor binding and subsequent clathrin-dependent internalization. Furthermore, the interaction with HSPG could facilitate B1-receptor binding by catching B1 in the HSPG network, bringing the vector

particles closer to their receptor, a phenomenon that was previously shown to be important for FGF-FGFR interaction and signalling [187].

Caveolar endocytosis was recently postulated to play an important role in the uptake of AAV5, which resulted in accumulation of viral particles in the Golgi compartment [14],[15]. Inhibitor studies with Genistein should reveal a potential participation of the caveolar pathway in the uptake of rAAV2 and the four peptide insertion mutants, especially B1 in a low particle to cell ratio and D5 that were not internalized clathrin-dependently. Apparently, neither rAAV2 nor any of the insertion mutants rely on caveolar endocytosis, since the addition of Genistein did not lead to a reduction of cell transduction.

In line with the current literature, rAAV2 was shown to be competed by soluble Heparin and internalized by clathrin-mediated endocytosis. The same was observed for the insertion mutant B1 with a high particle to cell ratio, even though it was less sensitive to Heparin. Structural rearrangements in the AAV2 capsid after primary receptor binding are believed to facilitate co-receptor binding; thus, HSPG- and co-receptor binding should happen one after another, explaining the dependency of rAAV2 on HSPG for infectivity. However, since transduction of rAAV2 and B1 was only partially reduced by inhibition of clathrin-mediated endocytosis, a portion of vector particles might have been forced to be internalized in complex with HSPG. Inhibition of clathrin-mediated endocytosis in combination with blocking rAAV2 and B1 vector particles with Heparin at their respective IC_{50} led to a notably higher inhibition compared to CPZ treatment alone. This observation showed that HSPG-binding was not only required to alleviate co-receptor binding but that rAAV2 and B1 are likely to be taken up via clathrin-coated pits and in complex with HSPG.

The uptake mechanism of rAAV2 and the four peptide insertion mutants was assayed by inhibitor studies and Heparin competition: D5 used neither the clathrin-dependent pathway nor caveoli to transduce cells. The three-fold positively charged targeting insertion of D5 and its high sensitivity to Heparin strongly suggest a proteoglycan-dependent internalization of the vector, similar to cationic polymers [18],[23],[56]. B1 seems to be capable to enter cells in a clathrin- and/or in a proteoglycan-mediated fashion depending on vector dose. As mentioned above, at a high particle to cell ratio, B1 can be taken up by clathrin-mediated endocytosis, while at a low particle to cell ratio, B1 showed the same phenotype as D5, proposing proteoglycan-dependent internalization. The insertions of A2 and C2 equipped the respective mutants with the ability to transduce cells in an HSPG-independent, clathrin-mediated fashion. Strikingly, rAAV2 was not exclusively internalized in a clathrin-dependent way, but, in addition, seemed to use its primary receptor HSPG not only for facilitation of co-receptor binding but also for vector uptake. Obviously, the peptide ligands inserted into the AAV capsid determined the endocytotic pathway of the vectors, directing them either to HSPG-independent, clathrin-mediated uptake (A2 and C2), to an internalization route that

depends only on HSPG (D5) or a combination of both ways of uptake (B1). Ligand-mediated change in vector internalization mode has recently been demonstrated for targeted transduction by a surface-engineered lentiviral vector and a liposomal nano-carrier, respectively [188], [189]. A Sindbis-virus-envelope-pseudotyped lentiviral vector was shown to enter cells via clathrin-mediated endocytosis – like native Sindbis virus – and not via direct fusion with the plasma membrane, as it is naturally the case for lentiviruses [188]. Similarly, a liposomal nano-carrier mainly taken up via macropinocytosis, was directed to caveolae- and clathrin-mediated uptake by incorporation of an IRQ-peptide ligand selected by phage display [189]. Futhermore, viral and non-viral vectors could successfully be targeted to distinct endocytic pathways, i.e. to the clathrin-dependent entry route by incorporation of ligands like transferrin or RGD-containing peptides [51],[60],[78], implying that the determination of the endocytic pathway by the targeting ligand is a common phenomenon in the field of vector targeting.

In the current literature, transduction efficiency of targeted viral and non-viral vectors was predominantly assayed by measuring transgene expression using flow cytometry [57],[93],[94],[103],[87],[181],[188]. However, there are at least two major steps contributing to transduction efficiency: cell entry – or crossing the cellular membrane – and intracellular processing leading to transgene expression. Flow cytometry measurements can not provide detailed information about the uptake process itself. In this study, cell entry of rAAV2 and the peptide insertion mutants was therefore monitored as a separate event by quantifying intracellular vector genomes via qPCR.

Transduction of human melanoma cells (BLM), human embryonic kidney cells (HEK293), human epithelial cervix adenocarcinoma cells (HeLa) and human epithelial hepatocellular carcinoma cells (HepG2) with rAAV2 and the peptide insertion mutants revealed significant differences in vector entry efficiency. While the HSPG-binder mutants B1 and D5 entered cells with comparable (HeLa and HEK293) or higher efficiency (BLM and HepG2) than rAAV2, the HSPG-non-binder mutants A2 and C2 were significantly less efficiently taken up into all cell lines tested. This difference in vector internalization strongly suggests that clathrin-mediated endocytosis of A2 and C2 is not as efficient as proteoglycan-dependent uptake of D5 or the combination of both entry pathways in case of rAAV2 and B1 in several human cell types. The reason for this could be the above mentioned association with the extracellular HSPG network, which catches the HSPG-binder mutants and rAAV2 in close proximity to the cellular membrane leading to a higher probability of subsequent vector uptake compared to A2 and C2, which solely rely on the interaction with their receptor for internalization into the cell. Moreover, HSPG molecules were shown to cluster upon cationic

particle binding, leading to cortical actin rearrangement and particle engulfment [18],[23], which could well be a mechanism for enhanced uptake of HSPG-binder vectors.

A time course analysis of rAAV vector uptake on HeLa cells further revealed different internalization rates for HSPG-binder vectors including rAAV2 and the HSPG-non-binder mutants. One hour p.t., similar amounts of vector genomes of HSPG-binder vectors and rAAV2 were detected inside the cell, whereas compared to rAAV2, 8.22- and 12.48-times less intracellular genomes of the HSPG-non-binder mutants A2 and C2, respectively, were detected. Since the cellular receptors of A2 and C2 are unknown, the uptake of a rAAV2 vector with the well characterized RGD4C peptide inserted at position 587 was additionally analyzed. The model peptide RGD4C has been shown to bind selectively to $\alpha_v\beta_5$ and $\alpha_v\beta_3$ integrins [177],[178]. HeLa cell transduction by rAAV2-RGD4C587 was recently observed to proceed in a HSPG-independent, peptide-mediated fashion [87]. Strikingly, though $\alpha_v\beta_5$ integrin is highly expressed on HeLa cells [181], the internalization rate of RGD4C was significantly different from rAAV2, which uses the same integrin as a co-receptor. The time course of RGD4C-mediated cell transduction was similar to that of the HSPG-non-binder mutants A2 and C2, indicating that indeed, HSPG-binding enhances rAAV vector uptake. The previously published induction of conformational changes in the AAV2 capsid upon HSPG binding [8],[131],[186] is likely to allow endocytosis of rAAV2 but not of the insertion mutants due to their peptide displayed at the site of the HSPG-binding motif. However, the data obtained in this study provide strong evidence that also HSPG-binding per se is sufficient to induce the uptake of rAAV2 particles independent of the described structural rearrangements.

Vector uptake is the first crucial step for efficient transgene delivery. The fact that cellular receptors have different expression profiles at the cell surface is of great importance for the comparison of ligand-mediated transduction by rAAV peptide insertion mutants in this study. In principle, it might have been possible that all receptors targeted by A2 and C2 were saturated when transducing HeLa cells with 5000 genomic particles per cell. This hypothesis can be rejected because transduction with 8.22- and 12.48-times higher genomic particles per cell of A2 and C2 than of rAAV2 was shown to compensate the significantly less efficient internalization of the HSPG-non-binder mutants compared to rAAV2. The calculation for the adjustment of intracellular particles based on 5000 g.p./cell was further shown to be transferable to a low particle to cell ratio of 200 g.p./cell, albeit with a higher variability. This kind of adjustment of intracellular vector particles has also been successfully applied in a recent study on adenoviral vectors [181]. Shayakhmetov and colleagues observed a reduced internalization rate of an adenoviral vector with an RGD motif deletion compared to an unmodified adenoviral vector. By applying a 10-times higher vector dose of the RGD-deletion

vector, the internalization rates of both vectors could be adjusted, which was a prerequisite to compare the intracellular trafficking of the two adenoviral vectors [181].

4.2 Intracellular vector fate

Besides biochemical approaches using substances that specifically inhibit cellular processes [9],[11],[136],[137], the intracellular trafficking of AAV2 has been monitored by imaging studies. Visualization of AAV2 particles inside cells was achieved by antibody-staining of the viral capsid, by conjugating viral particles with fluorescent dyes and by genetically fusing fluorescent proteins to the N-terminus of the viral capsid protein VP2 [9],[91],[135],[127]. In this study, genetic incorporation of GFP into the capsid of rAAV mutants displaying peptide insertions at amino acid position 587 was shown to be feasible. However, the need of $5x10^6$ capsids per cell (corresponding to roughly 10^5 g.p./cell) to visualize fluorescent-protein-tagged rAAV vectors impeded further imaging-based analysis, since substantial differences in vector uptake were observed already between 2000 and 5000 g.p./cell. Thus, in order to resolve rather low particle to cell ratios, the intracellular characteristics of rAAV peptide insertion mutants were assessed by molecular techniques.

The intracellular routing of rAAV targeting vectors has not been assessed so far and some steps even remain unclear in case of AAV2. Recent studies on adenoviral vectors revealed that targeting different receptors either by constructing chimeric vectors or by inserting ligands into the capsid will lead to an altered intracellular trafficking compared to unmodified adenoviral vectors [35],[51]. The exchange of Ad5 fiber knob to Ad35 fiber knob resulted in a de-targeting of the vector from CAR to CD46, which caused a change in the intracellular trafficking route of the chimeric Ad5/Ad35 vector [35]. The combined shielding of vector particles and geneti-chemical coupling of transferrin to the Ad5 fiber HI-loop gave rise to efficient de- and re-targeting of the vector to the transferrin-pathway [51]. Even non-viral vectors, that naturally face the problem of entrapment in the endosomal compartment, could overcome this barrier by targeting a specific receptor: transgene expression could be highly increased by using an EGFR-targeted polyplex, suggesting more efficient gene delivery following receptor-mediated endocytosis [67].

Since differences in receptor usage and uptake mechanism were observed for the rAAV peptide insertion mutants analyzed in this study, an altered intracellular routing was assumed, similar to the above mentioned observations made for adenoviral and non-viral vectors. Knowing, that there was no receptor saturation in case of the HSPG-non-binder mutants A2 and C2 and that the adjustment of intracellular particles in a high and in a low particle to cell ratio was feasible, intracellular events were analyzed with vector particles having entered the cell in a synchronized manner. Starting with adjusted intracellular particles, all insertion mutants and rAAV2 have the same precondition because the drawback

in cell entry efficiency has been corrected by raising the vector dose in case of the HSPG-non-binder mutants A2 and C2. Transduction of HeLa cells with adjusted intracellular particles revealed that rAAV2 was most efficient. Contrary to transduction efficiencies obtained without balancing the differences in cell entry, the HSPG-non-binder mutants A2 and C2 now reached the same transduction efficiency as B1 with a high particle to cell ratio and were even superior to B1 in a low particle to cell ratio. Remarkably, A2 and C2 transduced HeLa cells with equal efficiency as rAAV2 in a low particle to cell ratio. D5 showed significantly lower transduction efficiency than all other rAAV vectors. These observations indicate that intracellular routing following clathrin-mediated endocytosis resulted in more efficient transgene expression than intracellular trafficking subsequent to proteoglycan-dependent uptake. There are in principle three potential explanations for this phenomenon: First, those vectors that were internalized in a proteoglycan-dependent fashion could have been degraded to a higher extent than the vectors taken up via clathrin-mediated endocytosis. Second, vector uncoating could have been impaired in case of proteoglycan-dependently internalized vectors, and third, vector internalization via clathrin-coated pits could have directed the endocytosed vectors to an exceeding intracellular trafficking route leading to efficient transgene expression compared to a less efficient intracellular routing of vectors internalized proteoglycan-dependently.

With respect to the first explanation, AAV-mediated transduction was previously shown to be enhanced by inhibiting the proteasome which degrades ubiquitin-conjugated proteins in both cytosol and nucleus [136],[147],[151]. Here, the results obtained by inhibitor studies with MG-132, a potent inhibitor of the 26S proteasome, revealed that not only rAAV2 was a target of proteasomal degradation, but also cell transduction mediated by the peptide insertion mutants was enhanced in the presence of MG-132. However, no considerable differences were observed between the strength of enhancement detected for HSPG-binder mutants and HSPG-non-binder mutants. This finding points out that less efficient transgene expression was not the consequence of increased proteasomal degradation of vectors internalized in a proteoglycan-dependent fashion. Noteworthy, Douar and colleagues figured out, that MG-132 treatment led to an accumulation of single-stranded viral genomes that would possibly have been degraded in cells with an active proteasome [136]. Thus, by enriching single-stranded viral genomes, the chance to become converted into a transcriptionally active double-stranded DNA template might be increased for rAAV2 as well as for the insertion mutants.

Viral uncoating and the conversion of single-stranded viral genomes into the transcriptionally active double-stranded form are believed to be rate-limiting steps in the processing of AAV [183],[190]. In the absence of adenoviral genes, which were shown to facilitate the genome conversion, cellular factors may directly mediate second-strand synthesis [154],[155],[191].

The conversion of viral ssDNA into dsDNA was shown to be accomplished 24h after infection [192]. Accumulation of viral genomes in a perinuclear area was observed between 15 and 30min post infection and almost all transduced particles were nucleus-associated 3h p.i. [9],[11],[91]. Therefore, vector genome transcripts, appearing subsequent to intracellular vector trafficking and early after nuclear translocation of vector ssDNA and conversion to dsDNA, were assessed between 1 and 4h post transduction (p.t.). Since AAV was shown to accumulate in nuclear invaginations (tubular channels extending deeply into the nucleoplasm) during that time frame in HeLa cells [91], vector genome transcripts rather than intra-nuclear vector genomes were measured to exclude detection of virions that are not located inside the nucleus. Already 1h p.t., irrespective of the particle to cell ratio (5000 i.g.p./cell or 200 i.g.p./cell), vector genome transcripts of all analyzed rAAV vectors were detectable. Although transcript levels of rAAV2, A2, B1 and C2 were higher than those of D5, transcripts of vector genomes increased in case of all rAAV vectors from 2h p.t. onwards. Since vector genome transcription happened in a similar time frame in case of rAAV2 and all peptide insertion mutants, it can be concluded that vector uncoating is not likely to be impaired in any of the insertion mutants. In line with the observations made for the analysis of transduction efficiency by flow cytometry, significant differences in vector transcript levels were observed between the different rAAV vectors 4h p.t. Transduction with 5000 i.g.p./cell did not result in different levels of vector genome transcripts for rAAV2, A2, B1 and C2. These four vectors had in common, that they were – at least partially – internalized via clathrin-mediated endocytosis. For D5, which was taken up clathrin-independently, significantly less transcripts of vector genomes were observed. Intriguingly, transduction with 200 i.g.p./cell led to significantly different levels of vector genome transcripts between B1 and rAAV2, A2 and C2, which were not significantly different among each other. D5, as observed for the high particle to cell ratio, showed again significantly fewer transcripts of vector genomes compared to the other rAAV vectors. These observations support the hypothesis, that clathrin-mediated endocytosis of rAAV2, A2, C2 – and in a high particle to cell ratio also B1 – possibly directed the rAAV vectors to an efficient intracellular trafficking route that favours endosomal escape of vector particles, subsequent nuclear translocation of vector genomes and transgene expression. In contrast, proteoglycan-dependent uptake of D5 – and in a low particle to cell ratio also of B1 – may be inappropriate for endosomal escape of the insertion mutants, subsequently leading to less vector particles that can uncoat and whose vector genomes will be translocated to the nucleus and expressed. A possible explanation for this observation may be the electrostatic interaction of the two positively charged insertion mutants B1 and D5 with HSPG. D5 was shown to have a high sensitivity to Heparin and therefore the electrostatic interaction between D5 and HSPG is likely to be strong. B1 was less sensitive to Heparin and likewise its affinity to HSPG should be weaker compared to D5.

The effect of the different HSPG-affinities could be that B1 can dissociate from HSPG in the endosome with a higher chance than the tightly bound D5. Consequently, B1 can escape the endosome more efficiently than D5 prior to lysosomal degradation, resulting in significantly higher transcript levels of B1 compared to D5, as it was observed with the low particle to cell ratio. As proposed for the highly positively charged insertion mutant D5, cationic DNA complexes, that are internalized following electrostatic interaction with HSPG were shown to be entrapped in endosomes and degraded in lysosomes [18],[57].

Regarding the third explanation mentioned above, i.e. an altered intracellular routing of the insertion mutants following proteoglycan-dependent uptake, a study on adenoviral vectors recently demonstrated that the exchange of Ad5 fiber knob to Ad35 fiber knob gave rise to a change in intracellular trafficking of the chimeric Ad5/Ad35 vector caused by internalization via CD46 instead of CAR [35]. Based on electron microscopic visualization of adenoviral particles within different intracellular compartments, Shayakhmetov and colleagues depicted the intracellular distribution of Ad and Ad5/Ad35 vectors. Contrary to Ad5, which already escaped from early endosomes by 2h p.i. and was found mostly in the cytosol or perinuclear space, the majority of chimeric vectors still resided in the endosomal compartment and only few chimeric vector particles were detected in cytosol and perinuclear space. Thus, the authors proposed that chimeric Ad5/Ad35 vectors internalized via CD46 were directed to a less efficient intracellular trafficking route that probably trapped the majority of viruses in late/lysosomal compartments. In this study, the hypothesis that clathrin-mediated endocytosis could be superior to proteoglycan-dependent uptake with respect to intracellular processing of vector particles was further tested by monitoring the intracellular distribution of rAAV2 vector genomes compared to B1 and D5. The subcellular fractionation of HeLa cells transduced either with rAAV2 or the insertion mutants B1 and D5 revealed a picture resembling the one obtained for adenoviral vectors. Like adenovirus, AAV escapes from the endosomal compartment but it is still a matter of debate whether the release of AAV takes place in an early or late endosomal stage [11],[135],[136],[138],[152]. After HeLa cell fractionation 2h p.t., a minor proportion of rAAV2, B1 and D5 vector genomes were found in the cytosol. rAAV2 vector genomes were detected in membrane and nuclear fractions with a ratio of 0.7 reflecting vector genomes in membranes over vector genomes in nuclei. Thus, the major portion of rAAV2 vector genomes was present inside nuclei 2h p.t. In contrast, significantly higher ratios were obtained for B1 and D5, indicating that vector genomes of the HSPG-binder vectors B1 and D5 predominantly resided inside membrane-coated cellular compartments 2h p.t. From the fractionation procedure itself, the endosomal compartment could not be distinguished from mitochondria and the endoplasmic reticulum, since they were collected in the same fraction, but from the current knowledge AAV would most likely be found in endosomes [11],[135],[136],[138],[152]. Hence, 2h p.t., rAAV2 had already escaped

the endosome to a high extent and its vector DNA was nucleus-associated, while B1 and D5 were mainly present in the endosomal compartment and only a minor part of their vector genomes entered the nucleus. Presumably, as observed for the Ad5/Ad35 vector and already suggested above, proteoglycan-dependent uptake of B1 and D5 led to an altered intracellular routing that did not favour endosomal escape of the two peptide insertion mutants. Although assessing the same problem with different methods, similar conclusions to the chimeric adenoviral targeting vector could be drawn for the rAAV insertion mutants impaired in efficient transgene expression in this study.

Previous studies revealed that endosomal acidification is necessary for AAV2-mediated cell transduction [11],[136],[137]. Having proposed that the insertion mutants B1 and D5 could be directed to a distinct intracellular trafficking route, Bafilomycin A_1-treatment should clarify, whether endosomal maturation is required for cell transduction by B1 and D5. A hint towards an involvement of endosomal maturation in intracellular trafficking following HSPG-dependent uptake comes from the observation that HSPG degradation products could not be detected in Bafilomycin-treated rat hepatocytes, whereas in the absence of the drug, small HS fragments were found in lysosomes [193]. In addition to specific inhibition of the vacuolar ATPase, Bafilomycin was shown to block the transport from early to late endosomes, possibly by inhibiting the budding of vesicles from early endosomes [184],[193]. Strinkingly, cell transduction by rAAV2 as well as by B1 and D5 was almost completely abolished in the presence of Bafilomycin. This observation showed that endosomal maturation is crucial for intracellular processing of rAAV2 and the insertion mutants B1 and D5 irrespective of the endocytic mechanism. Recently, a clathrin- and caveolin-independent endocytic pathway has been identified in mammalian cells that was shown to be involved in the internalization and trafficking of cell surface proteoglycans and proteoglycan-binding ligands [56],[194]. The marker protein of this pathway, flotillin-1, has been identified in purified endosomes [194]. HSPG as well as HSPG-binding cationic polymers were shown to be internalized clathrin- and caveolin-independently, but dependent on flotillin-1 and dynamin. Subsequently, proteoglycan-bound ligands were found associated with flotillin-1-positive vesicles and efficiently trafficked to late endosomes. Interestingly, this proteoglycan-dependent pathway did not require phosphatidyl-inositol-3 kinase (PI3K)-dependent sorting from early endosomes [56], whereas endocytosis and nuclear trafficking of AAV2 was reported to be controlled by Rac1 and PI3K activation [9]. Therefore, PI3K-dependent sorting might be an essential process leading to efficient intracellular processing of rAAV2 and most likely also of the insertion mutants internalized in a clathrin-mediated fashion. The proteoglycan-dependent uptake of peptide insertion mutants might misguide the mutants to the flotillin-1 pathway lacking PI3K-dependent sorting, which could lead to an accumulation of the insertion mutants in late endosomal compartments that they are unable to escape from.

To gain additional knowledge of differences in endosomal trafficking between rAAV2 and the rAAV peptide insertion mutants, different endosomal compartments will have to be fractionated and subsequently analyzed regarding the presence of rAAV vector genomes and a well defined endosomal marker like flotillin-1 or Rab proteins to identify individual pathways.

## 4.3 Consequences of non-natural receptor binding: a model

The results obtained in this study provide evidence for a model that depicts the intracellular consequences of novel ligand-receptor interactions mediated by rAAV peptide insertion mutants.

As anticipated, the first interaction with the cell – i.e. primary receptor binding – differs between the analyzed rAAV vectors. In line with the current knowledge, rAAV2 attaches to its primary receptor HSPG, followed by co-receptor binding and clathrin-mediated endocytosis. The rAAV mutants A2 and C2 do not use HSPG as an attachment receptor but rely on their novel ligand-receptor interaction for clathrin-dependent uptake into the cell. Like rAAV2, the rAAV mutant B1 is able to bind to HSPG and to an additional internalization receptor, which mediates clathrin-dependent internalization of the vector. Since they differ in only one amino acid, B1 and C2 are likely to bind to the same or a very similar receptor. Contrary to C2, in case of B1, the affinity of the peptide ligand to its receptor may not be sufficient to trigger endocytosis. HSPG binding could enhance the ligand-receptor interaction of B1 or increase the chance of proper receptor binding by clustering numerous B1 vector particles at the cell surface. Consequently, if there are only few B1 vector particles present, the probability of being internalized via clathrin-mediated endocytosis decreases. The rAAV mutant D5 binds to HSPG with a high affinity and does not seem to use an additional receptor. The uptake of D5 and B1, if it can not be internalized in a clathrin-mediated fashion, is dependent on an electrostatic interaction of the positively charged peptide insertions of D5 and B1 with the negatively charged cell surface proteoglycans.

Following clathrin-mediated endocytosis, rAAV2 – and probably also A2, B1 and C2 – are efficiently processed inside endosomes. It is believed that rAAV2 trafficking is dependent on the activation of Rac1 and PI3K, the latter of which is involved in endosomal sorting. All vectors that are internalized in a clathrin-dependent fashion seem to efficiently escape from the endosomal compartment and to be processed efficiently: compared to rAAV2, no significant differences in vector degradation and uncoating or transgene expression were observed.

Proteoglycan-dependent internalization results in an altered intracellular routing of the rAAV mutants B1 and D5. Similar to vector trafficking following clathrin-mediated endocytosis, also vector trafficking subsequent to proteoglycan-dependent uptake relies on endosomal

maturation but it is not clear if both routes share an early endosomal compartment. The pathway following proteoglycan-dependent uptake of B1 and D5 is obviously not favourable for vector processing, since significantly more vector genomes are present in endosomes compared to rAAV2-mediated accumulation of vector genomes in the nucleus. Entrapment of B1 and D5 in endosomes could happen due to their electrostatic interaction with HSPG, leading to an impaired dissociation of the insertion mutants from the proteoglycan. Although with significantly lower levels compared to rAAV2, A2 and C2, vector genome transcripts of D5 and B1 appear in a similar time frame; hence, some of the internalized vector particles are able to escape from the endosome and to uncoat prior to lysosomal degradation. However, the question if B1- and D5-containing vesicles fuse with the pathway following clathrin-mediated endocytosis or if B1 and D5 escape from endosomes bypassing the sorting endosome remains to be answered.
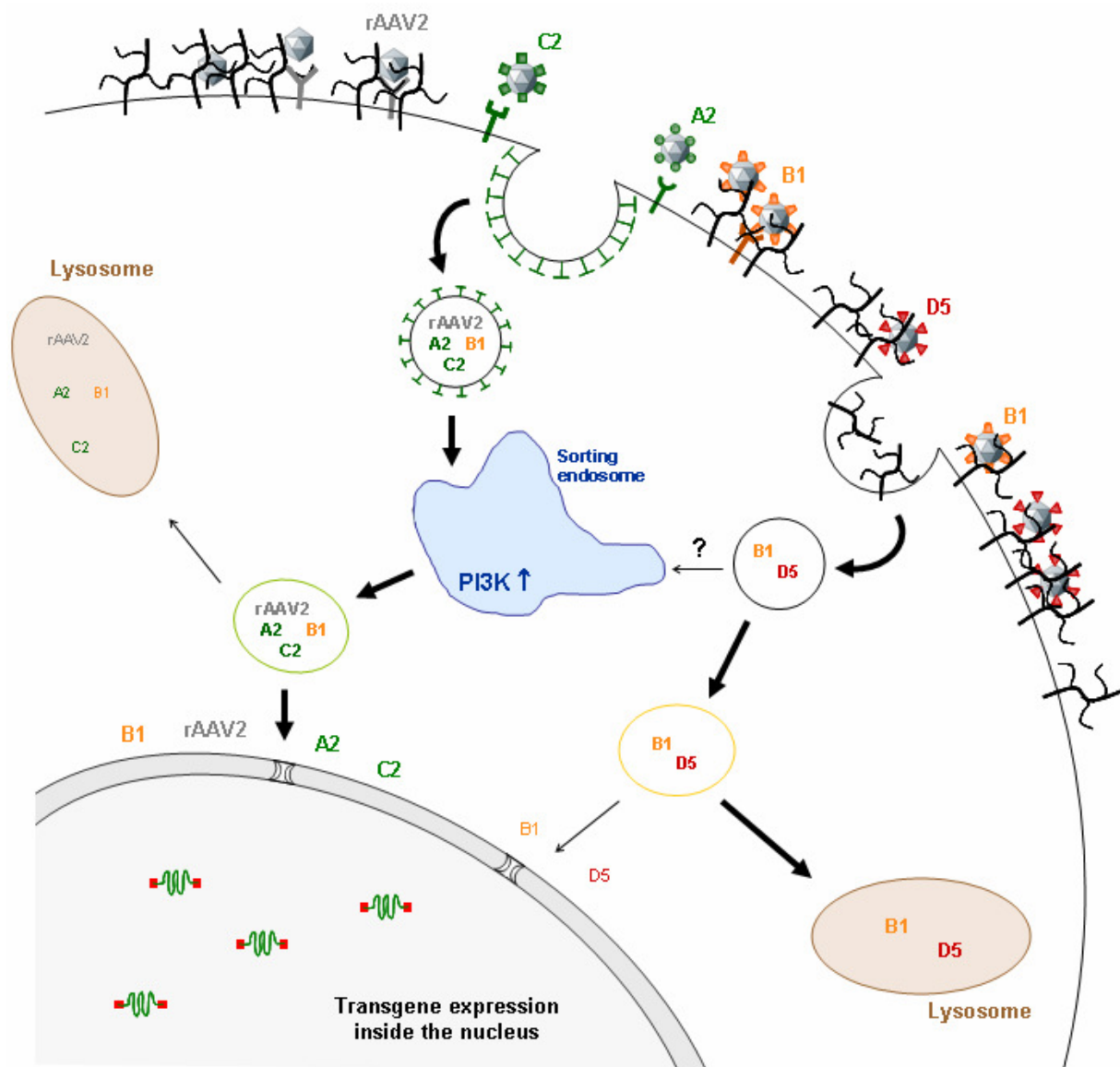
Figure 24: Model for the uptake of rAAV2 and rAAV peptide insertion mutants and the intracellular consequences

Like rAAV2, the insertion mutants A2, B1 and C2 are internalized into the cell in a clathrin-mediated fashion. Following clathrin-mediated endocytosis, rAAV2 and the insertion mutants A2 and C2 are efficiently processed, probably via early and late endosomes similar to rAAV2, which is assumed to include PI3K-dependent sorting in an early endosomal compartment. Subsequent to vector uncoating, efficient transgene expression takes place inside the nucleus. If B1 is able to bind to its receptor, which is likely to occur in a high particle number, this positively charged insertion mutant is also taken up via clathrin-coated pits and consequently takes the same pathway as described for rAAV2, A2 and C2. B1, like the highly positively charged insertion mutant D5, can also be taken up into the cell without binding to an additional receptor, presumably via electrostatic interaction with HSPG. Following proteoglycan-dependent internalization, the insertion mutants are inefficiently processed. Only a small proportion of vector particles that will subsequently uncoat and deliver their genome to the nucleus for expression are able to escape the endosome prior to lysosomal degradation.

In conclusion, this study provides strong evidence that the peptide ligand inserted into the AAV capsid determines the cell entry mode of the insertion mutant and thereby the efficiency of transgene delivery to the nucleus. To achieve efficient intracellular processing, the insertion mutant – like rAAV2 – has to target a specific cellular receptor triggering clathrin-mediated endocytosis. With regard to cell type specificity, the native tropism of AAV2, mediated by its HSPG-binding ability, should be ablated. Current studies carried out in our group point towards the achievement of a narrow tissue tropism by HSPG-non-binder mutants selected on primary human keratinocytes *in vitro* and BLM cells *in vivo* [John von Freyend and Sallach, unpublished data]. The *in vivo* selections further showed a redirection of the selected HSPG-non-binder mutants from the liver and other organs such as spleen, muscle, kidney and lung to the tumour [John von Freyend, unpublished data]. The re-targeting of a HSPG-non-binder mutant with the property of efficient transgene delivery to the cell type of interest, while de-targeting the rAAV insertion mutant from non-target cells can indirectly achieve vector-dose reduction. Therefore, an AAV targeting vector mediating efficient and specific gene expression *in vivo* should carry a peptide insertion that both ablates HSPG-binding and fosters clathrin-mediated endocytosis of the vector by binding to a cell-type-specific receptor.

5 References

[1]   D.V. Schaffer, J.T. Koerber, and K. Lim, "Molecular engineering of viral gene delivery vehicles," *Annual Review of Biomedical Engineering*, vol. 10, 2008, pp. 169-194.

[2]   A. Sharma, X. Li, D.S. Bangari, and S.K. Mittal, "Adenovirus receptors and their implications in gene delivery," *Virus Research*, vol. 143, Aug. 2009, pp. 184-194.

[3]   R. Waehler, S.J. Russell, and D.T. Curiel, "Engineering targeted viral vectors for gene therapy," *Nature Reviews. Genetics*, vol. 8, Aug. 2007, pp. 573-587.

[4]   P.L. Leopold and R.G. Crystal, "Intracellular trafficking of adenovirus: many means to many ends," *Advanced Drug Delivery Reviews*, vol. 59, Aug. 2007, pp. 810-821.

[5]   S. Kronenberg, J.A. Kleinschmidt, and B. Böttcher, "Electron cryo-microscopy and image reconstruction of adeno-associated virus type 2 empty capsids," *EMBO Reports*, vol. 2, Nov. 2001, pp. 997-1002.

[6]   C. Summerford and R.J. Samulski, "Membrane-associated heparan sulfate proteoglycan is a receptor for adeno-associated virus type 2 virions," *Journal of Virology*, vol. 72, Feb. 1998, pp. 1438-1445.

[7]   H. Büning, L. Perabo, O. Coutelle, S. Quadt-Humme, and M. Hallek, "Recent developments in adeno-associated virus vector technology," *The Journal of Gene Medicine*, vol. 10, Jul. 2008, pp. 717-733.

[8]   C. Summerford, J.S. Bartlett, and R.J. Samulski, "AlphaVbeta5 integrin: a co-receptor for adeno-associated virus type 2 infection," *Nature Medicine*, vol. 5, Jan. 1999, pp. 78-82.

[9]   S. Sanlioglu, P.K. Benson, J. Yang, E.M. Atkinson, T. Reynolds, and J.F. Engelhardt, "Endocytosis and nuclear trafficking of adeno-associated virus type 2 are controlled by rac1 and phosphatidylinositol-3 kinase activation," *Journal of Virology*, vol. 74, Oct. 2000, pp. 9184-9196.

[10]   D. Duan, Q. Li, A.W. Kao, Y. Yue, J.E. Pessin, and J.F. Engelhardt, "Dynamin is required for recombinant adeno-associated virus type 2 infection," *Journal of Virology*, vol. 73, Dec. 1999, pp. 10371-10376.

[11]   J.S. Bartlett, R. Wilcher, and R.J. Samulski, "Infectious entry pathway of adeno-associated virus and adeno-associated virus vectors," *Journal of Virology*, vol. 74, Mar. 2000, pp. 2777-2785.

[12]   N. Kaludov, K.E. Brown, R.W. Walters, J. Zabner, and J.A. Chiorini, "Adeno-associated virus serotype 4 (AAV4) and AAV5 both require sialic acid binding for hemagglutination and efficient transduction but differ in sialic acid linkage specificity," *Journal of Virology*, vol. 75, Aug. 2001, pp. 6884-6893.

[13]   G. Di Pasquale, B.L. Davidson, C.S. Stein, I. Martins, D. Scudiero, A. Monks, and J.A.

Chiorini, "Identification of PDGFR as a receptor for AAV-5 transduction," *Nature Medicine*, vol. 9, Oct. 2003, pp. 1306-1312.

[14] U. Bantel-Schaal, I. Braspenning-Wesch, and J. Kartenbeck, "Adeno-associated virus type 5 exploits two different entry pathways in human embryo fibroblasts," *The Journal of General Virology*, vol. 90, Feb. 2009, pp. 317-322.

[15] U. Bantel-Schaal, B. Hub, and J. Kartenbeck, "Endocytosis of adeno-associated virus type 5 leads to accumulation of virus particles in the Golgi compartment," *Journal of Virology*, vol. 76, Mar. 2002, pp. 2340-2349.

[16] C.J. Buchholz, M.D. Mühlebach, and K. Cichutek, "Lentiviral vectors with measles virus glycoproteins - dream team for gene transfer?," *Trends in Biotechnology*, vol. 27, May. 2009, pp. 259-265.

[17] M. Morille, C. Passirani, A. Vonarbourg, A. Clavreul, and J. Benoit, "Progress in developing cationic vectors for non-viral systemic gene therapy against cancer," *Biomaterials*, vol. 29, Sep. 2008, pp. 3477-3496.

[18] G.M.K. Poon and J. Gariépy, "Cell-surface proteoglycans as molecular portals for cationic peptide and polymer entry into cells," *Biochemical Society Transactions*, vol. 35, Aug. 2007, pp. 788-793.

[19] A. El Ouahabi, M. Thiry, S. Schiffmann, R. Fuks, H. Nguyen-Tran, J.M. Ruysschaert, and M. Vandenbranden, "Intracellular visualization of BrdU-labeled plasmid DNA/cationic liposome complexes," *The Journal of Histochemistry and Cytochemistry: Official Journal of the Histochemistry Society*, vol. 47, Sep. 1999, pp. 1159-1166.

[20] T. Merdan, K. Kunath, D. Fischer, J. Kopecek, and T. Kissel, "Intracellular processing of poly(ethylene imine)/ribozyme complexes can be observed in living cells by using confocal laser scanning microscopy and inhibitor experiments," *Pharmaceutical Research*, vol. 19, Feb. 2002, pp. 140-146.

[21] H. Matsui, L.G. Johnson, S.H. Randell, and R.C. Boucher, "Loss of binding and entry of liposome-DNA complexes decreases transfection efficiency in differentiated airway epithelial cells," *The Journal of Biological Chemistry*, vol. 272, Jan. 1997, pp. 1117-1126.

[22] R.P. Harbottle, R.G. Cooper, S.L. Hart, A. Ladhoff, T. McKay, A.M. Knight, E. Wagner, A.D. Miller, and C. Coutelle, "An RGD-oligolysine peptide: a prototype construct for integrin-mediated gene delivery," *Human Gene Therapy*, vol. 9, May. 1998, pp. 1037-1047.

[23] I. Kopatz, J. Remy, and J. Behr, "A model for non-viral gene delivery: through syndecan adhesion molecules and powered by actin," *The Journal of Gene Medicine*, vol. 6, Jul. 2004, pp. 769-776.

[24] Y. Xu and F.C. Szoka, "Mechanism of DNA release from cationic liposome/DNA

complexes used in cell transfection," *Biochemistry*, vol. 35, May. 1996, pp. 5616-5623.

[25] O. Zelphati and F.C. Szoka, "Mechanism of oligonucleotide release from cationic liposomes," *Proceedings of the National Academy of Sciences of the United States of America*, vol. 93, Oct. 1996, pp. 11493-11498.

[26] O. Boussif, F. Lezoualc'h, M.A. Zanta, M.D. Mergny, D. Scherman, B. Demeneix, and J.P. Behr, "A versatile vector for gene and oligonucleotide transfer into cells in culture and in vivo: polyethylenimine," *Proceedings of the National Academy of Sciences of the United States of America*, vol. 92, Aug. 1995, pp. 7297-7301.

[27] P. Kreiss, B. Cameron, R. Rangara, P. Mailhe, O. Aguerre-Charriol, M. Airiau, D. Scherman, J. Crouzet, and B. Pitard, "Plasmid DNA size does not affect the physicochemical properties of lipoplexes but modulates gene transfer efficiency," *Nucleic Acids Research*, vol. 27, Oct. 1999, pp. 3792-3798.

[28] J. Zabner, M. Seiler, R. Walters, R.M. Kotin, W. Fulgeras, B.L. Davidson, and J.A. Chiorini, "Adeno-associated virus type 5 (AAV5) but not AAV2 binds to the apical surfaces of airway epithelia and facilitates gene transfer," *Journal of Virology*, vol. 74, Apr. 2000, pp. 3852-3858.

[29] J.R. Smith-Arica, A.J. Thomson, R. Ansell, J. Chiorini, B. Davidson, and J. McWhir, "Infection efficiency of human and mouse embryonic stem cells using adenoviral and adeno-associated viral vectors," *Cloning and Stem Cells*, vol. 5, 2003, pp. 51-62.

[30] B.S. Schnierle, J. Stitz, V. Bosch, F. Nocken, H. Merget-Millitzer, M. Engelstädter, R. Kurth, B. Groner, and K. Cichutek, "Pseudotyping of murine leukemia virus with the envelope glycoproteins of HIV generates a retroviral vector with specificity of infection for CD4-expressing cells," *Proceedings of the National Academy of Sciences of the United States of America*, vol. 94, Aug. 1997, pp. 8640-8645.

[31] J. Cronin, X. Zhang, and J. Reiser, "Altering the tropism of lentiviral vectors through pseudotyping," *Current Gene Therapy*, vol. 5, Aug. 2005, pp. 387-398.

[32] J.C. Burns, T. Friedmann, W. Driever, M. Burrascano, and J.K. Yee, "Vesicular stomatitis virus G glycoprotein pseudotyped retroviral vectors: concentration to very high titer and efficient gene transfer into mammalian and nonmammalian cells," *Proceedings of the National Academy of Sciences of the United States of America*, vol. 90, Sep. 1993, pp. 8033-8037.

[33] A.S. Cockrell and T. Kafri, "Gene delivery by lentivirus vectors," *Molecular Biotechnology*, vol. 36, Jul. 2007, pp. 184-204.

[34] M.J.E. Havenga, A.A.C. Lemckert, O.J.A.E. Ophorst, M. van Meijer, W.T.V. Germeraad, J. Grimbergen, M.A. van Den Doel, R. Vogels, J. van Deutekom, A.A.M. Janson, J.D. de Bruijn, F. Uytdehaag, P.H.A. Quax, T. Logtenberg, M. Mehtali, and A.

Bout, "Exploiting the natural diversity in adenovirus tropism for therapy and prevention of disease," *Journal of Virology*, vol. 76, May. 2002, pp. 4612-4620.

[35] D.M. Shayakhmetov, Z. Li, V. Ternovoi, A. Gaggar, H. Gharwan, and A. Lieber, "The interaction between the fiber knob domain and the cellular attachment receptor determines the intracellular trafficking route of adenoviruses," *Journal of Virology*, vol. 77, Mar. 2003, pp. 3712-3723.

[36] G.T. Mercier, J.A. Campbell, J.D. Chappell, T. Stehle, T.S. Dermody, and M.A. Barry, "A chimeric adenovirus vector encoding reovirus attachment protein sigma1 targets cells expressing junctional adhesion molecule 1," *Proceedings of the National Academy of Sciences of the United States of America*, vol. 101, Apr. 2004, pp. 6188-6193.

[37] V. Krasnykh, N. Belousova, N. Korokhov, G. Mikheeva, and D.T. Curiel, "Genetic targeting of an adenovirus vector via replacement of the fiber protein with the phage T4 fibritin," *Journal of Virology*, vol. 75, May. 2001, pp. 4176-4183.

[38] B. Hauck, L. Chen, and W. Xiao, "Generation and characterization of chimeric recombinant AAV vectors," *Molecular Therapy: The Journal of the American Society of Gene Therapy*, vol. 7, Mar. 2003, pp. 419-425.

[39] J.E. Rabinowitz, D.E. Bowles, S.M. Faust, J.G. Ledford, S.E. Cunningham, and R.J. Samulski, "Cross-dressing the virion: the transcapsidation of adeno-associated virus serotypes functionally defines subgroups," *Journal of Virology*, vol. 78, May. 2004, pp. 4421-4432.

[40] Z. Wu, A. Asokan, and R.J. Samulski, "Adeno-associated virus serotypes: vector toolkit for human gene therapy," *Molecular Therapy: The Journal of the American Society of Gene Therapy*, vol. 14, Sep. 2006, pp. 316-327.

[41] L. Gigout, P. Rebollo, N. Clement, K.H. Warrington, N. Muzyczka, R.M. Linden, and T. Weber, "Altering AAV tropism with mosaic viral capsids," *Molecular Therapy: The Journal of the American Society of Gene Therapy*, vol. 11, Jun. 2005, pp. 856-865.

[42] B. Hauck, R.R. Xu, J. Xie, W. Wu, Q. Ding, M. Sipler, H. Wang, L. Chen, J.F. Wright, and W. Xiao, "Efficient AAV1-AAV2 hybrid vector for gene therapy of hemophilia," *Human Gene Therapy*, vol. 17, Jan. 2006, pp. 46-54.

[43] S. Snitkovsky and J.A. Young, "Cell-specific viral targeting mediated by a soluble retroviral receptor-ligand fusion protein," *Proceedings of the National Academy of Sciences of the United States of America*, vol. 95, Jun. 1998, pp. 7063-7068.

[44] M.A. Starovasnik, A.C. Braisted, and J.A. Wells, "Structural mimicry of a native protein by a minimized binding domain," *Proceedings of the National Academy of Sciences of the United States of America*, vol. 94, Sep. 1997, pp. 10080-10085.

[45] K. Morizono, G. Bristol, Y.M. Xie, S.K. Kung, and I.S. Chen, "Antibody-directed

targeting of retroviral vectors via cell surface antigens," *Journal of Virology*, vol. 75, Sep. 2001, pp. 8016-8020.

[46] K. Ohno, K. Sawai, Y. Iijima, B. Levin, and D. Meruelo, "Cell-specific targeting of Sindbis virus vectors displaying IgG-binding domains of protein A," *Nature Biotechnology*, vol. 15, Aug. 1997, pp. 763-767.

[47] I. Dmitriev, E. Kashentseva, B.E. Rogers, V. Krasnykh, and D.T. Curiel, "Ectodomain of coxsackievirus and adenovirus receptor genetically fused to epidermal growth factor mediates adenovirus targeting to epidermal growth factor receptor-positive cells," *Journal of Virology*, vol. 74, Aug. 2000, pp. 6875-6884.

[48] A.V. Pereboev, J.M. Nagle, M.A. Shakhmatov, P.L. Triozzi, Q.L. Matthews, Y. Kawakami, D.T. Curiel, and J.L. Blackwell, "Enhanced gene transfer to mouse dendritic cells using adenoviral vectors coated with a novel adapter molecule," *Molecular Therapy: The Journal of the American Society of Gene Therapy*, vol. 9, May. 2004, pp. 712-720.

[49] J. Lanciotti, A. Song, J. Doukas, B. Sosnowski, G. Pierce, R. Gregory, S. Wadsworth, and C. O'Riordan, "Targeting adenoviral vectors using heterofunctional polyethylene glycol FGF2 conjugates," *Molecular Therapy: The Journal of the American Society of Gene Therapy*, vol. 8, Jul. 2003, pp. 99-107.

[50] K. Ogawara, M.G. Rots, R.J. Kok, H.E. Moorlag, A. Van Loenen, D.K.F. Meijer, H.J. Haisma, and G. Molema, "A novel strategy to modify adenovirus tropism and enhance transgene delivery to activated vascular endothelial cells in vitro and in vivo," *Human Gene Therapy*, vol. 15, May. 2004, pp. 433-443.

[51] F. Kreppel, J. Gackowski, E. Schmidt, and S. Kochanek, "Combined genetic and chemical capsid modifications enable flexible and efficient de- and retargeting of adenovirus vectors," *Molecular Therapy: The Journal of the American Society of Gene Therapy*, vol. 12, Jul. 2005, pp. 107-117.

[52] S. Ponnazhagan, G. Mahendra, S. Kumar, J.A. Thompson, and M. Castillas, "Conjugate-based targeting of recombinant adeno-associated virus type 2 vectors by using avidin-linked ligands," *Journal of Virology*, vol. 76, Dec. 2002, pp. 12900-12907.

[53] J.S. Bartlett, J. Kleinschmidt, R.C. Boucher, and R.J. Samulski, "Targeted adeno-associated virus vector transduction of nonpermissive cells mediated by a bispecific F(ab'gamma)2 antibody," *Nature Biotechnology*, vol. 17, Feb. 1999, pp. 181-186.

[54] M.U. Ried, A. Girod, K. Leike, H. Büning, and M. Hallek, "Adeno-associated virus capsids displaying immunoglobulin-binding domains permit antibody-mediated vector retargeting to specific cell surface receptors," *Journal of Virology*, vol. 76, May. 2002, pp. 4559-4566.

[55] M. Ogris and E. Wagner, "Targeting tumors with non-viral gene delivery systems,"

Drug Discovery Today, vol. 7, Apr. 2002, pp. 479-485.

[56] C.K. Payne, S.A. Jones, C. Chen, and X. Zhuang, "Internalization and trafficking of cell surface proteoglycans and proteoglycan-binding ligands," *Traffic (Copenhagen, Denmark)*, vol. 8, Apr. 2007, pp. 389-401.

[57] J. Rejman, A. Bragonzi, and M. Conese, "Role of clathrin- and caveolae-mediated endocytosis in gene transfer mediated by lipo- and polyplexes," *Molecular Therapy: The Journal of the American Society of Gene Therapy*, vol. 12, Sep. 2005, pp. 468-474.

[58] L.C. Mounkes, W. Zhong, G. Cipres-Palacin, T.D. Heath, and R.J. Debs, "Proteoglycans mediate cationic liposome-DNA complex-based gene delivery in vitro and in vivo," *The Journal of Biological Chemistry*, vol. 273, Oct. 1998, pp. 26164-26170.

[59] A. Kichler, C. Leborgne, E. Coeytaux, and O. Danos, "Polyethylenimine-mediated gene delivery: a mechanistic study," *The Journal of Gene Medicine*, vol. 3, Apr. 2001, pp. 135-144.

[60] R. Kircheis, A. Kichler, G. Wallner, M. Kursa, M. Ogris, T. Felzmann, M. Buchberger, and E. Wagner, "Coupling of cell-binding ligands to polyethylenimine for targeted gene delivery," *Gene Therapy*, vol. 4, May. 1997, pp. 409-418.

[61] R. Kircheis, L. Wightman, A. Schreiber, B. Robitza, V. Rössler, M. Kursa, and E. Wagner, "Polyethylenimine/DNA complexes shielded by transferrin target gene expression to tumors after systemic application," *Gene Therapy*, vol. 8, Jan. 2001, pp. 28-40.

[62] M.A. Zanta, O. Boussif, A. Adib, and J.P. Behr, "In vitro gene delivery to hepatocytes with galactosylated polyethylenimine," *Bioconjugate Chemistry*, vol. 8, Dec. 1997, pp. 839-844.

[63] T. Bettinger, J.S. Remy, and P. Erbacher, "Size reduction of galactosylated PEI/DNA complexes improves lectin-mediated gene transfer into hepatocytes," *Bioconjugate Chemistry*, vol. 10, Aug. 1999, pp. 558-561.

[64] S.S. Diebold, H. Lehrmann, M. Kursa, E. Wagner, M. Cotten, and M. Zenke, "Efficient gene delivery into human dendritic cells by adenovirus polyethylenimine and mannose polyethylenimine transfection," *Human Gene Therapy*, vol. 10, Mar. 1999, pp. 775-786.

[65] S.S. Diebold, M. Kursa, E. Wagner, M. Cotten, and M. Zenke, "Mannose polyethylenimine conjugates for targeted DNA delivery into dendritic cells," *The Journal of Biological Chemistry*, vol. 274, Jul. 1999, pp. 19087-19094.

[66] P. Erbacher, J.S. Remy, and J.P. Behr, "Gene transfer with synthetic virus-like particles via the integrin-mediated endocytosis pathway," *Gene Therapy*, vol. 6, Jan.

1999, pp. 138-145.

[67]   T. Blessing, M. Kursa, R. Holzhauser, R. Kircheis, and E. Wagner, "Different strategies for formation of pegylated EGF-conjugated PEI/DNA complexes for targeted gene delivery," *Bioconjugate Chemistry*, vol. 12, Aug. 2001, pp. 529-537.

[68]   X. Li, P. Stuckert, I. Bosch, J.D. Marks, and W.A. Marasco, "Single-chain antibody-mediated gene delivery into ErbB2-positive human breast cancer cells," *Cancer Gene Therapy*, vol. 8, Aug. 2001, pp. 555-565.

[69]   T.J. Gollan and M.R. Green, "Redirecting retroviral tropism by insertion of short, nondisruptive peptide ligands into envelope," *Journal of Virology*, vol. 76, Apr. 2002, pp. 3558-3563.

[70]   N.V. Somia, M. Zoppé, and I.M. Verma, "Generation of targeted retroviral vectors by using single-chain variable fragment: an approach to in vivo gene delivery," *Proceedings of the National Academy of Sciences of the United States of America*, vol. 92, Aug. 1995, pp. 7570-7574.

[71]   S.J. Russell, R.E. Hawkins, and G. Winter, "Retroviral vectors displaying functional antibody fragments," *Nucleic Acids Research*, vol. 21, Mar. 1993, pp. 1081-1085.

[72]   M. Marin, D. Noël, S. Valsesia-Wittman, F. Brockly, M. Etienne-Julan, S. Russell, F.L. Cosset, and M. Piechaczyk, "Targeted infection of human cells via major histocompatibility complex class I molecules by Moloney murine leukemia virus-derived viruses displaying single-chain antibody fragment-envelope fusion proteins," *Journal of Virology*, vol. 70, May. 1996, pp. 2957-2962.

[73]   A.K. Fielding, M. Maurice, F.J. Morling, F.L. Cosset, and S.J. Russell, "Inverse targeting of retroviral vectors: selective gene transfer in a mixed population of hematopoietic and nonhematopoietic cells," *Blood*, vol. 91, Mar. 1998, pp. 1802-1809.

[74]   N. Kasahara, A.M. Dozy, and Y.W. Kan, "Tissue-specific targeting of retroviral vectors through ligand-receptor interactions," *Science (New York, N.Y.)*, vol. 266, Nov. 1994, pp. 1373-1376.

[75]   M. Katane, E. Takao, Y. Kubo, R. Fujita, and H. Amanuma, "Factors affecting the direct targeting of murine leukemia virus vectors containing peptide ligands in the envelope protein," *EMBO Reports*, vol. 3, Sep. 2002, pp. 899-904.

[76]   M.P. Chadwick, F.J. Morling, F.L. Cosset, and S.J. Russell, "Modification of retroviral tropism by display of IGF-I," *Journal of Molecular Biology*, vol. 285, Jan. 1999, pp. 485-494.

[77]   T.J. Wickham, E. Tzeng, L.L. Shears, P.W. Roelvink, Y. Li, G.M. Lee, D.E. Brough, A. Lizonova, and I. Kovesdi, "Increased in vitro and in vivo gene transfer by adenovirus vectors containing chimeric fiber proteins," *Journal of Virology*, vol. 71, Nov. 1997, pp. 8221-8229.

[78] I. Dmitriev, V. Krasnykh, C.R. Miller, M. Wang, E. Kashentseva, G. Mikheeva, N. Belousova, and D.T. Curiel, "An adenovirus vector with genetically modified fibers demonstrates expanded tropism via utilization of a coxsackievirus and adenovirus receptor-independent cell entry mechanism," *Journal of Virology*, vol. 72, Dec. 1998, pp. 9706-9713.

[79] S.A. Nicklin, D.J. Von Seggern, L.M. Work, D.C. Pek, A.F. Dominiczak, G.R. Nemerow, and A.H. Baker, "Ablating adenovirus type 5 fiber-CAR binding and HI loop insertion of the SIGYPLP peptide generate an endothelial cell-selective adenovirus," *Molecular Therapy: The Journal of the American Society of Gene Therapy*, vol. 4, Dec. 2001, pp. 534-542.

[80] N. Koizumi, H. Mizuguchi, N. Utoguchi, Y. Watanabe, and T. Hayakawa, "Generation of fiber-modified adenovirus vectors containing heterologous peptides in both the HI loop and C terminus of the fiber knob," *The Journal of Gene Medicine*, vol. 5, Apr. 2003, pp. 267-276.

[81] M.K. Magnusson, S.S. Hong, P. Henning, P. Boulanger, and L. Lindholm, "Genetic retargeting of adenovirus vectors: functionality of targeting ligands and their influence on virus viability," *The Journal of Gene Medicine*, vol. 4, Aug. 2002, pp. 356-370.

[82] S.J. Hedley, A. Auf der Maur, S. Hohn, D. Escher, A. Barberis, J.N. Glasgow, J.T. Douglas, N. Korokhov, and D.T. Curiel, "An adenovirus vector with a chimeric fiber incorporating stabilized single chain antibody achieves targeted gene delivery," *Gene Therapy*, vol. 13, Jan. 2006, pp. 88-94.

[83] P. Wu, W. Xiao, T. Conlon, J. Hughes, M. Agbandje-McKenna, T. Ferkol, T. Flotte, and N. Muzyczka, "Mutational analysis of the adeno-associated virus type 2 (AAV2) capsid gene and construction of AAV2 vectors with altered tropism," *Journal of Virology*, vol. 74, Sep. 2000, pp. 8635-8647.

[84] W. Shi, G.S. Arnold, and J.S. Bartlett, "Insertional mutagenesis of the adeno-associated virus type 2 (AAV2) capsid gene and generation of AAV2 vectors targeted to alternative cell-surface receptors," *Human Gene Therapy*, vol. 12, Sep. 2001, pp. 1697-1711.

[85] S.A. Loiler, T.J. Conlon, S. Song, Q. Tang, K.H. Warrington, A. Agarwal, M. Kapturczak, C. Li, C. Ricordi, M.A. Atkinson, N. Muzyczka, and T.R. Flotte, "Targeting recombinant adeno-associated virus vectors to enhance gene transfer to pancreatic islets and liver," *Gene Therapy*, vol. 10, Sep. 2003, pp. 1551-1558.

[86] A. Girod, M. Ried, C. Wobus, H. Lahm, K. Leike, J. Kleinschmidt, G. Deléage, and M. Hallek, "Genetic capsid modifications allow efficient re-targeting of adeno-associated virus type 2," *Nature Medicine*, vol. 5, Sep. 1999, pp. 1052-1056.

[87] J. Boucas, K. Lux, A. Huber, S. Schievenbusch, M.J. von Freyend, L. Perabo, S.

Quadt-Humme, M. Odenthal, M. Hallek, and H. Büning, "Engineering adeno-associated virus serotype 2-based targeting vectors using a new insertion site-position 453-and single point mutations," *The Journal of Gene Medicine*, vol. 11, Dec. 2009, pp. 1103-1113.

[88] X. Shi, G. Fang, W. Shi, and J.S. Bartlett, "Insertional mutagenesis at positions 520 and 584 of adeno-associated virus type 2 (AAV2) capsid gene and generation of AAV2 vectors with eliminated heparin- binding ability and introduced novel tropism," *Human Gene Therapy*, vol. 17, Mar. 2006, pp. 353-361.

[89] Q. Yang, M. Mamounas, G. Yu, S. Kennedy, B. Leaker, J. Merson, F. Wong-Staal, M. Yu, and J.R. Barber, "Development of novel cell surface CD34-targeted recombinant adenoassociated virus vectors for gene therapy," *Human Gene Therapy*, vol. 9, Sep. 1998, pp. 1929-1937.

[90] K.H. Warrington, O.S. Gorbatyuk, J.K. Harrison, S.R. Opie, S. Zolotukhin, and N. Muzyczka, "Adeno-associated virus type 2 VP2 capsid protein is nonessential and can tolerate large peptide insertions at its N terminus," *Journal of Virology*, vol. 78, Jun. 2004, pp. 6595-6609.

[91] K. Lux, N. Goerlitz, S. Schlemminger, L. Perabo, D. Goldnau, J. Endell, K. Leike, D.M. Kofler, S. Finke, M. Hallek, and H. Büning, "Green fluorescent protein-tagged adeno-associated virus particles allow the study of cytosolic and nuclear trafficking," *Journal of Virology*, vol. 79, Sep. 2005, pp. 11776-11787.

[92] W. Shi, "RGD inclusion in VP3 provides adeno-associated virus type 2 (AAV2)-based vectors with a heparan sulfate-independent cell entry mechanism," *Molecular Therapy*, vol. 7, 2003, pp. 515-525.

[93] S.A. Nicklin, H. Buening, K.L. Dishart, M. de Alwis, A. Girod, U. Hacker, A.J. Thrasher, R.R. Ali, M. Hallek, and A.H. Baker, "Efficient and selective AAV2-mediated gene transfer directed to human vascular endothelial cells," *Molecular Therapy: The Journal of the American Society of Gene Therapy*, vol. 4, Sep. 2001, pp. 174-181.

[94] M. Grifman, M. Trepel, P. Speece, L.B. Gilbert, W. Arap, R. Pasqualini, and M.D. Weitzman, "Incorporation of tumor-targeting peptides into recombinant adeno-associated virus capsids," *Molecular Therapy: The Journal of the American Society of Gene Therapy*, vol. 3, Jun. 2001, pp. 964-975.

[95] L. Perabo, H. Büning, D.M. Kofler, M.U. Ried, A. Girod, C.M. Wendtner, J. Enssle, and M. Hallek, "In vitro selection of viral vectors with modified tropism: the adeno-associated virus display," *Molecular Therapy: The Journal of the American Society of Gene Therapy*, vol. 8, Jul. 2003, pp. 151-157.

[96] O.J. Müller, F. Kaul, M.D. Weitzman, R. Pasqualini, W. Arap, J.A. Kleinschmidt, and M. Trepel, "Random peptide libraries displayed on adeno-associated virus to select for

targeted gene therapy vectors," *Nature Biotechnology*, vol. 21, Sep. 2003, pp. 1040-1046.

[97] L.M. Work, S.A. Nicklin, N.J.R. Brain, K.L. Dishart, D.J. Von Seggern, M. Hallek, H. Büning, and A.H. Baker, "Development of efficient viral vectors selective for vascular smooth muscle cells," *Molecular Therapy: The Journal of the American Society of Gene Therapy*, vol. 9, Feb. 2004, pp. 198-208.

[98] L.M. Work, H. Büning, E. Hunt, S.A. Nicklin, L. Denby, N. Britton, K. Leike, M. Odenthal, U. Drebber, M. Hallek, and A.H. Baker, "Vascular bed-targeted in vivo gene delivery using tropism-modified adeno-associated viruses," *Molecular Therapy: The Journal of the American Society of Gene Therapy*, vol. 13, Apr. 2006, pp. 683-693.

[99] D.A. Waterkamp, O.J. Müller, Y. Ying, M. Trepel, and J.A. Kleinschmidt, "Isolation of targeted AAV2 vectors from novel virus display libraries," *The Journal of Gene Medicine*, vol. 8, Nov. 2006, pp. 1307-1319.

[100] S.J. White, S.A. Nicklin, H. Büning, M.J. Brosnan, K. Leike, E.D. Papadakis, M. Hallek, and A.H. Baker, "Targeted gene delivery to vascular tissue in vivo by tropism-modified adeno-associated virus vectors," *Circulation*, vol. 109, Feb. 2004, pp. 513-519.

[101] A. Kern, K. Schmidt, C. Leder, O.J. Müller, C.E. Wobus, K. Bettinger, C.W. Von der Lieth, J.A. King, and J.A. Kleinschmidt, "Identification of a heparin-binding motif on adeno-associated virus type 2 capsids," *Journal of Virology*, vol. 77, Oct. 2003, pp. 11072-11081.

[102] S.R. Opie, K.H. Warrington, M. Agbandje-McKenna, S. Zolotukhin, and N. Muzyczka, "Identification of amino acid residues in the capsid proteins of adeno-associated virus type 2 that contribute to heparan sulfate proteoglycan binding," *Journal of Virology*, vol. 77, Jun. 2003, pp. 6995-7006.

[103] L. Perabo, D. Goldnau, K. White, J. Endell, J. Boucas, S. Humme, L.M. Work, H. Janicki, M. Hallek, A.H. Baker, and H. Büning, "Heparan sulfate proteoglycan binding properties of adeno-associated virus retargeting mutants and consequences for their in vivo tropism," *Journal of Virology*, vol. 80, Jul. 2006, pp. 7265-7269.

[104] R.W. ATCHISON, B.C. CASTO, and W.M. HAMMON, "ADENOVIRUS-ASSOCIATED DEFECTIVE VIRUS PARTICLES," *Science (New York, N.Y.)*, vol. 149, Aug. 1965, pp. 754-756.

[105] U. Bantel-Schaal and H. zur Hausen, "Characterization of the DNA of a defective human parvovirus isolated from a genital site," *Virology*, vol. 134, Apr. 1984, pp. 52-63.

[106] U. Bantel-Schaal, H. Delius, R. Schmidt, and H. zur Hausen, "Human adeno-associated virus type 5 is only distantly related to other known primate helper-dependent parvoviruses," *Journal of Virology*, vol. 73, Feb. 1999, pp. 939-947.

[107] M.D. Hoggan, N.R. Blacklow, and W.P. Rowe, "Studies of small DNA viruses found in various adenovirus preparations: physical, biological, and immunological characteristics," *Proceedings of the National Academy of Sciences of the United States of America*, vol. 55, Jun. 1966, pp. 1467-1474.

[108] B. Georg-Fries, S. Biederlack, J. Wolf, and H. zur Hausen, "Analysis of proteins, helper dependence, and seroepidemiology of a new human parvovirus," *Virology*, vol. 134, Apr. 1984, pp. 64-71.

[109] G. Gao, M.R. Alvira, L. Wang, R. Calcedo, J. Johnston, and J.M. Wilson, "Novel adeno-associated viruses from rhesus monkeys as vectors for human gene therapy," *Proceedings of the National Academy of Sciences of the United States of America*, vol. 99, Sep. 2002, pp. 11854-11859.

[110] G. Gao, L.H. Vandenberghe, M.R. Alvira, Y. Lu, R. Calcedo, X. Zhou, and J.M. Wilson, "Clades of Adeno-associated viruses are widely disseminated in human tissues," *Journal of Virology*, vol. 78, Jun. 2004, pp. 6381-6388.

[111] E.A. Rutledge, C.L. Halbert, and D.W. Russell, "Infectious clones and vectors derived from adeno-associated virus (AAV) serotypes other than AAV type 2," *Journal of Virology*, vol. 72, Jan. 1998, pp. 309-319.

[112] J.L. Melnick, H.D. Mayor, K.O. Smith, and F. Rapp, "Association of 20-Millimicron Particles with Adenoviruses," *Journal of Bacteriology*, vol. 90, Jul. 1965, pp. 271-274.

[113] S. Mori, L. Wang, T. Takeuchi, and T. Kanda, "Two novel adeno-associated viruses from cynomolgus monkey: pseudotyping characterization of capsid protein," *Virology*, vol. 330, Dec. 2004, pp. 375-383.

[114] M.A. Lochrie, G.P. Tatsuno, A.E. Arbetman, K. Jones, C. Pater, P.H. Smith, J.W. McDonnell, S. Zhou, S. Kachi, M. Kachi, P.A. Campochiaro, G.F. Pierce, and P. Colosi, "Adeno-associated virus (AAV) capsid genes isolated from rat and mouse liver genomic DNA define two new AAV species distantly related to AAV-5," *Virology*, vol. 353, Sep. 2006, pp. 68-82.

[115] P.J. Carter and R.J. Samulski, "Adeno-associated viral vectors as gene delivery vehicles," *International Journal of Molecular Medicine*, vol. 6, Jul. 2000, pp. 17-27.

[116] D.M. McCarty, J.H. Ryan, S. Zolotukhin, X. Zhou, and N. Muzyczka, "Interaction of the adeno-associated virus Rep protein with a sequence within the A palindrome of the viral terminal repeat," *Journal of Virology*, vol. 68, Aug. 1994, pp. 4998-5006.

[117] S.K. McLaughlin, P. Collis, P.L. Hermonat, and N. Muzyczka, "Adeno-associated virus general transduction vectors: analysis of proviral structures," *Journal of Virology*, vol. 62, Jun. 1988, pp. 1963-1973.

[118] R.J. Samulski, L.S. Chang, and T. Shenk, "A recombinant plasmid from which an infectious adeno-associated virus genome can be excised in vitro and its use to study

viral replication," *Journal of Virology*, vol. 61, Oct. 1987, pp. 3096-3101.

[119] R.O. Snyder, R.J. Samulski, and N. Muzyczka, "In vitro resolution of covalently joined AAV chromosome ends," *Cell*, vol. 60, Jan. 1990, pp. 105-113.

[120] R.O. Snyder, D.S. Im, T. Ni, X. Xiao, R.J. Samulski, and N. Muzyczka, "Features of the adeno-associated virus origin involved in substrate recognition by the viral Rep protein," *Journal of Virology*, vol. 67, Oct. 1993, pp. 6096-6104.

[121] R. Dubielzig, J.A. King, S. Weger, A. Kern, and J.A. Kleinschmidt, "Adeno-associated virus type 2 protein interactions: formation of pre-encapsidation complexes," *Journal of Virology*, vol. 73, Nov. 1999, pp. 8989-8998.

[122] J.A. King, R. Dubielzig, D. Grimm, and J.A. Kleinschmidt, "DNA helicase-mediated packaging of adeno-associated virus type 2 genomes into preformed capsids," *The EMBO Journal*, vol. 20, Jun. 2001, pp. 3282-3291.

[123] E.W. Lusby and K.I. Berns, "Mapping of the 5' termini of two adeno-associated virus 2 RNAs in the left half of the genome," *Journal of Virology*, vol. 41, Feb. 1982, pp. 518-526.

[124] S.R. Kyöstiö, R.A. Owens, M.D. Weitzman, B.A. Antoni, N. Chejanovsky, and B.J. Carter, "Analysis of adeno-associated virus (AAV) wild-type and mutant Rep proteins for their abilities to negatively regulate AAV p5 and p19 mRNA levels," *Journal of Virology*, vol. 68, May. 1994, pp. 2947-2957.

[125] R.H. Smith and R.M. Kotin, "The Rep52 gene product of adeno-associated virus is a DNA helicase with 3'-to-5' polarity," *Journal of Virology*, vol. 72, Jun. 1998, pp. 4874-4881.

[126] J.E. Rabinowitz and R.J. Samulski, "Building a better vector: the manipulation of AAV virions," *Virology*, vol. 278, Dec. 2000, pp. 301-308.

[127] G. Seisenberger, M.U. Ried, T. Endress, H. Büning, M. Hallek, and C. Bräuchle, "Real-time single-molecule imaging of the infection pathway of an adeno-associated virus," *Science (New York, N.Y.)*, vol. 294, Nov. 2001, pp. 1929-1932.

[128] Z. Wu, E. Miller, M. Agbandje-McKenna, and R.J. Samulski, "Alpha2,3 and alpha2,6 N-linked sialic acids facilitate efficient binding and transduction by adeno-associated virus types 1 and 6," *Journal of Virology*, vol. 80, Sep. 2006, pp. 9093-9103.

[129] J.E. Rabinowitz, F. Rolling, C. Li, H. Conrath, W. Xiao, X. Xiao, and R.J. Samulski, "Cross-packaging of a single adeno-associated virus (AAV) type 2 vector genome into multiple AAV serotypes enables transduction with broad specificity," *Journal of Virology*, vol. 76, Jan. 2002, pp. 791-801.

[130] B. Akache, D. Grimm, K. Pandey, S.R. Yant, H. Xu, and M.A. Kay, "The 37/67-kilodalton laminin receptor is a receptor for adeno-associated virus serotypes 8, 2, 3, and 9," *Journal of Virology*, vol. 80, Oct. 2006, pp. 9831-9836.

[131] A. Asokan, J.B. Hamra, L. Govindasamy, M. Agbandje-McKenna, and R.J. Samulski, "Adeno-associated virus type 2 contains an integrin alpha5beta1 binding domain essential for viral cell entry," *Journal of Virology*, vol. 80, Sep. 2006, pp. 8961-8969.

[132] E. Li, D. Stupack, G.M. Bokoch, and G.R. Nemerow, "Adenovirus endocytosis requires actin cytoskeleton reorganization mediated by Rho family GTPases," *Journal of Virology*, vol. 72, Nov. 1998, pp. 8806-8812.

[133] G. Odorizzi, M. Babst, and S.D. Emr, "Fab1p PtdIns(3)P 5-kinase function essential for protein sorting in the multivesicular body," *Cell*, vol. 95, Dec. 1998, pp. 847-858.

[134] J.T. Parsons, "Integrin-mediated signalling: regulation by protein tyrosine kinases and small GTP-binding proteins," *Current Opinion in Cell Biology*, vol. 8, Apr. 1996, pp. 146-152.

[135] W. Ding, L.N. Zhang, C. Yeaman, and J.F. Engelhardt, "rAAV2 traffics through both the late and the recycling endosomes in a dose-dependent fashion," *Molecular Therapy: The Journal of the American Society of Gene Therapy*, vol. 13, Apr. 2006, pp. 671-682.

[136] A.M. Douar, K. Poulard, D. Stockholm, and O. Danos, "Intracellular trafficking of adeno-associated virus vectors: routing to the late endosomal compartment and proteasome degradation," *Journal of Virology*, vol. 75, Feb. 2001, pp. 1824-1833.

[137] K. Pajusola, M. Gruchala, H. Joch, T.F. Lüscher, S. Ylä-Herttuala, and H. Büeler, "Cell-type-specific characteristics modulate the transduction efficiency of adeno-associated virus type 2 and restrain infection of endothelial cells," *Journal of Virology*, vol. 76, Nov. 2002, pp. 11530-11540.

[138] W. Xiao, K.H. Warrington, P. Hearing, J. Hughes, and N. Muzyczka, "Adenovirus-facilitated nuclear translocation of adeno-associated virus type 2," *Journal of Virology*, vol. 76, Nov. 2002, pp. 11505-11517.

[139] M. Marsh and A. Helenius, "Virus entry into animal cells," *Advances in Virus Research*, vol. 36, 1989, pp. 107-151.

[140] F. Sonntag, S. Bleker, B. Leuchs, R. Fischer, and J.A. Kleinschmidt, "Adeno-associated virus type 2 capsids with externalized VP1/VP2 trafficking domains are generated prior to passage through the cytoplasm and are maintained until uncoating occurs in the nucleus," *Journal of Virology*, vol. 80, Nov. 2006, pp. 11040-11054.

[141] S. Kronenberg, B. Böttcher, C.W. von der Lieth, S. Bleker, and J.A. Kleinschmidt, "A conformational change in the adeno-associated virus type 2 capsid leads to the exposure of hidden VP1 N termini," *Journal of Virology*, vol. 79, May. 2005, pp. 5296-5303.

[142] Z. Zádori, J. Szelei, M.C. Lacoste, Y. Li, S. Gariépy, P. Raymond, M. Allaire, I.R. Nabi, and P. Tijssen, "A viral phospholipase A2 is required for parvovirus infectivity,"

Developmental Cell, vol. 1, Aug. 2001, pp. 291-302.

[143] D. Mudhakir and H. Harashima, "Learning from the viral journey: how to enter cells and how to overcome intracellular barriers to reach the nucleus," *The AAPS Journal*, vol. 11, Mar. 2009, pp. 65-77.

[144] Z. Yan, R. Zak, G.W.G. Luxton, T.C. Ritchie, U. Bantel-Schaal, and J.F. Engelhardt, "Ubiquitination of both adeno-associated virus type 2 and 5 capsid proteins affects the transduction efficiency of recombinant vectors," *Journal of Virology*, vol. 76, Mar. 2002, pp. 2043-2053.

[145] Z. Yan, R. Zak, Y. Zhang, W. Ding, S. Godwin, K. Munson, R. Peluso, and J.F. Engelhardt, "Distinct classes of proteasome-modulating agents cooperatively augment recombinant adeno-associated virus type 2 and type 5-mediated transduction from the apical surfaces of human airway epithelia," *Journal of Virology*, vol. 78, Mar. 2004, pp. 2863-2874.

[146] L. Denby, S.A. Nicklin, and A.H. Baker, "Adeno-associated virus (AAV)-7 and -8 poorly transduce vascular endothelial cells and are sensitive to proteasomal degradation," *Gene Therapy*, vol. 12, Oct. 2005, pp. 1534-1538.

[147] D. Duan, Y. Yue, Z. Yan, J. Yang, and J.F. Engelhardt, "Endosomal processing limits gene transfer to polarized airway epithelia by adeno-associated virus," *The Journal of Clinical Investigation*, vol. 105, Jun. 2000, pp. 1573-1587.

[148] U.T. Hacker, L. Wingenfeld, D.M. Kofler, N.K. Schuhmann, S. Lutz, T. Herold, S.B.S. King, F.M. Gerner, L. Perabo, J. Rabinowitz, D.M. McCarty, R.J. Samulski, M. Hallek, and H. Büning, "Adeno-associated virus serotypes 1 to 5 mediated tumor cell directed gene transfer and improvement of transduction efficiency," *The Journal of Gene Medicine*, vol. 7, Nov. 2005, pp. 1429-1438.

[149] W. Ding, L. Zhang, Z. Yan, and J.F. Engelhardt, "Intracellular trafficking of adeno-associated viral vectors," *Gene Therapy*, vol. 12, Jun. 2005, pp. 873-880.

[150] K. Jennings, T. Miyamae, R. Traister, A. Marinov, S. Katakura, D. Sowders, B. Trapnell, J.M. Wilson, G. Gao, and R. Hirsch, "Proteasome inhibition enhances AAV-mediated transgene expression in human synoviocytes in vitro and in vivo," *Molecular Therapy: The Journal of the American Society of Gene Therapy*, vol. 11, Apr. 2005, pp. 600-607.

[151] J.S. Johnson and R.J. Samulski, "Enhancement of adeno-associated virus infection by mobilizing capsids into and out of the nucleolus," *Journal of Virology*, vol. 83, Mar. 2009, pp. 2632-2644.

[152] J. Hansen, K. Qing, and A. Srivastava, "Infection of purified nuclei by adeno-associated virus 2," *Molecular Therapy: The Journal of the American Society of Gene Therapy*, vol. 4, Oct. 2001, pp. 289-296.

[153] J.C. Grieger, S. Snowdy, and R.J. Samulski, "Separate basic region motifs within the adeno-associated virus capsid proteins are essential for infectivity and assembly," *Journal of Virology*, vol. 80, Jun. 2006, pp. 5199-5210.

[154] F.K. Ferrari, T. Samulski, T. Shenk, and R.J. Samulski, "Second-strand synthesis is a rate-limiting step for efficient transduction by recombinant adeno-associated virus vectors," *Journal of Virology*, vol. 70, May. 1996, pp. 3227-3234.

[155] K.J. Fisher, G.P. Gao, M.D. Weitzman, R. DeMatteo, J.F. Burda, and J.M. Wilson, "Transduction with recombinant adeno-associated virus for gene therapy is limited by leading-strand synthesis," *Journal of Virology*, vol. 70, Jan. 1996, pp. 520-532.

[156] R.M. Kotin, J.C. Menninger, D.C. Ward, and K.I. Berns, "Mapping and direct visualization of a region-specific viral DNA integration site on chromosome 19q13-qter," *Genomics*, vol. 10, Jul. 1991, pp. 831-834.

[157] R.M. Kotin, R.M. Linden, and K.I. Berns, "Characterization of a preferred site on human chromosome 19q for integration of adeno-associated virus DNA by non-homologous recombination," *The EMBO Journal*, vol. 11, Dec. 1992, pp. 5071-5078.

[158] J.R. Brister and N. Muzyczka, "Mechanism of Rep-mediated adeno-associated virus origin nicking," *Journal of Virology*, vol. 74, Sep. 2000, pp. 7762-7771.

[159] B.E. Redemann, E. Mendelson, and B.J. Carter, "Adeno-associated virus rep protein synthesis during productive infection," *Journal of Virology*, vol. 63, Feb. 1989, pp. 873-882.

[160] R.M. Linden, E. Winocour, and K.I. Berns, "The recombination signals for adeno-associated virus site-specific integration," *Proceedings of the National Academy of Sciences of the United States of America*, vol. 93, Jul. 1996, pp. 7966-7972.

[161] R.M. Linden, P. Ward, C. Giraud, E. Winocour, and K.I. Berns, "Site-specific integration by adeno-associated virus," *Proceedings of the National Academy of Sciences of the United States of America*, vol. 93, Oct. 1996, pp. 11288-11294.

[162] M.D. Weitzman, S.R. Kyöstiö, R.M. Kotin, and R.A. Owens, "Adeno-associated virus (AAV) Rep proteins mediate complex formation between AAV DNA and its integration site in human DNA," *Proceedings of the National Academy of Sciences of the United States of America*, vol. 91, Jun. 1994, pp. 5808-5812.

[163] K.I. Berns and C. Giraud, "Biology of adeno-associated virus," *Current Topics in Microbiology and Immunology*, vol. 218, 1996, pp. 1-23.

[164] U.T. Hacker, F.M. Gerner, H. Büning, M. Hutter, H. Reichenspurner, M. Stangl, and M. Hallek, "Standard heparin, low molecular weight heparin, low molecular weight heparinoid, and recombinant hirudin differ in their ability to inhibit transduction by recombinant adeno-associated virus type 2 vectors," *Gene Therapy*, vol. 8, Jun. 2001, pp. 966-968.

[165] X. Xiao, J. Li, and R.J. Samulski, "Production of high-titer recombinant adeno-associated virus vectors in the absence of helper adenovirus," *Journal of Virology*, vol. 72, Mar. 1998, pp. 2224-2232.

[166] D. Hanahan, "Studies on transformation of Escherichia coli with plasmids," *Journal of Molecular Biology*, vol. 166, Jun. 1983, pp. 557-580.

[167] F.L. Graham, J. Smiley, W.C. Russell, and R. Nairn, "Characteristics of a human cell line transformed by DNA from human adenovirus type 5," *The Journal of General Virology*, vol. 36, Jul. 1977, pp. 59-74.

[168] W.F. SCHERER, J.T. SYVERTON, and G.O. GEY, "Studies on the propagation in vitro of poliomyelitis viruses. IV. Viral multiplication in a stable strain of human malignant epithelial cells (strain HeLa) derived from an epidermoid carcinoma of the cervix," *The Journal of Experimental Medicine*, vol. 97, May. 1953, pp. 695-710.

[169] B.B. Knowles, C.C. Howe, and D.P. Aden, "Human hepatocellular carcinoma cell lines secrete the major plasma proteins and hepatitis B surface antigen," *Science (New York, N.Y.)*, vol. 209, Jul. 1980, pp. 497-499.

[170] C.B. Lozzio and B.B. Lozzio, "Human chronic myelogenous leukemia cell-line with positive Philadelphia chromosome," *Blood*, vol. 45, Mar. 1975, pp. 321-334.

[171] L. Perabo, H. Büning, D.M. Kofler, M.U. Ried, A. Girod, C.M. Wendtner, J. Enssle, and M. Hallek, "In vitro selection of viral vectors with modified tropism: the adeno-associated virus display," *Molecular Therapy: The Journal of the American Society of Gene Therapy*, vol. 8, Jul. 2003, pp. 151-157.

[172] H. Mizukami, N.S. Young, and K.E. Brown, "Adeno-associated virus type 2 binds to a 150-kilodalton cell membrane glycoprotein," *Virology*, vol. 217, Mar. 1996, pp. 124-130.

[173] M. Marsh and A. Helenius, "Virus entry: open sesame," *Cell*, vol. 124, Feb. 2006, pp. 729-740.

[174] L.H. Wang, K.G. Rothberg, and R.G. Anderson, "Mis-assembly of clathrin lattices on endosomes reveals a regulatory switch for coated pit formation," *The Journal of Cell Biology*, vol. 123, Dec. 1993, pp. 1107-1117.

[175] K. Miller, M. Shipman, I.S. Trowbridge, and C.R. Hopkins, "Transferrin receptors promote the formation of clathrin lattices," *Cell*, vol. 65, May. 1991, pp. 621-632.

[176] E. Van Hamme, H.L. Dewerchin, E. Cornelissen, B. Verhasselt, and H.J. Nauwynck, "Clathrin- and caveolae-independent entry of feline infectious peritonitis virus in monocytes depends on dynamin," *The Journal of General Virology*, vol. 89, Sep. 2008, pp. 2147-2156.

[177] E. Koivunen, B. Wang, and E. Ruoslahti, "Phage libraries displaying cyclic peptides with different ring sizes: ligand specificities of the RGD-directed integrins,"

Bio/Technology (Nature Publishing Company), vol. 13, Mar. 1995, pp. 265-270.

[178] W. Arap, R. Pasqualini, and E. Ruoslahti, "Cancer treatment by targeted drug delivery to tumor vasculature in a mouse model," *Science (New York, N.Y.)*, vol. 279, Jan. 1998, pp. 377-380.

[179] M. Chalfie, Y. Tu, G. Euskirchen, W.W. Ward, and D.C. Prasher, "Green fluorescent protein as a marker for gene expression," *Science (New York, N.Y.)*, vol. 263, Feb. 1994, pp. 802-805.

[180] P. Desai and S. Person, "Incorporation of the green fluorescent protein into the herpes simplex virus type 1 capsid," *Journal of Virology*, vol. 72, Sep. 1998, pp. 7563-7568.

[181] D.M. Shayakhmetov, A.M. Eberly, Z. Li, and A. Lieber, "Deletion of penton RGD motifs affects the efficiency of both the internalization and the endosome escape of viral particles containing adenovirus serotype 5 or 35 fiber knobs," *Journal of Virology*, vol. 79, Jan. 2005, pp. 1053-1061.

[182] D.H. Lee and A.L. Goldberg, "Proteasome inhibitors: valuable new tools for cell biologists," *Trends in Cell Biology*, vol. 8, Oct. 1998, pp. 397-403.

[183] C.E. Thomas, T.A. Storm, Z. Huang, and M.A. Kay, "Rapid uncoating of vector genomes is the key to efficient liver transduction with pseudotyped adeno-associated virus vectors," *Journal of Virology*, vol. 78, Mar. 2004, pp. 3110-3122.

[184] N. Bayer, D. Schober, E. Prchla, R.F. Murphy, D. Blaas, and R. Fuchs, "Effect of bafilomycin A1 and nocodazole on endocytic transport in HeLa cells: implications for viral uncoating and infection," *Journal of Virology*, vol. 72, Dec. 1998, pp. 9645-9655.

[185] S. Michelfelder, J. Kohlschütter, A. Skorupa, S. Pfennings, O. Müller, J.A. Kleinschmidt, and M. Trepel, "Successful expansion but not complete restriction of tropism of adeno-associated virus by in vivo biopanning of random virus display peptide libraries," *PloS One*, vol. 4, 2009, p. e5122.

[186] H.C. Levy, V.D. Bowman, L. Govindasamy, R. McKenna, K. Nash, K. Warrington, W. Chen, N. Muzyczka, X. Yan, T.S. Baker, and M. Agbandje-McKenna, "Heparin binding induces conformational changes in Adeno-associated virus serotype 2," *Journal of Structural Biology*, vol. 165, Mar. 2009, pp. 146-156.

[187] M. Mohammadi, S.K. Olsen, and O.A. Ibrahimi, "Structural basis for fibroblast growth factor receptor activation," *Cytokine & Growth Factor Reviews*, vol. 16, Apr. 2005, pp. 107-137.

[188] M. Liang, K. Morizono, N. Pariente, M. Kamata, B. Lee, and I.S.Y. Chen, "Targeted transduction via CD4 by a lentiviral vector uses a clathrin-mediated entry pathway," *Journal of Virology*, vol. 83, Dec. 2009, pp. 13026-13031.

[189] D. Mudhakir, H. Akita, E. Tan, and H. Harashima, "A novel IRQ ligand-modified nano-carrier targeted to a unique pathway of caveolar endocytic pathway," *Journal of*

Controlled Release: Official Journal of the Controlled Release Society, vol. 125, Jan. 2008, pp. 164-173.

[190] B. Hauck, W. Zhao, K. High, and W. Xiao, "Intracellular viral processing, not single-stranded DNA accumulation, is crucial for recombinant adeno-associated virus transduction," *Journal of Virology*, vol. 78, Dec. 2004, pp. 13678-13686.

[191] K. Qing, B. Khuntirat, C. Mah, D.M. Kube, X.S. Wang, S. Ponnazhagan, S. Zhou, V.J. Dwarki, M.C. Yoder, and A. Srivastava, "Adeno-associated virus type 2-mediated gene transfer: correlation of tyrosine phosphorylation of the cellular single-stranded D sequence-binding protein with transgene expression in human cells in vitro and murine tissues in vivo," *Journal of Virology*, vol. 72, Feb. 1998, pp. 1593-1599.

[192] N. Vincent-Lacaze, R.O. Snyder, R. Gluzman, D. Bohl, C. Lagarde, and O. Danos, "Structure of adeno-associated virus vector DNA following transduction of the skeletal muscle," *Journal of Virology*, vol. 73, Mar. 1999, pp. 1949-1955.

[193] M. Egeberg, R. Kjeken, S.O. Kolset, T. Berg, and K. Prydz, "Internalization and stepwise degradation of heparan sulfate proteoglycans in rat hepatocytes," *Biochimica Et Biophysica Acta*, vol. 1541, Dec. 2001, pp. 135-149.

[194] O.O. Glebov, N.A. Bright, and B.J. Nichols, "Flotillin-1 defines a clathrin-independent endocytic pathway in mammalian cells," *Nature Cell Biology*, vol. 8, Jan. 2006, pp. 46-54.

Cited unpublished manuscript:

S. Stahnke, K. Lux, S. Uhrig, F. Kreppel, M. Hösel, O. Coutelle, M. Ogris, M. Hallek, and H. Büning, "Intrinsic phospholipase A2 activity of adeno-associated virus is involved in endosomal escape of incoming particles," Mar. 2010, *Virology*, in revision.

Cited dissertations:

J. Bouças, "Engineering AAV-2 Targeting Vectors: A New Insertion Site and scFv Driven Vectors," Aug. 2008.

D. Goldnau, "New strategies for the application of Adeno-Associated Virus type 2 targeting vectors," Mar. 2006.

N. Huttner, "Adeno-associated virus type 2 as vector for human gene therapy: Characterization of virus-host interactions," May 2003.

S. Stahnke, „Die Funktion der viralen Phospholipase A2 während der Infektion des Adeno-assoziierten Virus 2," Dez. 2008.

Danksagung

Ganz herzlich möchte ich mich bei PD Dr. Hildegard Büning für die Möglichkeit zur Erstellung dieser Arbeit bedanken, insbesondere für die Überlassung eines vielseitigen Projekts und ihre ständige Bereitschaft, über Ergebnisse, Probleme und deren Lösungsmöglichkeiten zu diskutieren.

Bei Prof. Dr. Michael Hallek bedanke ich mich für Möglichkeit, meine Promotion an der Klinik I für Innere Medizin der Uniklinik Köln in einem hochrangigen wissenschaftlichen Umfeld durchführen zu dürfen.
Den Mitgliedern des DFG-Schwerpunktprogramms 1230, besonders Dr. Manfred Ogris und Dr. Florian Kreppel, danke ich für die gute Zusammenarbeit im Forschungsfeld Gentransfer-Vektoren.

Prof. Dr. Dagmar Knebel-Mörsdorf und Prof. Dr. Herbert Pfister danke ich für die kompetente Tutorenschaft im Rahmen des IPMM-Programms, sowie für die Begutachtung dieser Arbeit.

Bei Prof. Dr. Hinrich Abken und Prof. Dr. Günter Schwarz bedanke ich mich für die Bereitschaft, als Prüfer in meiner Disputation zur Verfügung zu stehen.
Prof. Dr. Mats Paulsson danke ich für die Übernahme des Prüfungsvorsitzes.

Besonderer Dank gilt meinen Kollegen aus der AG Büning und den anderen Arbeitsgruppen der ZMMK-Ebene 5 / LFI-Ebene 4, die mir stets mit Rat und Tat zur Seite standen und durch den einen oder anderen netten Plausch auf dem Flur zu einer abwechslungsreichen Doktorandenzeit in angenehmer Arbeitsatmosphäre beigetragen haben.

Nicht zuletzt geht ein großes Dankeschön an meine Eltern, meine Schwestern und natürlich an Patrick, die mich durch die Höhen und Tiefen der letzten Jahre begleitet, Freude und Niedergeschlagenheit mit mir geteilt und mich bei Problemen aller Art immer nach Kräften unterstützt haben. Ihr seid einfach die Besten!

Erklärung

Ich versichere, dass ich die von mir vorgelegte Dissertation selbständig angefertigt, die benutzten Quellen und Hilfsmittel vollständig angegeben und die Stellen der Arbeit – einschließlich Tabellen, Karten, und Abbildungen –, die anderen Werken im Wortlaut oder dem Sinn nach entnommen sind, in jedem Einzelfall als Entlehnung kenntlich gemacht habe; dass diese Dissertation noch keiner anderen Fakultät oder Universität zur Prüfung vorgelegen hat; dass sie – abgesehen von unten angegebenen Teilpublikationen – noch nicht veröffentlicht worden ist sowie, dass ich eine solche Veröffentlichung vor Abschluss des Promotionsverfahrens nicht vornehmen werde.

Die Bestimmungen dieser Promotionsordnung sind mir bekannt. Die von mir vorgelegte Dissertation ist von PD Dr. Hildegard Büning im Labor für AAV-Vektorentwicklung an der Klinik I für Innere Medizin der Uniklinik Köln betreut worden.

Teilpublikationen:

S. Stahnke, K. Lux, **S. Uhrig**, F. Kreppel, M. Hösel, O. Coutelle, M. Ogris, M. Hallek, and H. Büning, "Intrinsic phospholipase A2 activity of adeno-associated virus is involved in endosomal escape of incoming particles," Mar. 2010, *Virology*, in revision.

S. Uhrig, M. Hösel, L. Perabo, M. Hallek and H. Büning, "Targeted transduction of recombinant adeno-associated viral vectors uses a clathrin-mediated entry pathway," manuscript in preparation.

Teile dieser Arbeit wurden auf folgenden Kongressen vorgestellt:

Poster presentations:

11th Annual Meeting of the American Society of Gene Therapy (ASGT), 2008.

15th Annual Meeting of the German Society of Gene Therapy (DG-GT), 2008.

16th Annual Congress of the European Society of Gene and Cell Therapy (ESGCT), 2008.

Oral presentations:

Combined Meeting of the ESGCT, GSZ, DG-GT and ISCT, 2009.

13th Annual Meeting of the ASGT, 2010.

Ich versichere, dass ich alle Angaben wahrheitsgemäß nach bestem Wissen und Gewissen gemacht habe und verpflichte mich, jedmögliche, die obigen Angaben betreffenden Veränderungen, dem Promotionsausschuss unverzüglich mitzuteilen.

....

Datum   Unterschrift

Lebenslauf

Persönliche Daten

Name	Silke Uhrig
Geburtsdatum	3. August 1981
Geburtsort	Köln
Familienstand	ledig

Schulische Ausbildung

1988 – 1992	Ildefons-Herwegen-Grundschule, Köln
1992 – 2001	Liebfrauenschule Köln, Gymnasium
06/2001	Allgemeine Hochschulreife (Note: 1,5)

Akademische Ausbildung

2001 – 2006	Universität zu Köln, Diplom Biologie
09/2003	Vordiplom (Note: 1,5)
05/2006	Diplom (Note: 1,0)
	Hauptfach: Botanik
	1. Nebenfach: Genetik
	2. Nebenfach: Biochemie
06/2005 – 05/2006	**Diplomarbeit** am Botanischen Institut III der Universität zu Köln unter der Leitung von Prof. Dr. Martin Hülskamp zum Thema "Genetische, molekulare und zellbiologische Analyse von *scar*-Mutanten in *Arabidopsis thaliana*".
06/2006 – 09/2006	Wissenschaftliche Mitarbeit am Botanischen Institut III der Universität zu Köln
10/2006 – 03/2007	Promotion gefördert durch die "International Max-Planck Research School" der Max-Planck-Gesellschaft am Botanischen Institut III der Universität zu Köln
2007 – 2010	**Promotion** an der Uniklinik Köln im Labor für AAV-Vektorentwicklung unter der Leitung von PD Dr. Hildegard Büning zum Thema „The impact of peptide insertions on adeno-associated viral vector fate".
2008 – 2010	Interdisziplinäres Promotionsstudium „Molekulare Medizin" des Zentrums für Molekulare Medizin Köln (ZMMK)

Publikationen

2007	Joachim F. Uhrig, Moola Mutondo, Ilona Zimmermann, Michael J. Deeks, Laura M. Machesky, Philipp Thomas, Silke Uhrig, Claudia Rambke, Patrick J. Hussey and Martin Hülskamp (2007). **The Role of *Arabidopsis SCAR* genes in Arp2/3-dependent cell morphogenesis.** *Development* **134,** 967-977.
2010	Stefanie Stahnke, Kerstin Lux, Silke Uhrig, Florian Kreppel, Marianna Hösel, Oliver Coutelle, Manfred Ogris, Michael Hallek and Hildegard Büning (2010). **Intrinsic phospholipase A2 activity of adeno-associated virus is involved in endosomal escape of incoming particles.** *Virology*, in Revision.
2010	Silke Uhrig, Marianna Hösel, Luca Perabo, Michael Hallek and Hildegard Büning (2010). **Targeted transduction of recombinant adeno-associated viral vectors uses a clathrin-mediated entry pathway.** Manuskript in Vorbereitung.

Poster

05/2008	<u>Silke Uhrig</u>, Luca Perabo, Michael Hallek and Hildegard Büning (2008). **Cell infection by capsid engineered AAV vectors: variations from the common scheme?** *ASGT Meeting (Boston, USA).*
10/2008	<u>Silke Uhrig</u>, Luca Perabo, Michael Hallek and Hildegard Büning (2008). **Consequences of capsid engineering for AAV mediated cell infection.** *DG-GT Meeting (Berlin, Deutschland).*

Vorträge

11/2009	<u>Silke Uhrig</u>, Marianna Hösel, Luca Perabo, Michael Hallek and Hildegard Büning (2009). **HSPG-independent, clathrin-mediated endocytosis of AAV targeting vectors fosters cell type specificity and intracellular processing.** *ESGCT Meeting (Hannover, Deutschland).*
2010	<u>Silke Uhrig</u>, Jessica Sallach, David Gomez Almarza, Luca Perabo, Sabine Eming, Fernando Laguzzi Larcher, Michael Hallek and Hildegard Büning (2010). **Cell entry pathway defines efficiency and specificity of rAAV targeting vectors.** *ASGT Meeting (Washington, USA)*

Berufserfahrung

Praktika

1997	Betriebspraktikum im Bereich Krankenpflegedienst, St. Elisabeth-Krankenhaus, Köln-Hohenlind
2000	Praktikum am Institut für Rechtsmedizin der Universität zu Köln
2001	Praktikum im molekularbiologischen Bereich am Max-Planck-Institut für Züchtungsforschung in der Arbeitsgruppe von PD Dr. Klaus Theres

Arbeitserfahrung

2002	Studentische Hilfskraft im molekularbiologischen Bereich am Max-Planck-Institut für Züchtungsforschung in der Arbeitsgruppe von PD Dr. Klaus Theres
2004	Studentische Hilfskraft im molekularbiologischen Bereich am Institut für Botanik III der Universität zu Köln in der Arbeitsgruppe von Prof. Dr. Martin Hülskamp
2005, 2006	Betreuung von Studenten im Botanik Grund- und Hauptstudium, Universität zu Köln

Weiterbildung

2008	BioScript Workshop „Advanced Scientific Writing"
2009	BioScript Workshop „Presenting with Confidence"

Sonstige Tätigkeit

2008 – 2010	Studentische Vertreterin im Vorstand des Zentrums für Molekulare Medizin Köln (ZMMK)
2008	Organisation des Doktorandenseminars der Klinik I für Innere Medizin, Uniklinik Köln
2009 – 2010	Mitglied der Deutschen Gesellschaft für Gentherapie e.V.

Köln, den ……………….................

………………………………………..